1977

The in vivo and in vitro assembly of cell walls in the marine coccolithophorid, Hymenomonas carterae

David Charles Flesch
Iowa State University

INFORMATION TO USERS

This material was produced from a microfilm copy of the original document. While the most advanced technological means to photograph and reproduce this document have been used, the quality is heavily dependent upon the quality of the original submitted.

The following explanation of techniques is provided to help you understand markings or patterns which may appear on this reproduction.

1. The sign or "target" for pages apparently lacking from the document photographed is "Missing Page(s)". If it was possible to obtain the missing page(s) or section, they are spliced into the film along with adjacent pages. This may have necessitated cutting thru an image and duplicating adjacent pages to insure you complete continuity.

2. When an image on the film is obliterated with a large round black mark, it is an indication that the photographer suspected that the copy may have moved during exposure and thus cause a blurred image. You will find a good image of the page in the adjacent frame.

3. When a map, drawing or chart, etc., was part of the material being photographed the photographer followed a definite method in "sectioning" the material. It is customary to begin photoing at the upper left hand corner of a large sheet and to continue photoing from left to right in equal sections with a small overlap. If necessary, sectioning is continued again — beginning below the first row and continuing on until complete.

4. The majority of users indicate that the textual content is of greatest value, however, a somewhat higher quality reproduction could be made from "photographs" if essential to the understanding of the dissertation. Silver prints of "photographs" may be ordered at additional charge by writing the Order Department, giving the catalog number, title, author and specific pages you wish reproduced.

5. PLEASE NOTE: Some pages may have indistinct print. Filmed as received.

University Microfilms International
300 North Zeeb Road
Ann Arbor, Michigan 48106 USA
St. John's Road, Tyler's Green
High Wycombe, Bucks, England HP10 8HR

The *in vivo* and *in vitro* assembly of cell walls in the marine coccolithophorid, *Hymenomonas carterae*

by

David Charles Flesch

A Dissertation Submitted to the

Graduate Faculty in Partial Fulfillment of

The Requirements for the Degree of

DOCTOR OF PHILOSOPHY

Major: Molecular, Cellular, and
Developmental Biology

Approved:

Signature was redacted for privacy.

In Charge of Major Work

Signature was redacted for privacy.

For the Major Department

Signature was redacted for privacy.

For the Graduate College

Iowa State University
Ames, Iowa

1977

TABLE OF CONTENTS

DEDICATION

This work is dedicated to my father, Laverne E. Flesch, whose sacrifices as a parent and provider should not be allowed to pass unrecognized.

INTRODUCTION

Present on most, if not all, cells is an extracellular layer comprised of a variety of molecular units; the cell wall is one example of an extracellular coat. In bacteria and plants, these walls become very elaborate; in the latter, cellulose assumes a major role. However, the chemical structure of any higher plant cell wall has not been worked out, nor is it understood how the cell elongates during growth. There is a need to know much more about the specific cellular and biochemical mechanisms involved with the cell wall including its chemical structure, its biosynthesis, assembly, and disassembly.

It has been our thesis that a primitive form of the higher plant cell might be more accessible experimentally. The unicellular, marine alga Hymenomonas carterae seemed an excellent choice on the following grounds: (1) its cell wall is assembled as a series of discrete units with the largest of these, the coccolith, being visible with the light microscope so that formation and wall placement can be observed in vivo; (2) sequential assembly of parts in the Golgi can be followed with electron microscopy; (3) it can be grown axenically in large quantities for biochemical studies; (4) its cell division can be synchronized for cell cycle relationships to cell wall growth; and finally (5) protoplast production for following cell wall biosynthesis and assembly seemed feasible since Hymenomonas cell walls possess cellulose, pectin, and probably hemicellulose just as higher plant cell walls do.

This work tells something about how the cell wall is formed, how it grows, how it can sometimes be shed or partially resorbed, how it is held

together, what some of its parts look like, and of what it is made. In a real sense, this is a progress report; it includes information about the course of cell wall formation from protoplasts (*in vivo* cell wall assembly) and about how the cell wall is reassembled from dissociated parts (*in vitro* cell wall assembly).

LITERATURE REVIEW

The Organism

General features

Hymenomonas carterae is a member of an ancient group of organisms, the coccolithophorids, so named because of their production of calcareous scales called coccoliths. The coccolithophorids have external appendages, flagella, and a haptonema; the haptonema is a bulbous structure found between the two flagella and may serve as an attachment organelle and aid in controlling movement (Manton, 1968). The coccolithophorids' habitat is predominantly marine with samples taken from tropic, temperate, and arctic seas (Pautard, 1970) where they help to make up a substantial portion of the plankton; one fresh water form has been reported (Manton and Peterfi, 1969). They also have made significant contributions to the fossil record (Pautard, 1970). Hymenomonas has been referred to in the literature by the genus names Cricosphaera and Syracosphaera (Paasche, 1968); for my work, I will use Hymenomonas for the genus name following the recommendations of Manton and Peterfi (1969). These phytoflagellates are classified by the International Committee for Botanical Nomenclature as belonging in the order Coccolithophorales, in the class Haptophyceae, and in the phylum Chrysophyta and by the International Committee for Zoological Nomenclature as belonging in the order Coccolithophorida, in the class Mastigophora, and in the phylum Protozoa (Pautard, 1970). It is not the intention of this report to enter into this controversy. Reviews of coccolithophorids and Hymenomonas can be found in Paasche (1968), Pautard (1970), and Williams (1972).

The life cycle of Hymenomonas and the other coccolithophorids has been investigated by several authors (Brown and Romanovicz, 1976; Leadbeater, 1970, 1971; Lefort, 1971; Manton and Peterfi, 1969; Parke and Adams, 1960; Paddock, 1968; Pienaar, 1976; Rayns, 1962; Stosch, 1967). These authors are in general agreement that there exists a motile and nonmotile phase for these algae. In the motile stage, the cells bear coccoliths, and in the nonmotile, vegetative or benthic stage, the cells lack coccoliths (Leadbeater, 1970, 1971). In this paper coccolith bearing organisms are referred to as Hymenomonas, and the nonmotile stage is referred to as Pleurochrysis. These stages can be transformed into one another by amino acid addition or withdrawal (Brown and Romanovicz, 1976). The stages are thought to be linked through meiosis (meiospores) and syngamy (gametes) (Leadbeater, 1971; Rayns, 1962; Stosch, 1967). From a chromosome study of these two stages (Rayns, 1962), the motile stage was reported as diploid and the benthic stage was haploid; these results have been reiterated by others (Leadbeater, 1971; Stosch, 1967) without any additional evaluation. Parke and Adams (1960), working with Coccolithus pelagicus, have reported that motile stages are haploid and the nonmotile stages are diploid; this information contradicts the previous work. However, a report to be released soon (Safa, A. R., Unpublished report, Department of Biochemistry and Biophysics, Iowa State University, 1977) will show results from chromosome squashes and a quantitative measurement of DNA content per nucleus by microspectrophotometry that the motile, coccolith-bearing stages are haploid and nonmotile, noncoccolith-bearing stages are diploid. Thus a unity would be established between the life cycle of Hymenomonas and the

coccolithophorids to the other algae, for example, the green alga Chlamydomonas (Ebersold, 1963, 1967; Levine and Ebersold, 1960).

The coccoliths of the coccolithophorids contain calcium carbonate crystals in the form of calcite. These crystals, along with the organic constituents of the coccolith, have particular sizes and shapes, often quite elaborate, and are, therefore, of primary value in the taxonomy of the group. A tremendous variety of coccolith types are found in nature and in the fossil record and, with this diversity, there has arisen some complex terminology for describing and classifying coccoliths which has been summarized by Braarud et al. (1955). The coccoliths of Hymenomonas are in the heterococcolith category and cricolith subdivision which means the calcite crystal is of a rhombohedral shape, but the crystal faces become partially or wholly obliterated. The other main category of coccoliths is the heterococcoliths which are formed from a large number of regularly packed calcite crystals of simple hexagonal or rhombohedral shape. Lefort (1971) has reported that cricolith-producing Hymenomonas can undergo a third life cycle stage in which the heterococcoliths are different from the cricoliths. The identification of calcite in coccoliths of Coccolithus was demonstrated first on a morphological basis by Black (1962) and later from electron diffraction analysis by Watabe (1967) where the calcite is arranged radially with the c-axis projecting outward. Calcification involves a biphasic system where calcium carbonate is deposited upon a preformed matrix (Klaveness, 1972, 1976; Manton and Leedale, 1969; Pienaar, 1971b; Outka and Williams, 1971; Williams, 1972). At first the carbonate of the coccolith calcite was postulated to come from bicarbonate ions (Crenshaw, 1964; Paasche, 1962), but more recent work with carbonic

anhydrase inhibitors refutes this idea (Paasche, 1968; Williams, 1972). The coccoliths made by this algal group are most elaborate, and recently several SEM and TEM micrographs have been published of them (Gaarder and Heimdal, 1977; Klaveness, 1976; Mills, 1975; Pienaar, 1976).

Investigations of factors affecting growth have been confined to primarily two species of coccolithophorids, Hymenomonas carterae and Coccolithus huxleyi, and these studies have been reviewed by Blankley (1971), Paasche (1968), and Williams (1972). Light has generally been considered a necessity for these organisms, but Blankley (1971) has been able to grow both organisms in the dark with the same growth rates as light grown cells. Light intensity does influence autotrophic growth (Blankley, 1971; Paasche, 1967) with reduced growth below 2,000 lux and unchanged growth rates from 2,000 to 14,000 lux. Paasche (1967) has found that daylengths shorter than 16 hours of light reduced growth, but the growth rate was unchanged with 16-24 hours of light; a synchronized division occurred during the dark. The optimum temperature for growth has been demonstrated by Paasche (1967) and Blankley and Lewin (1976) to be 20°C. The optimum pH has been 7.8-8.0 for the few species tested (Blankley, 1971; Paasche, 1964; Swift and Taylor, 1966). Mineral cofactors also influence growth. Isenberg et al. (1963a), Weiss et al. (1976), and Williams (1972, 1974) had shown that 1×10^{-2} M calcium was optimal for growth and, under reduced calcium concentrations, strontium was found, in all cases, to substitute for the calcium and allow cell division to occur; the calcium transport inhibitors, lanthanum chloride, oligomycin, and ethacrynic acid reduce growth also (Dorigan and Wilbur, 1973). Magnesium had no effect on growth when added to the growth medium (Williams, 1972), but when magnesium was absent from

the medium ($\leq 4 \times 10^{-5}$ M) cell division ceased (Weiss et al., 1976). Finally, Blankley (1971) has found that aeration and CO_2 exchange must be increased to improve growth.

Coccolith formation

In this section coccolith formation will be divided into two main categories: (1) the physiological and nutritional factors affecting coccolith production and (2) the structural studies with the electron microscope which established the developmental sequence for the intracellular manufacture of coccoliths within the Golgi apparatus. Both of these categories have been reviewed by Paasche (1968), Pautard (1970), and Williams (1972).

Physiological and nutritional studies Light is one physiological factor affecting coccolith formation. Numerous investigators have shown that coccolith production requires light (Crenshaw, 1964; Dorigan and Wilbur, 1973; Paasche, 1964, 1966a, 1966b, 1968; Williams, 1972; 1974); however, Blankley (1971) has reported that, when glycerol was present in growth medium with cells in the dark, coccolith production was equal to or greater than coccolith production in the light. Dorigan and Wilbur (1973) were unable to get decalcified cells to produce coccoliths in the dark (after seven days with glycerol present), but apparently they should have allowed more time to elapse before terminating their experiment because it normally took six days or more for the cells to convert to heterotrophic growth (Blankley, 1971). Paasche (1966b) found that coccolithogenesis functioned optimally at a wavelength of 440 nm while photosynthesis was more efficient at 670 nm. Paasche suggests that two photochemical reactions may be involved in the light reactions associated with coccolith

production. An extrachloroplastic pigment body from Hymenomonas has been isolated which absorbs maximally in the blue range (Olson et al., 1967), but its relationship, if any, to coccolith formation is unclear. The nature of the relationship of light and coccolithogenesis is presently uncertain.

At this point an explanation of how coccolith formation is measured would be helpful because numerous differences in technique do arise. Wilbur and Watabe (1963) and Crenshaw (1964) were the first to make coccolithogenic measurements which were later revised (Dorigan and Wilbur, 1973); they decalcified the cells by bubbling CO_2 through the medium for 20-60 minutes to reduce the pH 5.5-6.0; the coccolith formation was determined by (1) detection of birefringence with the polarization microscope produced from the calcite crystals, (2) counting at least one coccolith on a cell after seven days was considered sufficient to score it as a calcified cell, and (3) calcium content measurements from 10^6 cells with the aid of an atomic absorption spectrophotometer. Carbon-14 uptake was utilized by Paasche (1964, 1966a), and the rate of coccolith formation was determined by radioactivity differences between light and dark grown cells. Blankley (1971) filtered sample aliquots and measured calcium levels with an automatic absorption spectrophotometer. The simplest and probably the most accurate method was devised by Williams (1972, 1974) who decalcified the cells by placing the cells in calcium-free medium at pH 5.5 and returning them to normal growth medium where he counted the number of coccoliths per cell with the aid of Nomarski interference contrast light microscopy, until the cells had at least 40 coccoliths. Only with

Williams' method has a coccolithogenic rate been reported, which can be as high as 10 coccoliths per cell per hour.

The incubation temperature affects the coccolith dimensions, according to Watabe and Wilbur (1966). They found no overall change in coccolith length or width from cultures maintained between $7^{o}C$ to $18^{o}C$, but the width and length decreased when incubation temperatures rose above $18^{o}C$.

Mineral cofactors such as calcium, strontium, and magnesium have been investigated for their influence on coccolithogenesis by several authors (Blackwelder *et al.*, 1976; Crenshaw, 1964; Isenberg *et al.*, 1963a; Paasche, 1964; Williams, 1972, 1974). *C. huxleyi* has a calcium saturation level for coccolith formation at 2×10^{-3} M (Paasche, 1964) for one strain and at 10^{-2} M for a different strain (Crenshaw, 1964) with no coccolith formation at 10^{-3} M. For *Hymenomonas* Williams (1972) demonstrated that 10^{-2} M calcium was optimal for growth and coccolithogenesis and that if the calcium concentration was increased (10^{-1} M) or decreased (10^{-4} M), the coccolith formation rate would be reduced. This work on *Hymenomonas* was verified by Blackwelder *et al.* (1976) except that no coccoliths were made at 10^{-4} M calcium. When strontium was added to these calcium inhibited cells, calcified coccoliths reappeared, and no strontium was present; the number of calcified cells increased with increased strontium concentration. This is in agreement with the results of Isenberg *et al.* (1963a) but in disagreement with Williams (1972) who showed an inhibitory effect on coccolithogenesis with strontium. An explanation for these discrepancies is not available. Additional supportive evidence of calcium's importance to coccolithogenesis comes from the work of Blankenship and Wilbur (1975) who showed that coccolith production was reduced in the presence of cobalt, a

calcium transport inhibitor. Also DDT will inhibit calcification of scales of C. huxleyi (Elder et al., 1972); however, the mechanism of DDT action on calcification is not known.

Magnesium had an unusual effect on coccolith formation (Blackwelder et al., 1976). In the absence of magnesium, coccoliths were made at a reduced rate, and calcite was the only form of calcium carbonate deposited but in low magnesium concentrations (10^{-4}-10^{-6} M) the coccoliths made contained 60% calcite and 40% aragonite. Excess quantities of magnesium (10^{-1} M) had no effect on coccolith production (Williams, 1972).

Calcium's partner in the calcite of coccoliths is the carbonate ion which presumably originates from CO_2. Numerous studies have been conducted with inhibitors of metabolism (Paasche, 1964) including inhibitors of carbonic anhydrase, an enzyme which catalyzes the interconversion of molecular CO_2 and carbonic acid (Crenshaw, 1964; Isenberg et al., 1963b; Williams, 1972), to determine how CO_2 is converted to CO_3^{-2} in $CaCO_3$. Paasche (1964) concluded that coccolith formation was dependent on photosynthesis. Coccolith formation was inhibited by hydrocyanic acid, an inhibitor of both photosynthesis and respiration, and 2,4-dinitrophenol, an uncoupler of oxidative phosphorylation, with coccolith formation being affected more than photosynthesis. A Hill reaction inhibitor (photolysis of H_2O and evolution of O_2) affected coccolith formation to a lesser extent. Paasche interprets this as evidence supporting a role for photosynthesis and respiration in coccolith formation. The carbonic anhydrase inhibitors had no effect on coccolith production for Crenshaw (1964) or Williams (1972), but coccolith production was completely inhibited for Isenberg et al. (1963b). Williams (1972) and Isenberg et al. (1963b) were working with Hymenomonas carterae

and the same inhibitor, sodium acetazolamide. Their differences may be the result of variations in experimental technique; however, we would tend to discount Isenberg's results on several grounds; certainly Williams' method of counting new coccoliths was more direct and accurate and was in agreement with the general conclusions reached by Crenshaw (1964) and Paasche (1968).

Structural studies It is now generally accepted that coccoliths are made intracellularly in the Golgi apparatus (Dorigan and Wilbur, 1973; Klaveness, 1976; Manton and Leedale, 1969; Manton and Peterfi, 1969; Outka and Williams, 1971; Pienaar, 1971b; Williams, 1972), a method also employed for uncalcified scale production in other haptophyceae (Brown, 1969; Brown et al., 1970, 1973; Manton, 1967a, 1967b, 1968), and other algae (Manton, 1966), and fungi (Darley et al., 1973). Such a method also shows certain homologies with the biosynthesis of higher plant cell walls (Chrispeels, 1976; Loewus, 1973; Pickett-Heaps, 1967, 1968).

A discussion of the intracellular formation of coccoliths requires some knowledge of coccolith structure itself. Detailed observations of coccoliths are restricted to electron microscopy because their minute size (approx. 0.25 to 1.5 μm) requires higher resolution for studying any coccolith substructure than can be attained with the light microscope. Three distinct morphological components of the coccolith can be seen with the electron microscope: (1) $CaCO_3$ which is present in all coccoliths (Paasche, 1968), (2) a subtending scale-like base (Brown and Romanovicz, 1976; Crenshaw, 1964; Klaveness, 1972, 1976; Leadbeater, 1970, 1971; Manton and Leedale, 1969; Manton and Peterfi, 1969; Outka and Williams, 1971; Paddock, 1968; Pienaar, 1969a, 1969b; Wilbur and Watabe, 1963; Williams,

1972), and (3) an organic sheath or matrix which encases the $CaCO_3$ (Crenshaw, 1964; Klaveness, 1972, 1976; Leadbeater, 1971; Manton and Leedale, 1969; Manton and Peterfi, 1969; Outka and Williams, 1971; Williams, 1972). In addition, the organic matrix has a characteristic morphology consisting of several elements which can form "H" configurations at juncture points (Pienaar, 1969a). Outka and Williams (1971) and Williams (1972) have shown two types of rim elements--A and B--with an anvil shape which alternate about the base periphery. The base of the coccolith has two morphologically discrete units--radials, numerous lines or spokes which radiate from the scale-like base, and concentrics, a microfibril whorl spun atop the base (Outka and Williams, 1971; Williams, 1972).

The developmental sequence of intracellular coccoliths has had a series of transformations since the original proposal of Golgi involvement in coccolith formation (Parke and Adams, 1960). Wilbur and Watabe (1963) first described intracellular calcification for C. huxleyi as occurring between the nucleus proximally and a "reticular" body distally with calcification proceeding from centers near the future base. They proposed that a matrix region predetermines the coccolith shape prior to calcification. Isenberg and Lavine (1973) and Isenberg et al. (1966) proposed a somewhat different theoretical pathway for mineralization in coccolithophorids. They hypothesized that the Golgi apparatus gives rise to a reticular (ww) body and a mineral reservoir which, in turn, gives rise to an intracellular coccolith precursor body (ICP) via intermediate fibrous elements. The ICP then forms a coccolith leaving behind some portion which can be either reincorporated into a new ICP or degenerated into a fat body. A similar proposal to this was made by Pienaar (1969b), but both proposals have since

been discredited on a morphological and developmental basis (Manton and Leedale, 1969; Outka and Williams, 1971; Williams, 1972) with the intermediate fibrous structures now identified as scales and on a cytochemical basis (Pienaar, 1971a), which identified lysosomal enzymes in the (ICP) bodies, thereby supporting a degradative function. Investigators in this field now have accepted the developmental sequence postulated by Outka and Williams (1971) with the possible exception of Isenberg and Lavine (1973) who continued to promote their ICP hypotheses (Isenberg et al., 1966) without publishing any additional scientific information.

The currently accepted hypothesis of coccolith formation proposes a more direct involvement of the Golgi apparatus in coccolith "synthesis" (Outka and Williams, 1971) with supportive evidence from Manton and Leedale (1969), Manton and Peterfi (1969), and Williams (1972). Manton and her co-workers concluded that calcification began as a marginal deposit on a preformed organic scale and hypothesized that coccolith morphology was determined by an organic matrix. Outka and Williams (1971) propose that the Golgi apparatus is responsible for the synthesis and assembly of coccoliths. The first stages involve synthesis and accumulation of electron dense bodies (coccolithosomes) in lateral earpockets of the Golgi cisternae and a simultaneous independent development of scale-like bases in the immature regions of the Golgi apparatus. Subsequently, the coccolithosomes are transferred to the base-containing vacuoles where they condense at the base periphery forming a sheath-like matrix. The Golgi membranes help mold the shape of the matrix. Calcification now proceeds from nucleation sites within the matrix material. The completed coccolith, still in a Golgi vesicle, is next channeled within a "microtubule basket" to the anterior

region of the cell where the Golgi membranes fuse with the plasma membrane and the coccoliths are deposited extracullularly.

Klaveness (1976) working with Emiliania huxleyi has found a similar scheme except that matrix formation occurs within the endoplasmic reticulum and without any coccolithosomes; this has been interpreted by Klaveness as reflecting a variation of the endomembrane system like that proposed by Morre and Mollenhauer (1974). Klaveness (1976) does not view the matrix as a vehicle for nucleation and directed crystal growth as do Outka and Williams (1971), but instead the matrix acts to suppress uncontrolled nucleation by acting as a filtering medium to permit homogeneous nucleation. Klaveness may be correct in proposing this function for the matrix; however, this is probably just an additional function for the matrix to perform without eliminating the other two proposed by Outka and Williams. In support of this statement are the findings of Luben et al. (1973), who have shown that specific nucleation sites for calcium phosphate deposition are present in the matrix of beef tendon collagen. Also Wolter and Tawashi (1977) have studied calcite growth using a gelatin "gel" medium and found that the organic matrix material, temperature, diffusion fluctuation, and additives exert a control over calcite structure; furthermore, nucleation appears to be determined by the nature of the gel substrate which provides limited sites for nucleation.

The transformation of Pleurochrysis stages into Hymenomonas stages (Brown and Romanovicz, 1976; Brown et al., 1970; Manton and Leedale, 1969) and vice versa provides homology between coccoliths and noncalcified scales of other haptophycean algae (Brown, 1969; Brown and Romanovicz, 1976; Brown et al., 1970, 1973; Manton, 1966, 1967a, 1967b; Pienaar, 1969b; Romanovicz

and Brown, 1976) and becomes pertinent to a further understanding of coccolith formation. If one also assumes a structural homology between the coccolith and nonmineralized haptophycean scales, a developmental process for coccolith base formation can be inserted into the coccolith formation picture. Brown and his co-workers (Brown and Romanovicz, 1976; Brown et al., 1970, 1973) have pieced together an elaborate developmental scheme for scale formation in Pleurochrysis scherffelii from morphological and cytochemical investigations. In scale biogenesis, enzymes for scale synthesis and precursors for radial formation are made in the endoplasmic reticulum and immature face of the Golgi; radial microfibrils are crystallized from the precursors in close association with cisternal membranes. The membranes assume a folded configuration having a "Z" shape (Z-stage) which unfolds bringing about a quadrilateral arrangement of radial microfibrils. At the same time that the radials were being formed in central dialations of the Golgi cisternae, glucose was being converted to cellulose. At some point after unfolding, feeding tubules begin to add cellulose microfibrils (the aforementioned concentrics) to the top of the radial microfibrils which are being sulfated. As the Golgi cisternae with the scales move distally, amorphous pectin-like subcomponents are added. (For coccolith formation, the coccolithosomes would now begin to condense to form rim elements.) The Golgi membranes migrate to the plasmalemma where the two fuse. New scales are added to the wall by exocytosis. Colchicine will inhibit the deposition of both coccoliths (Williams, 1972) and scales (Brown et al., 1973).

Coccoliths are components of the cell wall of Hymenomonas and other coccolithophorids, but present in the wall are several other morphological

units which need to be described. The cell wall consists of fibrils projecting from the plasma membrane known as columnar material which may be involved with holding the wall together (Manton and Leedale, 1969), a layer of scales which are embedded in an amorphous electron transport material for Pleurochrysis stages and an additional outer covering of exposed coccoliths for Hymenomonas stages (Manton and Leedale, 1969; Outka and Williams, 1971; Williams, 1972). The coccolith bases are presumed to be chemically and structurally similar except that the coccolith base is thicker, has sites for matrix deposition, and has calcified rim elements attached. In addition the haptophyceae have smaller elliptical scales that are found associated with the haptonema (Manton, 1968; Outka and Williams, 1971; Williams, 1972). In the biosynthesis of the scales of Pleurochrysis there is a rotation of the protoplast while the wall remains stationary; this allows an even distribution of scales around the cell. Brown and Romanovicz (1976) reported a similar protoplast rotation during coccolith formation with the Hymenomonas stage transformed from a Pleurochrysis stage. However, Williams (1972, 1974) found no protoplast rotation in Hymenomonas carterae and expressed his doubt that such an event could occur because of the haptonema and flagella connections to the cytoplasm. Protoplast rotation will be considered further in the discussion section of this report.

Coccolith and scale chemistry

The chemistry of coccoliths and scales will be considered together since they probably contain some homologous molecules (Kuratana, 1974). The chemical nature of haptophycean scales has received little attention

with work restricted to Chrysochromulina chiton (Green and Jennings, 1967), Pleurochrysis scherffelii (Brown and Romanovicz, 1976; Brown et al., 1970, 1973; Herth et al., 1972, 1975; Romanovicz and Brown, 1976), Coccolithus huxleyi (Westbroek et al., 1973), and Hymenomonas carterae (Isenberg and Lavine, 1973; Isenberg et al., 1966; Kuratana, 1974). Two sugars which are shared by these scales are galactose and ribose (Brown et al., 1970; Green and Jennings, 1967; Kuratana, 1974); the presence of ribose as a structural unit is somewhat surprising since the only other reported location of ribose is in the formation of nucleic acid molecules (White et al., 1968), and its role in the scales and coccoliths is unknown.

A nondialyzable fraction (F_1) from isolated coccoliths of Hymenomonas was reported which contained a glycoprotein (5% protein) with a hydroxyproline-rich peptide and several carbohydrate moities (glucose, hexuronic acid, methyl pentose, and no amino sugars) (Isenberg and Lavine, 1973; Isenberg et al., 1966). The F_1 fraction was a single unit with an estimated molecular weight of 40,000-50,000 daltons and 25% of the amino acids were dicarboxylic acids. Whole coccoliths only had trace amounts of hydroxyproline. In a similar study by Kuratana (1974), no hydroxyproline was found in a corresponding F_1 fraction, and the molecular weight of the principal globular unit was only 8,000 daltons, based on sedimentation data. The hydroxyproline found in Isenberg's F_1 fraction probably is contamination from other wall material because cell walls are known to contain hydroxyproline-rich glycoproteins (Lamport, 1970), and, in a personal communication, Lamport has found hydroxyproline in whole walls of Pleurochrysis.

Decalcified coccoliths of Hymenomonas were 12% protein and 70% carbohydrate with organic matter comprising 40-50% of the whole coccoliths (Kuratana, 1974). Using gas chromotography, Kuratana's isolated coccoliths and their fractions maintained a constant relative amount of carbohydrate monomers with glucose the predominant sugar followed by nearly equal amounts of galactose, mannose, and arabinose and trace amounts of xylose, fucose, and rhamnose. Neither the relative amounts nor the carbohydrate moieties themselves varied significantly among the whole coccoliths, bases, and matrix material.

In C. huxleyi Westbroek et al. (1973) treated lyophilized cells sequentially with chloroform-methanol, SDS and pronase, the oxidizing agents NaOCl and $KMnO_4$, EDTA, and finally separated a soluble intracrystalline fraction (SIF) on Sephadex G-50. Colorimetric tests indicated that SIF contained 26% uronic acid, some methyl pentose, and no amino sugars. SIF was polyanionic since it preceded bromophenol blue on polyacrylamide gels. SIF was apparently protected from these harsh treatments by the calcite because isolated SIF was readily degraded with the same chemicals used for isolation. It has been suggested that SIF is trapped inside the rim elements during the calcification process (Klaveness, 1976). Also SIF may be dissimilar to the F_1 fraction of Isenberg et al. (1966) and the matrix material obtained by Kuratana (1974) because no amino acids were found in SIF; however, it seems reasonable that the isolation procedure could cleave a peptide chain from the molecule.

The scales of Pleurochrysis scherffelii have been studied the most extensively of any of the haptophycean scales with regard to their chemical composition and molecular components. Whole scales were comprised of 3-9%

protein, and the carbohydrate content was primarily galactose and ribose with traces of arabinose and glucose (Brown et al., 1970). A scale fraction was isolated and contained predominantly glucose; this fraction was identified as cellulose and was assigned morphologically to the concentric whorls atop the scale. The authors postulated that cellulose was biosynthesized in the Golgi apparatus. Brown's postulate received the criticism that this fraction was not cellulose, and even if it was, it could not be synthesized in the Golgi (Preston, 1974). In two papers (Brown and Romanovicz, 1976; Brown et al., 1973), Brown and his co-workers showed that concentrics are laid down in the Golgi apparatus. The proof that they had cellulose came from a series of studies (Herth et al., 1972, 1975) on isolated concentric microfibrils with electron and x-ray diffraction data and a latest paper (Romanovicz and Brown, 1976) in which comparisons were made of sizes, x-ray diffraction patterns, and infrared absorption spectra between isolated concentrics and cotton cellulose; all of this accumulated data confirms that cotton cellulose and scale concentrics are identical. X-ray diffraction patterns of isolated coccoliths reveal a cellulose II structure (Kuratana, 1974).

During the struggle to convince everyone of cellulose's presence in Pleurochrysis, Brown and his associates experimented further with the scale and wall structure. The scale concentric microfibrils were not just cellulose but were 2:1 cellulose to protein (Brown et al., 1973) with protein covalently linked to the cellulose; amino acids from this protein contained 38% hydroxyl groups and 25% carboxyl groups. The radial spokes were thought to be pectin, but no uronic acids have been identified chemically (Romanovicz and Brown, 1976); the pectin staining characteristics were

presumably caused from dicarboxylic acid groups of amino acids in short polypeptides. From a more detailed extraction with trifluoracetic acid (Romanovicz and Brown, 1976), the scale was divided into four subcomponents: (1) an amorphous polysaccharide which was 6% protein and 94% carbohydrate with galactose, glucose, and fucose as the principal sugars; (2) radial microfibrils were 7% protein and 93% carbohydrate with galactose, arabinose, and fucose predominating; (3) a spiral microfibril coating containing 9% protein with hydroxyproline the dominant amino acid and 91% carbohydrate with the principal sugars being galactose, glucose, and mannose; and (4) spiral microfibrils of 37% protein and 63% carbohydrate with glucose only present. Alcian blue staining indicated that the scales had sulfate groups which were thought to be responsible for binding cationized ferritin. Douglas et al. (1967) also used Alcian blue staining, presumably specific for sulfated molecules under their conditions; they found Alcian blue positive staining of wall material but not the coccolith, thus suggesting some chemical dissimilarity between scales and coccoliths.

The Cell Walls of Other Organisms

Bacteria

Hymenomonas and the other coccolithophorids are eukaryotic cells possessing a "true" double membrane-bounded nucleus with membranous or organelles, etc., and, as such, their organization should relate most closely to that of other eukaryotic cells including higher plants and more distantly to prokaryotes. Nevertheless, an extremely brief description of prokaryotic cell walls seems appropriate to see if there are any common

features including especially methods of assembly. The basic molecular units of bacterial cell walls are peptidoglycans with some attached lipopolysaccharides and lipoproteins in Gram-negative bacteria (Baddiley, 1975; Drews, 1974) and covalently linked teichoic acids and/or techuronic acid in Gram-positive bacteria (Drews, 1974; Ivatt and Gilvag, 1977). The synthesis and addition of sugars involve nucleoside diphosphates, and their transport across the membranes is aided by a lipid carrier (Baddiley, 1975; Drews, 1974); the synthesis of peptides generally occurs extracellularly and the one amino acid strikingly absent from bacterial cell walls is hydroxyproline (Bricas, 1973). (For a discussion of hydroxyproline in eukaryotic cell walls see Lamport (1970).) The growth of Gram-negative cell walls occurs in a single, equatorial plane, while Gram-positive cell walls elongate all along the lateral wall from the random insertion of peptidoglycan (Glaser, 1973). One of the very few demonstrated examples of cellulose in prokaryotic cell walls is in Acetobacter xylinium, and in contrast to eukaryotic cells that require membranes for cellulose biosynthesis (Westafer and Brown, 1976; Mueller et al., 1976; Preston, 1974), the biosynthesis of cellulose appears to occur without any direct plasma membrane involvement (Brown et al., 1976). Although the final assembly of most bacterial cell walls appears to be closely coupled with the activity of special exoenzymes (Drews, 1974; Glaser, 1973), at least in one case, that of the wall of Acinetobacter, there is a layer of protein subunits which self-assemble and form ionic associations with the outer wall membrane (Thorne et al., 1975); this system will be discussed in greater detail in the Discussion section. More information concerning bacterial cell walls is

available from recent reviews by Baddiley (1975), Bricas (1973), Drews (1974), and Glaser (1973).

Fungi and yeasts

Most of the work on fungal and yeast cell walls has been restricted to biochemical analyses with some supportive light microscopy; only a small number of investigations has attempted to study cell wall structure or follow cell wall formation with the electron microscope. The cell walls of fungi and yeasts are composed of two major polysaccharides with predominantly chitin-glycan in fungi and glucan-mannan in yeasts (Gander, 1974), and they apparently lack cellulose. Their cell walls are unlike the bacterial cell wall in that there is no evidence for muramic acid-containing peptidoglycan, teichoic acid, or lipopolysaccharides (Gander, 1974); however, hydroxyproline is present in the walls (Taylor and Cameron, 1973). The synthesis of new wall from protoplasts of fungi involves first chitin and an S-glucan (α-1,3 glucan) synthesis followed by a cytochemically positive R-glucan (β-1,3-β-1,6 glucan); no wall primer was required for wall synthesis (Van der Valk and Wessels, 1976). In vitro synthesis of chitin has been reported; it apparently requires the presence of a special granular structure called a chitosome which has been isolated (Bracker et al., 1976). Electron microscopy of fungal and yeast cell walls has been limited because fixation procedures have not been satisfactorily developed (Cabib, 1975); however, they have been good enough to identify membranous vesicles in the cell walls which were originally referred to as lomosomes by Moore and McAlear (1961). Lomosomes will be described in the Discussion section. Also, the Golgi apparatus is involved in polysaccharide synthesis

(Van der Valk and Wessels, 1976), and in one fungal species, galactose-containing scales were manufactured in the Golgi (Darley et al., 1973). During glycoprotein synthesis, nucleotide diphosphates are used as glycosyl donors, and dolichol phosphates are used as glycosyl carriers (Gander, 1974). Some current reviews of yeast and fungal cell-walls are Brody (1973), Cabib (1975), Gander (1974), and Taylor and Cameron (1973).

Algae other than coccolithophorids

Research on algal cell walls has centered on cellulose biosynthesis in some green algae, the chemistry of noncellulosic polysaccharides in brown and red algae, and some concentrated studies on wall proteins and assembly processes in Chlamydomonas, a green alga lacking cellulose. A wide variety of carbohydrate monomers occurs in algal polysaccharides, with glucose, galactose, xylose, rhamnose, fucose, arabinose, and mannose being common as homopolymers or heteropolymers; uronic acid and sulfate groups are prevalent but amino sugars are absent (Haug, 1974). Matrix polysaccharides are those which are extracted with hot water or alkali and generally are polyanionic; fibrillar material remains insoluble under these conditions and is composed of cellulose, β-1,3 linked xylan or β-1,4 linked mannan with some heteropolymers (Haug, 1974). A hydroxyproline-rich glycoprotein component has been found in Chlamydomonas where the hydroxyproline is linked glycosidically to galactose (Miller et al., 1972) instead of the arabinoside linkage of most plants (Lamport, 1969, 1970, 1973; Miller et al., 1974). Haug (1974) and Preston (1974) have reviewed algal cell walls, and Evans and Callow (1976) have reviewed walls of brown and red algae.

The red and brown algal polysaccharides and their gel properties have been studied extensively (Evans and Callow, 1976; Haug, 1974) and suggest similarities with the cell wall study reported here. The alginate of brown algae is composed of D-mannuronic acid and L-guluronic with varying proportions of each from 1:3 to 3:1; it exists as a mixed salt with calcium, magnesium, and sodium; calcium alginate is insoluble and sodium alginate is soluble (Haug, 1974). Guluronic acid has a higher affinity for calcium than magnesium while mannuronic acid has about the same affinity for both. Experiments have shown that the calcium ions are selectively bound in long sequences between the polyguluronate chain in the gel (Haug, 1974). The carrageenans (β-1,3 and α-1,4 linked galactose units) of red algae, which are the source of agar, will gel in monovalent cations like potassium, rubidium, cesium, and ammonium with some affinity for sodium or lithium while divalent cations have no effect on gel strength. For purposes of comparison, the walls of Nitella, a green alga, will soften in the presence of magnesium and harden the greatest with aluminum and some with calcium (Métraux and Tais, 1977).

In the green algae, cellulose biosynthesis occurs on the outer surface of the plasma membrane (Brown and Montezinos, 1976; Preston, 1974). For Oocystis, Preston (1974) has proposed that granule bands on the plasma membrane are responsible for cellulose biosynthesis, but Brown and Montezinos (1976) have shown a linear enzyme complex which they propose is responsible for cellulose-biosynthesis. They too observed the granules and, in addition, some associated ridges which together function to orient the cellulose microfibrils. A self-assembly proposal for cellulose microfibril orientation comes from studies of Chara vulgaris by Neville et al. (1976).

Using a tilting stage in an electron microscope, they discovered that all fibers in one layer are parallel and that the different angles between layers are so varied that membrane granules could not explain these numerous orientations. The self-assembly model is not substantiated by studies of colchicine-inhibited wall biosynthesis in Oocystis (Grimm et al., 1976); in this instance, cellulose continues to be synthesized in the presence of colchicine, but the microfibril orientation is random and remains that way even when the colchicine is removed. A similar result was obtained with lettuce hypocotyl cells (Srivastava et al., 1977). These results implicate an involvement of microtubules in cellulose orientation as suggested by Palevitz and Hepler (1976); however, it is not known if this disorientation of microfibrils by colchicine is a result of redistributing the granular bands and associated ridges (Brown and Montezinos, 1976) or whether the reduced number of microtubules while the cells are in colchicine might act to prevent the flow and subsequent release of some other factors related to microfibril orientation (Packard and Stack, 1976).

The self-assembly of a cell wall glycoprotein has been reported in Chlamydomonas (Hills, 1973) and should be elaborated here. The cell wall of Chlamydomonas reinhardii has seven layers with a central layer consisting of an elaborate crystal lattice (Roberts and Hills, 1976). This lattice is a glycoprotein with a high hydroxyproline content (Roberts et al., 1972), and its assembly depends on a heritable factor (Davies and Lyall, 1973). In an extension of this study, Roberts (1974) tested other species of Chlamydomonas and found the same, conserved glycoprotein; expanding their coverage to include different members of the class Chlaymdomonaceae, two major glycoproteins have been found (Roberts and Hills, 1976). Cell

walls dissociated by lithium chloride reassembled upon dialysis against water; a nucleation site on the inner wall was required for reassembly (Hills, 1973). The self-assembly was not dependent on ions and continues to occur at a pH range of 4.5 to 8.5 (Hills et al., 1975). The self-assembly glycoprotein has a molecular weight of 298,000 d. and is 35% protein with arabinose, galactose, and high levels of hydroxyproline (Catt et al., 1976). The implications and importance of self-assembly to cell wall construction cannot be fully determined until other cell wall systems are investigated for the presence of this phenomenon.

Higher plants

In this section a brief description of polysaccharide synthesis with emphasis on cellulose biosynthesis, the role of protoplasts in cell wall investigations, and some cell wall models will be presented. More information is available in reviews on cell wall structure and chemistry (Albersheim, 1975, 1976; Bateman and Basham, 1976; Cook and Stoddart, 1973; Franke et al., 1974; Lamport, 1970; Northcote, 1972; Preston, 1974; Rayle and Zenk, 1973; Roland, 1973) and on cell wall biosynthesis (Chrispeels, 1976, Cocking, 1972; Cook and Stoddart, 1973; Franke et al., 1974; Karr, 1976; Loewus, 1973; Preston, 1974; O'Brien, 1972; Willison, 1976).

From ultrastructural studies, Whaley and Mollenhauer (1963) were among the first to demonstrate that the Golgi apparatus was involved in cell plate formation in dividing plant cells. Biochemical support for this claim came from autoradiographic studies (Pickett-Heaps, 1967, 1968) which showed UDP-glucose incorporation in the Golgi. The synthesis of cell wall polysaccharides probably involves nucleotide diphosphates as direct

glycosyl donors although clear *in vitro* experiments demonstrating this in plants is not available (Karr, 1976). There appears to be a pattern emerging for the use of lipid carriers or intermediates like dolichol phosphates (see Waechter and Lennarz (1976) for a review of dolichol phosphates). Although such carriers have not been isolated from higher plant cells, they are a definite possibility (Karr, 1976); the lipid carriers are well-known for bacterial systems (Baddiley, 1975) and glycoprotein synthesis in animal cells (Montreuil, 1975). In general, synthesis of cell walls occurs in two stages: (1) primary cell wall growth consisting of pectin and hemicellulose secretion and (2) secondary wall thickening when, primarily, cellulose is synthesized along with some hemicellulose but not pectin (Dalessandro and Northcote, 1977). In cotton cells, the Golgi apparatus is directly involved in the secretion of primary cell wall components, but during secondary wall growth, the endoplasmic reticulum assumes a major role (Westafer and Brown, 1976). However, in numerous other cell types, cellulose synthesizing enzymes have been found in the Golgi apparatus (Helsper *et al.*, 1977; Kiermayer and Dobberstein, 1973; Roland and Pilet, 1974; Van Der Woude *et al.*, 1974), and, in one reported case, an x-ray diffraction pattern identified as cellulose was obtained from within the Golgi apparatus (Engels, 1974). These examples represent some of the heterogeneity that exists within the endomembrane systems of plants and animals (Morre and Mollenhauer, 1974), and just because enzymes are present in these Golgi fractions does not mean that they are active there; most examples of cellulose biosynthesis still show that synthesis is at the plasma membrane level (Brown and Montezinos, 1976; Mueller *et al.*, 1976; Preston, 1974).

The employment of protoplasts to study cell wall formation has progressed rapidly since Cocking (1972) predicted a marked increase in their usage. Some selected examples of cell wall formation studies which have combined electron microscopy and protoplasts are presented here. The cell surfaces of protoplasts actively synthesizing new wall material have numerous projections or protrusions with closely associated microfibrils (Burgess and Fleming, 1974; Burgess and Linstead, 1977; Williamson et al., 1977; Willison and Cocking, 1975); these protrusions resemble the globular complexes found in freeze etch preparations of corn roots which have been postulated as cellulose synthesizing centers (Mueller et al., 1976). In these studies, the growth of microfibrils was inhibited with coumarin, but the wall projections were still present. According to Hara et al. (1973), coumarin is the only reported inhibitor of cell wall biosynthesis, and it may inhibit cellulose biosynthesis. The time required to synthesize the microfibrils apparently varies with the cell type because, for tobacco mesophyll protoplast microfibrils, it required 24 hours before microfibrils were visible (Willison and Cocking, 1975); in the case of Vicia hajastona protoplasts, microfibrils were observed in 10-25 minutes (Williamson et al., 1977). A weakly-acidic, pectin-like material was obtained from the culture medium of growing protoplasts (Hanke and Northcote, 1974); this has been used as support of the hypothesis that pectins secreted during cell plate formation are more acidic than pectins made during extension growth. The cementing role of xylans has been demonstrated when an endoxylanase was added to cells in primary cell wall growth (Ruel et al., 1977); xylan distribution was uneven in a given wall, and fibrillar elements were released during this xylan lysis. A final example of investigations using

protoplasts is the demonstration of membrane mobility in plants; using concanavalin A (Con A), which binds to glucose or mannose units, and soybean protoplasts, Williamson et al. (1976) found Con A to occur in clusters which got tighter as cellulose was synthesized; whereas, if these cells were first fixed for electron microscopy, Con A was evenly distributed over the cell surface. Such studies of protoplasts are contributing to an understanding of plant cell walls, but much more work is needed to determine the function of the structures being reported on protoplast surfaces.

The exact structure of any one plant cell wall still remains unknown, but the most well-developed model comes from the study of sycamore cells grown in suspension cultures (Keegstra et al., 1973), which has been applied as a model to explain cell walls in general. It was developed and presented in a series of three papers by Albersheim and his co-workers (Bauer et al., 1973; Keegstra et al., 1973; Talmadge et al., 1973) and has reappeared in later publications (Albersheim, 1975, 1976; Bateman and Basham, 1976). In the Albersheim model, there is H-bonding of a xyloglucan to cellulose and covalent bonding of the xyloglucan to a single arabinogalactan; the arabinogalactan is linked covalently to a single rhamnogalacturonan, and the single rhamnogalacturonan is linked covalently to several arabinogalactans. This is linked covalently to a glycoprotein, extensin, and the structure works backwards from the extensin to another cellulose microfibril. In this model, covalent bonding predominates. In order for wall growth or extension to occur, an enzyme must cleave a bond, shift over one fiber, and then join the new wall component to the old wall. No such enzyme has been isolated. The model has been subjected to recent criticism for not being flexible enough to allow cell wall extension.

Monro *et al*. (1976) has proposed another model having fewer covalent bonds and substituting ionic bonds between the pectins, hemicellulose, and glycoprotein and allowing a more direct interaction between glycoprotein and cellulose. Both of these models are based on biochemical data accumulated by employing numerous more or less specific enzymes to cleave specific linkage groups with the products of the enzymatic digestions being analyzed. A self-assembly mechanism has been introduced, from ultrastructural studies, to help explain the addition of hemicellulose (Roland *et al*., 1975, 1977). These investigators found that the staining pattern of intact walls and precipitated hemicellulose were identical. *In vivo* additions of wall material show a gradual transition from unordered to ordered fibrils with increasing distance from the cell membrane; presumably the latter acts as a suitable interface for polysaccharide condensation.

The cell walls of plants are poorly understood in regard to their chemical structure, molecular arrangements, biosynthesis, and assembly. However, a great deal of renewed interest in plant cell walls has been stimulated by the possibility of cell fusion studies and their potential for genetic engineering; adding to this interest is an ongoing excitement about self-assembly systems. Together, these two areas of genetic engineering and self-assembly have measurably heightened research on plant cell walls.

MATERIALS AND METHODS

General Procedures

Standard culture conditions

Hymenomonas (*Syracosphaera*, *Cricosphaera*) *carterae* Plymouth Culture Collection No. 181 was maintained on an artificial sea water medium which was based on that of Isenberg *et al.* (1963a) and modified by Williams (1972, 1974) and will be referred to as PMW_{II}. The cells were grown in 500 ml stainless steel-capped Delong flasks containing 100-150 ml of PMW_{II} at pH 7.7-7.9. They were incubated at 17-19°C in a Precision Scientific controlled-temperature incubator with a light intensity of about 4450 lux from 14-watt cool-white fluorescent tubes on a repeating cycle of 16 hours light and 8 hours dark. Transfers were made on a 48-hour schedule with inoculation occurring between the second and fourth hour of the light period. Inocula resulted in initial cell densities of 5×10^4 to 1×10^5 organisms/ml and in maximum cell densities of 1.5×10^5 to 3×10^5 organisms/ml after two days of growth,[1] which enabled experiments to be carried out with midlog phase cells. Growth determinations for all experiments were completed in triplicate using direct cell counts on an A. O. Spencer haemocytometer chamber. Aliquots were taken and counted either live or fixed in Gram's iodine (Pearse, 1968).

---

[1] Growth is defined as the increase in cell number per unit volume of culture medium.

Microscopic procedures

P_1 experimental and control cells were examined and photographed with a Zeiss photomicroscope in the fluorescent, phase contrast, dark field, or Nomarski differential interference contrast mode. A Hitachi HU-11E-1 was used to make transmission electron microscope observations and a JSM 35 was utilized to make scanning electron microscope observations.

Thin sectioned material was fixed in glutaraldehyde at 4°C, postfixed in osmium tetroxide at 4°C, washed in distilled water at room temperature, decalcified with ethanolic uranyl acetate, dehydrated in a graded acetone series, and embedded in Spurr's ERL, mixture E (Spurr, 1969). When cells were not decalcified, the uranyl acetate step was eliminated and 0.01 M $CaCl_2$ was added to all solutions through 95% acetone. The sections were cut on an LKB Ultratome I or a Reichert OM U2 with a DuPont diamond knife. The sections were stained sequentially with uranyl acetate and lead citrate according to Venable and Coggeshall (1965) or Reynolds (1963).

The Biology of Hymenomonas

General morphological procedures

The preservation of the cell surface of Hymenomonas was studied with the scanning electron microscope following three drying techniques: air-drying, freeze drying, and critical point drying. For air drying, fixed, dehydrated cells were placed in partially opened Petri dishes overnight at room temperature. Unfixed cells for freeze drying were placed in aluminum foil molds, cooled to liquid nitrogen temperatures, and dried in an Edwards EF_2 freeze dryer (Edwards High Vacuum, Inc., Grand Island, N.Y.) for 48 hours. The critical point drying process followed the guidelines

established by Cohen (1974), which involved fixation of the cells as for transmission electron microscopy, dehydration in alcohol, gradual replacement of the alcohol with Freon TF and exchanging Freon TF with CO_2, and finally "drying" at the critical point of CO_2, namely, a critical pressure of 72 atmospheres and a critical temperature of 36.5°C. After drying, all specimens were placed on brass disks which contained a moist overcoat of silver conducting paint. The disks were transferred to a Varian VE-30M vacuum evaporator for a coating of carbon and gold during rotation. The specimens were removed and stored in a desiccator until examination with the JSM 35 scanning electron microscope.

Responses to diverse culture environments

The growth of Hymenomonas as related to the surface area of the culture was investigated. Five hundred ml Delong flasks, containing in each set 100, 200, 300, 400, and 500 ml of PMW_{II}, which yielded surface to volume ratios of 62.3, 27.3, 14.7, 9.1, and 2.1 cm^2/ml, respectively, were given the same size inoculation and allowed to grow at 17-19°C under 4450 lux illumination with a light-dark cycle. Samples were taken daily to follow growth effects.

In order to obtain sufficient yields for cell fractionation and wall analysis, growth of cells in large batch cultures was necessary. This was carried out in five gallon carboys containing 15 liters of PMW_{II} at 18-20°C under a bank of 8-40 watt, cool white fluorescent tubes providing a light intensity of 2700-5400 lux from the bottom to the top of the carboy. The effect of forced air on growth in the carboys was studied by comparing growth in a carboy plugged with cotton, a carboy plugged with a rubber

stopper assembly, but no forced air, and a rubber stopped carboy with forced air supplied from an aquarium pump. The forced air carboy assembly was as follows: air was pumped thru rubber tubing to a sterilized cotton air filter attached to a 500 ml flask containing 300 ml of sterile water (to prevent evaporation from forcing dry air thru the medium); from the water, the air passed into the carboy and thence to rubber tubing that extended to the bottom of the carboy; after passing thru the medium, the air left the carboy thru an outlet to a 125 ml flask equipped with a glass tube to the bottom of the flask (this last was for moisture to collect in the flask and not in the cotton plug at the flask outlet). The flask outlet consisted of a bent piece of glass tubing resting inside a cotton plugged vial. The carboy of medium, the forced air assembly from the sterilized cotton air filter to the outlet flask, and the water were sterilized separately and then assembled aseptically as a unit. (If the water was not sterilized separately, it would back up into the tubing and dampen the cotton air filter.) The aquarium pump was capable of pumping air to four carboys at once. The carboy with no forced air had only rubber tubing hanging down from the air inlet and outlet ports and nothing extending into the medium. Inoculation of carboys was made aseptically from a single carboy by the gravity displacement of 3 l of medium plus cells into 12 l of fresh medium.

The Kinetics of Wall Formation

Pattern of coccolithogenesis after treatment of cells with EDTA

Standardization of EDTA treatment Midlog phase cells were spun out and resuspended in a volume of 5 mM Na_2 EDTA (disodium ethylenedinitrilo

tetraacetate) at pH 5.5 equal to one-half the volume of the original growth medium for twenty minutes at room temperature in the light. The EDTA solution was filter-sterilized and added aseptically. After the treatment, the cells were washed 3 times with PMW_{II}. PMW_{II} equal to one-half of the original PMW_{II} volume was added to the cells, which were then incubated at 17-19°C in the light at an intensity of 4450 lux in metal-capped or Kaput-capped Delong flasks. Samples were removed at specified times, and the number of coccoliths per cell was counted for 50 cells, either live or fixed in the "standard" glutaraldehyde solution, using Nomarski differential interference contrast (Williams, 1972, 1974). Unless otherwise stated, these were the standard conditions for EDTA treatment.

Concentration effects (EDTA) Cells were treated with EDTA solutions in concentrations of 1 mM, 5mM, 10 mM, 50 mM, 100 mM, or 500 mM (saturated solution). Cells were incubated for 4 hours in 16 ml of PMW_{II} in 50 ml Kaput-capped Delong flasks.

Time effects Cells were extracted with EDTA for the following lengths of time: 20, 40, 60, 90, and 120 minutes. The cells recovered for 4 hours in 8 ml of PMW_{II} contained in 50 ml Kaput-capped Delong flasks.

Morphology of regeneration Samples of the EDTA treatment and various stages of recovery were preserved for observation with the transmission and scanning electron microscope.

Pattern of coccolithogenesis after treatment of the cells with pronase

Standardization of pronase treatment Midlog phase cells were centrifuged from their growth medium during the twelfth to fourteenth hour of the light period, placed in 2-4 mg/ml of pronase, B grade (Calbiochem,

San Diego, Calif.), and dissolved in PMW_{II}, which was filter sterilized. The flask was placed in the dark at room temperature for 12-13 hours. Then the cells were washed three times in PMW_{II} and returned to PMW_{II} for incubation in the 17-19°C incubator with a light intensity of 4450 lux in metal-capped, 500 ml Delong flasks or gauze-covered 2800 ml Fernbach flasks. The volume of all incubation media equaled one-half the original PMW_{II} volume and was done to prevent unusually high cell densities. Samples were removed at specified times, and the coccoliths on 50 cells were counted as for the EDTA treated cells. Unless otherwise stated, these were the standard conditions for pronase treatment.

Concentration effects Cells were treated with a pronase solution at a concentration of 1 mg/ml, 2 mg/ml, 4 mg/ml, or 10 mg/ml. The number of coccoliths per cell were counted at the end of the treatment and after five hours of recovery in the light.

Time effects Midlog phase cells were concentrated by centrifugation, resuspended in two different media--PMW_{II} and PMW_{II} plus 2 mg/ml pronase and placed in the dark at room temperature. Samples from both were taken after 0, 3, 6, 9, 12, and 15 hrs in the dark and washed 3 times in PMW_{II}. The cells were dispersed in fresh PMW_{II} and the coccoliths of 50 cells without recovery in the light were counted and so were the coccoliths of 50 cells with 4 hours recovery in the light. A second sample of each culture was taken after 0, 3, 6, 9, 12, and 15 hrs in the dark and washed 3 times in PMW_{II}. These second samples were treated for twenty minutes in Na_2 EDTA and washed 3 times in PMW_{II}. After resuspending the cells in fresh PMW_{II}, the cells were placed in the 17-19°C incubator for 4 hours. The coccoliths on fifty cells were counted for each sample at each time.

Coccolith production following pronase and EDTA treatment Cells were enzymatically digested with 4 mg/ml pronase for 13 hours, washed 3 times, and incubated in the light. Samples of recovering cells were taken at 0, 6, 11, 24, 33, and 49 hrs. The cells were treated with EDTA for 20 minutes, washed 3 times, and incubated for 4 hours in the light. The coccoliths on 50 cells were counted for each sample.

Morphology of regeneration Samples of the pronase treatment and various stages of recovery were taken and observed with the transmission and scanning electron microscope.

The Chemistry of the Cell Wall

Disassembly and reassembly of the wall

Fractionation Different homogenizations were compared to optimize the fractionation procedure. A small glass hand homogenizer (Kontes Glass Co., Vineland, N.J.), a Teflon-glass homogenizer (A. H. Thomas Co., Philadelphia, Pa.), a French Press (American Instrument Co., Inc., Silver Spring, Md.), and a Servall Omni-Mixer (Ivan Sorvall, Inc., Norwalk, Conn.) attached to an Adjust-A-volt (Standard Elect. Product Co., Dayton, Ohio) for variable speed adjustments were employed to disrupt the cells.

Two different homogenization media were devised for homogenization depending on the fraction desired. The first will be referred to as Morre's homogenization medium (MHM) because of its similarity to the rat liver homogenization used by Morre et al. (1969). Morre's homogenization medium consisted of 37.5 mM Tris-Maleate buffer, pH 7.5-7.8, 250 mM sucrose, 5 mM $MgCl_2$, 10 mM $CaCl_2$, 1% dextran--Lot number D-5126 234,000 Daltons (Sigma Chemical Company, St. Louis, Mo.), and 5 mM mercaptoethanol

(Sigma Chemical Company, St. Louis, Mo.). The variation on Morre's rat liver homogenization was the addition of $CaCl_2$ to prevent coccolith decalcification. The second homogenization medium, PMW_{III}, contained 37.5 mM Tris-Maleate buffer, pH 7.9, 340 mM NaCl, 8 mM KCl, 5 mM $MgCl_2$, 10 mM $CaCl_2$ and 5 mM mercaptoethanol.

The standard homogenization procedure utilized cells from five gallon carboys. The cells were harvested at cell densities of 150,000 to 300,000 cells per ml on a Sharples Super centrifuge (The Sharples Corporation, Philadelphia, Pa.) through a continuous flow rotor at 22,000 rpm (14,000 g) at 4°C. The cells were homogenized immediately or frozen to liquid nitrogen temperatures and stored at -20°C. For cell organelle preparations, live cells were suspended in 100 ml of MHM, homogenized for 10 minutes at 90 volts using the large blade and standard cup of the Servall Omni-Mixer. For cell wall studies, fresh or frozen cells were suspended in 100 ml of PMW_{III} and homogenized for 15 minutes at 110 volts of the Servall Omni-Mixer.

Dissociation Chaotropic agents were successfully used for cell wall dissociation in Chlamydomonas (Hills, 1973) and were tested on Hymenomonas. Live cells or cell walls from homogenized cells (either live or frozen) were treated with 10 M lithium chloride (LiCl) or 6 M sodium perchlorate ($NaClO_4$-H_2O) which was buffered in 37.5 mM tris/maleate at pH 6.8. A suspension from 0.2 to 0.5 ml of wet pellet was made in 10 ml of 10 M LiCl or 6 $NaClO_4$-H_2O for 2-48 hours at room temperature. The effects of the treatments were observed with the light and electron microscope.

For electron microscopy, cell walls from cells homogenized in MHM buffer were suspended in 10 M LiCl or 6 M $NaClO_4$-H_2O and one drop of

suspension was placed on 200 mesh, collodion-coated, copper grids for one minute; the grids were washed seven times with double distilled water (one drop per wash) and negatively stained with one drop of 1% ammonium molybdate, pH 7.9, with the stain removed immediately. At each step, all liquids were absorbed by touching small wedges of Whatman No. 1 filter paper to the edge of the grid.

Reassociation The LiCl and $NaClO_4$-H_2O solubilized suspensions in 1 to 5 ml amounts were dialyzed against double distilled water (d_2H_2O) at room temperature. The reassociated material was observed at the electron microscope level as described in the previous section.

Factors affecting the reassociation process were investigated with LiCl solubilized cell walls from whole or homogenized cells. The LiCl solubilized wall suspensions were centrifuged for 5000 g-minutes (1000 g for five minutes) in a floor model centrifuge (International Equipment Co., Needham Heights, Mass.). The supernatant was dialyzed against 5 mM Na_2 EDTA in 8.3 mM Tris, pH 7.7 overnight at room temperature; the dialysis bag was transferred to d_2H_2O, with at least two changes, for 24-48 hours. At this point the cell wall material remained in suspension and the fraction was called the dialyzate and labeled L_1. This fractionation scheme is summarized in Figure 43a.

The effect of monovalent and divalent ions on reassociation was tested on the dialyzate. The dialyzate was divided into two ml samples and placed in 4 cm diameter dialysis tubing forming dialysis bags 4 cm long. L_1 was dialyzed against 100 ml of 0.01 M $CaCl_2$ or 0.3 M $CaCl_2$, $Ca(NO_3)_2$, $CaSO_4$, $MgCl_2$, $MgSO_4$, NaCl, Na_2SO_4, or KCl in 8.3 mM Tris, pH 7.5, at room temperature for a maximum time of two hours.

The effect of pH on the reassociation process was examined for the dialyzate. As described above, L_1 was dialyzed against 0.01 M $CaCl_2$ at pH 2.0, 4.5, 6.0, 7.5, 9.0, or 11.8. The buffer was 37.5 mM Tris maleate except for pH 11.8 which was 0.1 M NaOH. The time required for the onset of visible reaggregation was recorded. If reassociation did not occur within two hours, it was considered as no reassociation.

Biochemical analysis Live cells were extracted with 15 ml of 5 mM Na_2 EDTA in PMW_{II}, pH 5.5, for two hours at room temperature. The cells were concentrated at 5000 g-min; the supernatant was saved. An additional 15 ml of EDTA was added for another two hours and handled similarly. A third 15 ml EDTA extraction was carried out for three hours, and the supernatant again was saved. The cell pellet was resuspended in 15 ml of EDTA and saved. The four samples were analyzed for the amount of protein and carbohydrate by the Lowry method (Lowry et al., 1951) and phenol-sulfuric method (Hodge and Hofreiter, 1962), respectively. All samples were done in triplicate and averaged. Bovine Serum albumin fraction V (Miles Laboratories, Inc., Kankakee, Ill.) and D-glucose (Mallinckrodt Chemical Works, St. Louis, Mo.) were utilized as protein and carbohydrate standards, respectively.

Using whole cells, a molecular analysis of the dialyzate (L_1), the reassociated product (L_2), and reassociated supernatant (L_3) was conducted utilizing the disc-gel electrophoresis technique of Weber and Osborn (1969). The dialyzate was dialyzed against 0.1 M $CaCl_2$ in 37.5 M Tris-Maleate, pH 7.5, and the reaggregated product (L_2) was centrifuged at 39,000 g-min; 5 ml of supernatant (L_3) was removed with a disposable pasteur pipette and the pellet placed into 5 ml of fresh dialyzing

solution. Five ml of the three fractions were placed in dialysis bags and dialyzed against 1% SDS (sodium dodecyl sulfate, Sigma Chemical Company, St. Louis, Mo.), 1% MCE (β-mercaptoethanol, Sigma Chemical Company, St. Louis, Mo.), and 20 mM Tris-acetate, pH 8.0 overnight at room temperature. The dialyzates were removed from the dialysis bags, and their volumes were equalized with dialyzing solution.

The 10% polyacrylamide gels were made according to Weber and Osborn (1969). They were made fresh daily and were approximately 8 cm long. For each gel, 50 μl of sample, 30 μl of 8 M urea, 3 μl of tracking dye (0.3% (w/v) Bromphenol blue, 32% (v/v) MCE, 5.2% (w/v) SDS, 20% (v/v) glycerol in 0.1 M sodium phosphate buffer, pH 7.0, were placed in depression spot plates, mixed, and placed on the gels. The tubes were then filled to the top edge with gel buffer (0.1% SDS in 0.1 M sodium phosphate buffer, pH 7.0). The electrophoretic run was performed at 6 ma per gel with the positive electrode in the lower chamber. It took approximately seven hours for the tracking dye to traverse about 80% of the gel. The gels were removed from the tubes. The length of the gel and the distance traveled by the marker dye were measured.

The electrophoretic samples were run in duplicate for comparative staining for proteins and carbohydrates. The protein staining was with Coomassie blue (2 g Coomassie Brilliant Blue R, Sigma Chemical Company, St. Louis, Mo., per 250 ml of 50% (v/v) methanol, 9.2% (v/v) glacial acetic acid) by one of two methods. In the first method by Weber and Osborn (1969), the gels were stained for 5-6 hours and destained for 12-24 hours in each of three successive solutions: (1) overnight 5% (v/v) methanol and 9.2% (v/v) glacial acetic acid; (2) 5% (v/v) methanol and 9.2% (v/v)

glacial acetic acid; (3) 7.5% (v/v) glacial acetic acid. In the second method by Segrest and Jackson (1972), the gels were fixed overnight in 50% (v/v) methanol and 5% (v/v) glacial acetic acid, stained for 60 minutes and destained for 12 hours in 5% (v/v) methanol and 7.5% (v/v) glacial acetic acid and 24 hours in 7.5% (v/v) glacial acetic acid. In both cases all staining and destaining occurred at room temperature, and all gels were stored in 7.5% (v/v) glacial acetic acid at room temperature.

Carbohydrate staining was carried out using the periodic acid-Schiff (PAS) method of Segrest and Jackson (1972). Each gel was fixed overnight in 40% (v/v) ethanol and 5% (v/v) glacial acetic acid. The gels were treated for 3 hours with 0.7 (w/v) periodic acid which was followed by approximately 3 hours of treatment in 0.2% (w/v) sodium metabisulfite with one solution change after 30 minutes. After the gels had cleared, the Schiff reagent was added and the tubes capped with plastic tops. Staining was completed within 18 hours, and the gels were stored at $4^{\circ}C$. The Schiff reagent was made up using 10 g of basic fuchsin, 2 liters of distilled water, 200 ml of 1 N HCl, and 17 g of sodium metabisulfite; it was decolorized with charcoal, filtered through glass wool until clear and colorless, and stored in a brown bottle at $4^{\circ}C$.

Whole cells were treated with 5 mM disodium EDTA for two hours and then subjected to centrifugation at 5000 g-minute. The supernatant was dialyzed against double distilled water. This fraction, the dialyzate (E_1), was transferred to 0.1 M $CaCl_2$ in 8.3 mM Tris, pH 7.7, for reassociation. Reassociated material was centrifuged at 39,000 g-minute, and the pellet (E_2) and the supernatant (E_3) were separated by removing E_3 with a disposable pasteur pipette as summarized in Figure 43b. The volume of E_2

and E_3 were equalized with the $CaCl_2$ solution and placed in dialysis bags for exchange with the SDS solution described earlier for L_1, L_2, L_3 electrophoretic preparation. The three samples were run on polyacrylamide gels and stained for protein and carbohydrate as described earlier for LiCl treated cells.

Ionic interactions of the wall with cationized ferritin

Binding in normal cells Midlog phase cells on 16 hours of light and 8 hours of dark were treated with cationized ferritin (Danon, 1972) during the third hour of the light period. The cationized ferritin (Miles Laboratories, Inc., Elkhart, Ind.) was diluted to a final concentration of 0.7 mg/ml with PMW_{II} forming a stock solution. Approximately 0.1 ml of pelleted cells were resuspended in 1 ml of cationized ferritin stock solution for 30 minutes in the light at room temperature. The cells were washed three times with PMW_{II} to remove excess ferritin and then fixed by the standard procedures for observation with the electron microscope.

Binding in dark-incubated cells Midlog phase cells were treated with cationized ferritin for 30 minutes as above, washed three times in PMW_{II}, placed in the dark for 12 hours at room temperature, and placed back again in the light for seven hours at 17-19°C. The cells were fixed, sectioned, and observed with the electron microscope.

A second group of midlog phase cells was placed in the dark for 12 hours, was treated with cationized ferritin as above, washed three times, and incubated in the light for seven hours. The cells were fixed, processed, and observed with the electron microscope.

Binding in pronase treated cells Midlog phase cells were treated with 4 mg/ml of pronase in the dark at room temperature for 12 hours. The cells were washed three times in PMW_{II} to remove the pronase and divided in half. The first half was treated with cationized ferritin, washed three times with PMW_{II}, and allowed to recover in the light at 17-19°C for seven hours. The second half was placed in the light for seven hours immediately after the pronase was washed out, then treated with cationized ferritin, and washed three times with PMW_{II}. Both samples were processed and observed with the electron microscope.

The Biological Degradation of the Cell Wall

Multiple scale and coccolith-containing vesicles and hydrolytic enzymes

Enzyme localization Three liters of medium with cells were removed from a 15 liter culture that had been growing for six days under aeration. The cells were centrifuged and divided equally for the localization of two hydrolytic enzymes--acid phosphatase and aryl sulfatase. All samples were fixed in 4% Na cacodylate buffered glutaraldehyde for 45 minutes, washed three times in cacodylate buffer, and stored for 24 hours in buffer.

Acid phosphatase activity was localized according to Wachstein and Meisel (1957) as performed by Trout (1977). The pH of the incubation medium was adjusted to 5.0 and β-glycerophosphate was used as the substrate. The incubation medium was composed of the following:

20 ml 0.125% β-glycerophosphate

20 ml 0.2 M Tris-maleate buffer, pH 5.0

3 ml 1.0% Pb NO_3 (Fresh)

2 ml double distilled water

My modification of this medium was the elimination of 0.1 M $MgCl_2$ to prevent nonspecific lead deposits. The tissue was incubated for 60 minutes at room temperature. A substrateless control and a 0.1 M Na F inhibited control were run in parallel. The release of the phosphate group by the action of acid phosphatase on β glycerophosphate yields an insoluble product $(Pb)_3(PO_4)_2$ at the site of the acid phosphatase enzyme.

Aryl sulfatase localization was carried out by Trout's modification (1977) of the Hopsu-Havu et al. method (1967). The substrate was ρ-nitrocatechol sulfate (Sigma Chemical Company, St. Louis, Mo.) with lead as the precipitating agent. The incubation medium consisted of:

40 mg ρ-nitrocatechol sulfate in 1.0 ml double distilled water

3 ml 0.1 M Tris-maleate buffer, pH 5.0

1 ml 8% Pb NO_3 (fresh)

The same substrateless control from the acid phosphatase localization was used for aryl sulfatase. The reaction depends on the deposit of insoluble Pb SO_4 at the site of aryl sulfatase when the sulfate group is cleaved.

The cells were incubated for 60 minutes at room temperature. All samples were washed for 5-10 minutes in 3% acetic acid (to remove any spurious lead deposits) and then washed with 0.1 M Tris-maleate pH 5.0. The samples were fixed overnight in 1% OsO_4, decalcified, dehydrated and embedded by standard procedures. All sections were observed unstained.

Enzyme activity of homogenates A carboy of cells was harvested and the cells were suspended in 20% (w/v) cold 1% KCl with 0.5% Triton X-100. The suspension was homogenized using a Tekmar polytron homogenizer operated at medium speed. This homogenate was used for the enzyme activity assays

of acid phosphatase, aryl sulfatase, and cathepsin D and for protein determinations.

Acid phosphatase with ρ-nitrophenyl phosphate was assayed according to the method of Seed et al. (1967). The incubation medium consisted of the following components:

0.5 ml ρ-nitrophenyl phosphate

0.5 ml commercial citrate buffer, pH 4.8
(Sigma Chemical Company, St. Louis, Mo.)

0.2 ml homogenate

Nonspecific activity was determined by adding 0.1 ml of 0.1 M NaF to the incubation medium and was subtracted from the uninhibited sample for the final specific activity. The samples were incubated for 30 minutes at 37°C. The reaction was stopped with 5.0 ml of 0.1 N NaoH, and the absorbance was read at 410 nm. The mechanism of the reaction is that ρ-nitrophenyl phosphate is colorless in acid or alkali, but the ρ-nitrophenol formed from the acid phosphatase hydrolysis is colorless in acid and yellow in alkali with an absorption maximum near 410 nm. The results were converted to the amount of inorganic phosphate (Pi) released, and the activity was expressed as M Pi/mg of protein per hour.

The aryl sulfatase activity was assayed by the hydrolysis of ρ-nitrophenyl sulfate to ρ-nitrophenol and sulfate ion (Sigma Technical Bulletin). The assay conditions were as follows:

0.5 ml of 0.2 M sodium acetate buffer, pH 5.0

0.4 ml of 0.00625 M ρ-nitrophenyl sulfate

0.1 ml of enzyme preparation

The samples were incubated in a water bath at 37°C for 30 minutes. The reaction was stopped with the addition of 5.0 ml of 1.0 N NaOH. The absorbance was read at 410 nm after 10 minutes. The enzyme activity was determined from a standard curve of known ρ-nitrophenol concentrations and expressed as μ M ρ-nitrophenol per mg protein per hour.

Anson's assay method (1939) for cathepsin D activity was utilized. This assay is based on the hydrolysis of hemoglobin into TCA soluble amino acids and polypeptides. The substrate medium consisted of the following components:

50 ml 5.0% (w/v) Sigma Type II hemoglobin dialyzed for 48 hours against double distilled water at 4°C

25 ml 1.35 M acetate buffer, pH 3.8

50 ml double distilled water

The incubation medium components were:

1.0 ml substrate solution

0.5 ml enzyme preparation

The samples were incubated for 30 minutes at 37°C. The reaction was stopped with 3.0 ml of cold, 5% TCA which was then filtered through Whatman #42 filter paper, and 1.0 ml of filtrate was transferred to a clean test tube. To the filtrate 2.0 ml of 0.5 N NaOH was added followed by 0.6 ml of 2N phenol reagent. Exactly five minutes after the addition of the phenol reagent the absorbance of each tube was read at 600 nm. The activity was determined from a tyrosine standard curve and expressed as μ M tyrosine per mg protein per hour.

Neutral red staining vesicles A stock solution of 2.9×10^{-4} g/ml of neutral red (Eastman Kodak Company, Rochester, N.Y.) was made in double

distilled water. This solution was diluted to 1.4×10^{-5} g/ml in PMW_{II} for a working solution.

Midlog phase cells were centrifuged, and 5 ml of the neutral red working solution was added for five minutes. The cells were centrifuged again and observed with the light microscope. The number of neutral red staining vesicles was counted for 25 cells for each sample. Samples were taken at 3, 7, 11, 15, 25, and 28 hours; this time span included an eight-hour dark period between the 15 and 25 hour samples.

RESULTS

The Biology of Hymenomonas

General morphology

The general morphological characteristics of Hymenomonas carterae which are seen at the light and transmission electron microscope levels are presented in Figures 1 and 2 primarily for orientation. Figure 1 is a Nomarski differential interference control light micrograph showing an optical section thru a typical cell. The cells are 10-15 μm in diameter with two flagella on either side of a bulbous haptonema. The cell surface consists of a layer of 100-200 calcium carbonate-containing scales called coccoliths; the calcium carbonate is in the form of calcite crystals. Two chloroplasts flank the nucleus and are responsible for the yellow-green color of the cells. An internal coccolith in the anterior region near the flagella is visible in Figure 1.

Figure 2 is a survey transmission electron micrograph showing the internal and external morphology of Hymenomonas. Inside the cell there are two chloroplasts surrounding the nucleus. The posterior region normally has a large vacuole or tonoplast and several small vesicles. Anteriorly there is a polarized Golgi apparatus with its typical cisternal stacking. A small portion of an internal coccolith and several coccolithosomes (coccilith precursors) are visible. Coccolith formation and structure were previously described (see p. 15). The cell wall consists of columnar material, small fibrils radiating from the plasma membrane, three layers of scales embedded in electron transparent material, and an exposed layer of coccoliths. The coccoliths have been decalcified in this preparation, but

Figure 1. Nomarski differential interference contrast light micrograph showing an optical section of a living H. carterae. Visible are the two flagella (F), the coccolith exoskeleton, two chloroplasts (Ch), and an internal coccolith (arrow). X 3,000

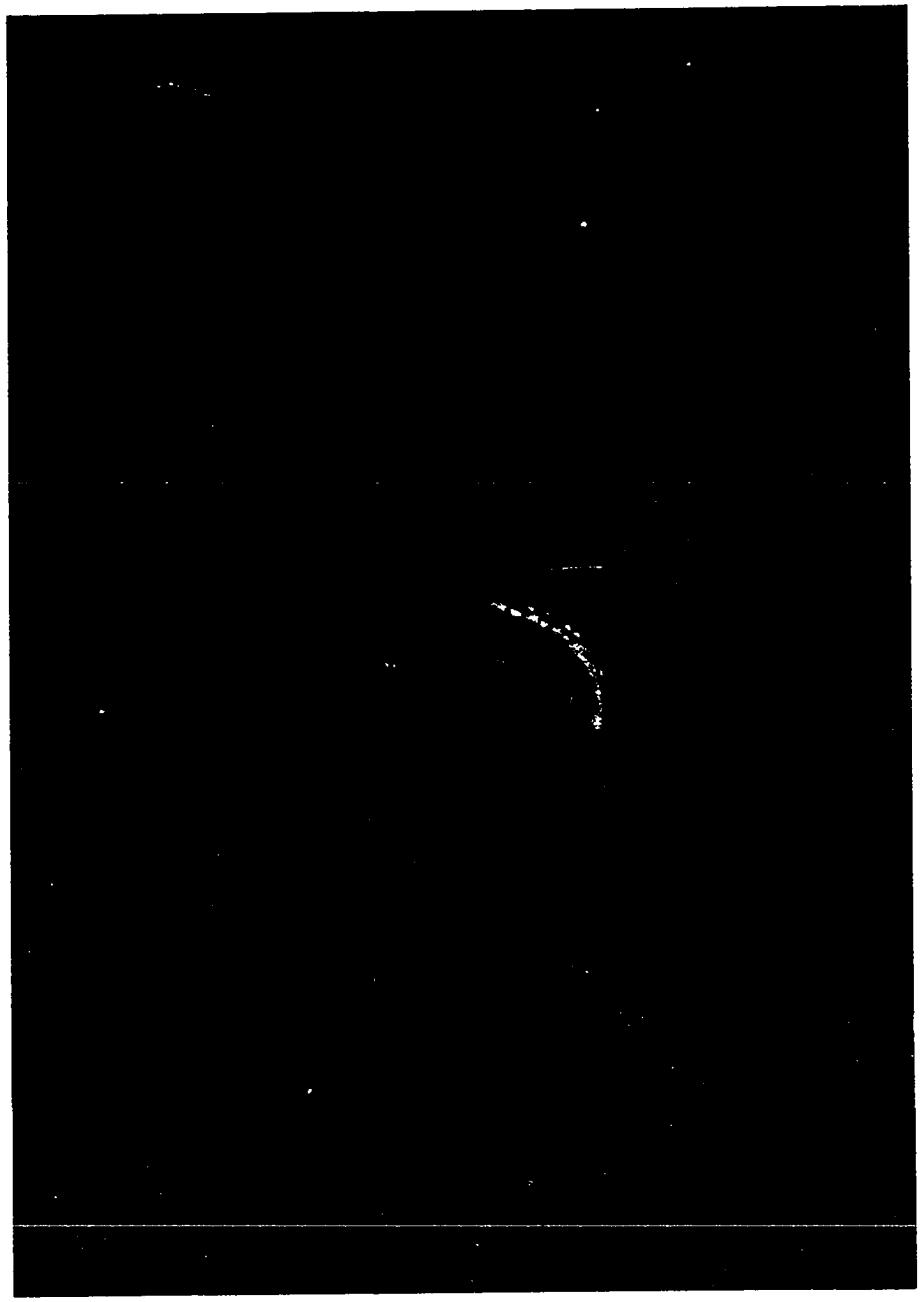

Figure 2. A survey transmission electron micrograph of a longitudinal section thru H. carterae. The following structures are visible: chloroplast (Ch), nucleus (N), golgi apparatus (G), coccolithosomes (arrows), internal coccolith (iC), mitochondrion (M), microtubule bundle (Mb), columnar material radiating from the plasma membrane (P), coccoliths (C) with their bases (B) and rims (R), and scales (S). X 20,000

the characteristic shape of the rims is preserved by the matrix. The coccoliths are decalcified to facilitate sectioning and prevent holes in the sections when the calcium drops out following sectioning.

The preservation of cell shape and surface structures for scanning electron microscopy was compared for three drying techniques--air drying, freeze drying, and critical point drying. Figures 3-5 show the differences in these techniques. The air dried cells (Figure 3) have a shrunken or shriveled appearance with a bumpy wall surface. The coccolith rims are present, but the coccoliths are sunken into the wall. The air dried cells are not well-preserved. The freeze drying technique preserved the cell shape and resulted in a smooth wall surface. The coccolith rims and bases are visible; the grooves formed by the alternating A and B elements around the coccolith base can be seen. The bases have a granular appearance. The number and distribution of coccoliths are easily observed. The critical point drying technique (Figure 5) maintains a well-preserved cell shape with a fibrous cell wall surface. The coccolith rims are visible, and the coccoliths are covered with a reticular network which I refer to as a coccolithonet. Figure 5b gives a better view of the coccolithonets which are connected to the rims and traverse the base. The coccolithonet can be seen passing over the rims to the wall surface. Often the nets will radiate from the wall surface and connect to the coccolith edges. The coccolithonets have not been reported before.

Since more surface structures are preserved and the technique is so much more rapid (1 hr vs 1 day for freeze-drying), critical point drying was performed for all additional SEM preparations.

Figures 3-5. Comparison of air-drying, freeze-drying, and critical point drying techniques for specimen preservation in the scanning electron microscope

Figure 3. Air-drying. Cell shape is not well-preserved. X 9,000

Figure 4. Freeze-drying. Cell shape is generally preserved. Note the grooves formed from the coccolith rims (arrows). X 9,000

Figure 5a. Critical point drying. Cell shape is well-preserved. The coccoliths are covered with a reticular material called a coccolithonet (cn). X 9,000

Figure 5b. A higher resolution view of the coccolithonets. Note the fibril connection of the coccolith and the wall and the nets passing over the rim (arrow). X 24,000

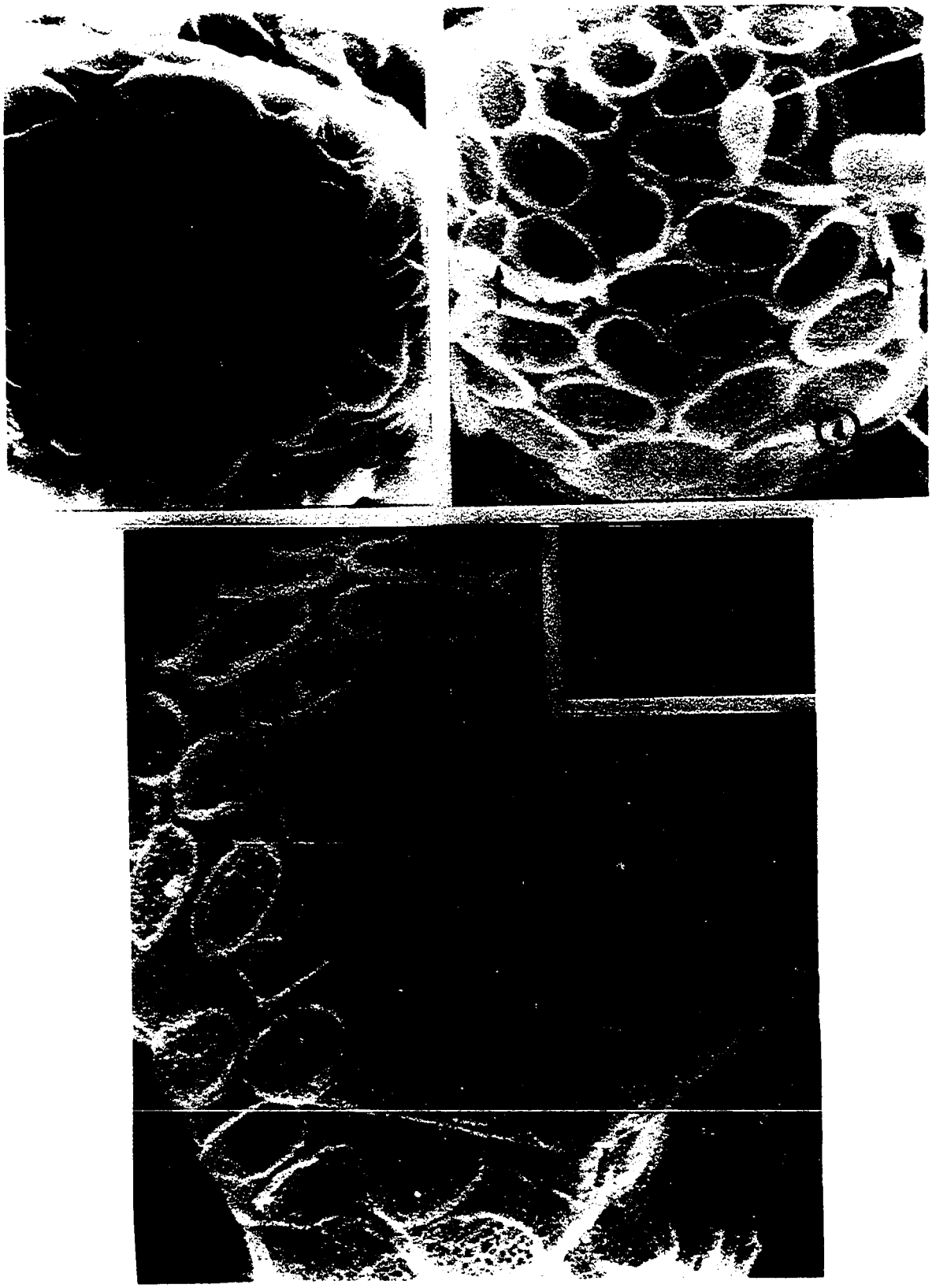

Responses to diverse culture environments

The effect of surface to volume (s/v) ratios of the culture medium on growth is shown in Figure 6. Logarithmic or optimal growth at a rate of 0.7-1.0 generations per day was maintained for 5-6 days for the highest s/v flask (62.3 cm^2/ml) and for 2-3 days for the lowest s/v flask (2.1 cm^2/ml). The maximum cell density possible for these flasks was 1-3 million and 100,000-125,000 cells per milliliter, respectively.

To obtain enough cells and cell wall material for cell fractionation studies, it was necessary to grow the cells in large batch culture. From the above data, carbon dioxide exchange had to be maximized to improve yields. Table 1 shows the effects on growth of forcing air through 15 liters of medium in five carboys with an aquarium pump. The cell density can be improved 2-3 fold when air is forced through the growth medium. The surface to volume ratio of the 15 liters of medium in the carboy is 3.24 cm^2/ml and is nearly equal to the smallest s/v ratio (2.1 cm^2/ml) flask shown in Figure 6. The inoculum size is also important because small inocula result in reduced maximum cell density.

The cultures shown in Figure 6 were grown using 16 hour light-8 hour dark diurnal cycles. If continuous light was substituted, the growth rate increased slightly. This increase was not enough to outweigh the advantages of maintaining 70-80% division synchrony that was achieved by using the light dark cycle.

If cells are allowed to grow beyond 6 to 7 divisions or to achieve cell densities of approximately 400,000 cells/ml, a phase change results (Williams, 1972, 1974) with the release of meiospores. To avoid this,

Figure 6. Effect of surface to volume ratio on cell growth in 500 ml Delong flasks. The results show that as the surface to volume ratio increases so does the length of the logarithmic growth phase and the maximum cell density.

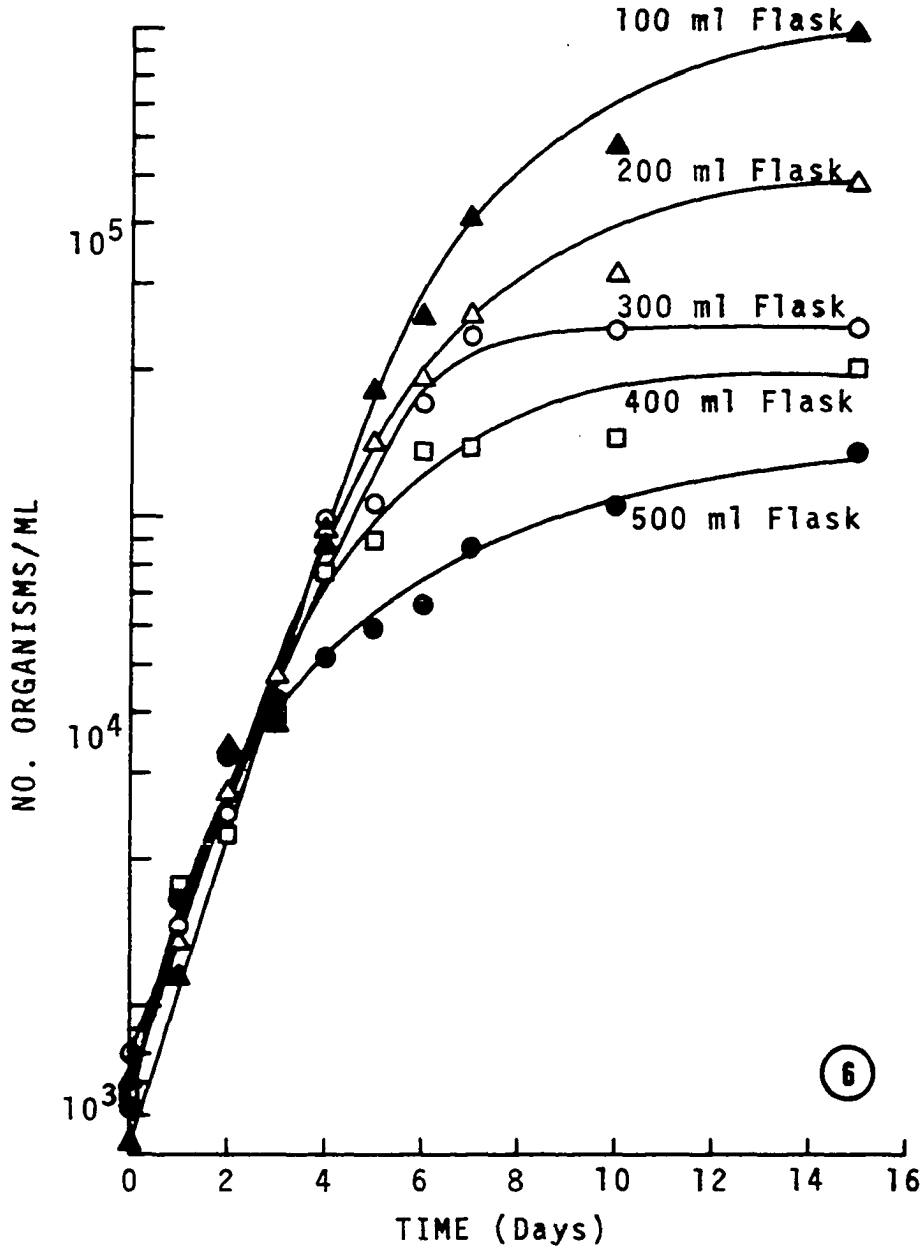
100 ml Flask
200 ml Flask
300 ml Flask
400 ml Flask
500 ml Flask
10^5
10^4
10^3
NO. ORGANISMS/ML
0
2
4
6
8
10
12
14
16
TIME (Days)
6

Table 1. Effects of forced air on growth in five gallon carboys with 15 liters of medium

Carboy condition	0 days growth[a]	6 days growth	12 days growth
Cotton plugged[b]	50,000	109,000	120,000
Rubber stoppered[c]	3,300	16,000	20,600
Forced air 1[d]	6,800	105,000	144,000
Forced air 2[d]	55,500	247,000	--

[a]Growth units equal to number of cells per milliliter.

[b]No forced air.

[c]No forced air but stoppered identically to forced air carboys.

[d]Rubber stoppered but filtered forced air passed thru medium in carboy.

cultures were routinely maintained on a 48 hour transfer schedule where cell densities were between 150,000 and 300,000 cells/ml.

The Kinetics of Wall Formation

Pattern of coccolithogenesis after treatment of cells with EDTA

Concentration effects Figure 7 shows the effect of varying the EDTA concentration on the cell's ability to make coccoliths. The minimum concentration to remove the calcium from the coccoliths is 5 mM Na_2 EDTA, and it also gives the best coccolithogenic rate of the EDTA treatments. The rate decreases as the EDTA concentration increases. The hardiness of these cells is shown when 20-25% of cells treated with a 500 mM (saturated) EDTA solution survive to produce coccoliths.

Figure 7. Effect of different EDTA concentrations on coccolithogenesis after 4 hours recovery

Figure 8. Effect of varying time of EDTA treatment on coccolithogenesis after 4 hours recovery

Figure 9. Kinetics of coccolith formation following 20 minutes of 5 mM Na_2 EDTA treatment. The rate of coccolith formation is 7.5-8.0 coccoliths per cell per hour

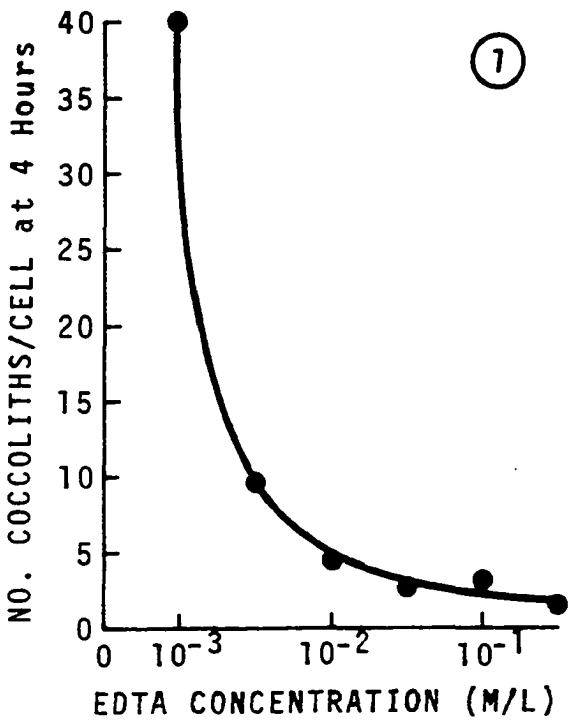
NO. COCCOLITHS/CELL at 4 Hours
40
35
30
25
20
15
10
5
0
0
10^{-3}
10^{-2}
10^{-1}
EDTA CONCENTRATION (M/L)
7

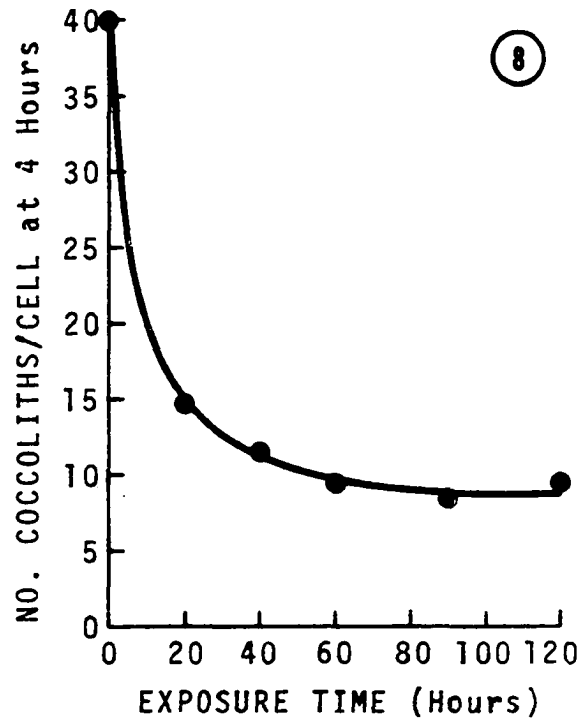
NO. COCCOLITHS/CELL at 4 Hours
40
35
30
25
20
15
10
5
0
0
20
40
60
80
100
120
EXPOSURE TIME (Hours)
8

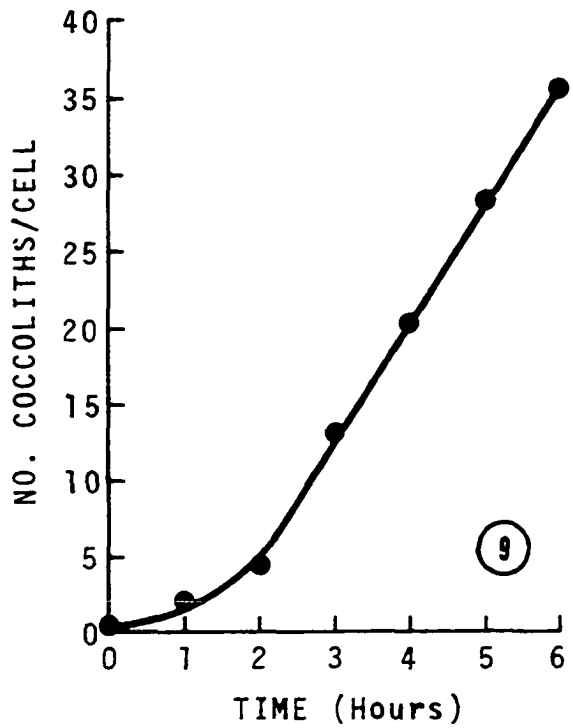
NO. COCCOLITHS/CELL
40
35
30
25
20
15
10
5
0
0
1
2
3
4
5
6
TIME (Hours)
9

Time effects Figure 8 shows the effects of varying the time the cells are exposed to 5 mM EDTA on coccolith production. After 4 hours of recovery, more coccoliths were made by cells treated for 20 minutes than any other treatment time, but the effect levels off after 60 minutes. Thus the ability of cells to make coccoliths is dependent on how long they are subjected to EDTA treatment. From Figures 7 and 8 the optimum conditions for maximum coccolith production following EDTA treatment is 5 mM EDTA for 20 minutes.

Coccolithogenesis When 5 mM Na_2 EDTA for 20 minutes is used as the wall treatment, the cells generate coccoliths at a rate of 7.5-8.0 coccoliths per cell per hour (Figure 9). At the end of the treatment, no coccoliths are present, and a 1-2 hour lag period is necessary before new coccoliths are made at a steady rate. After washing out the EDTA, the cells aggregate into a large mass or several small masses which do not break up until 7-8 hours of recovery. New coccoliths are clustered near the anterior end of the cell. These characteristics are summarized and compared to pronase recovery characteristics in Table 3.

The deposition of new coccoliths on the cell surface is easily viewed with Nomarski interference contrast in living cells following EDTA treatment. Internal coccoliths are seen in the anterior regions of the cell, they disappear, there is a contraction of the cell in this region, and a new coccolith will emerge onto the cell surface. This process takes less than 5 seconds. From the time of appearance of the internal coccolith to its deposition on the cell surface takes 20-30 minutes, and usually more than one coccolith is visible inside the cell at the same time. Once outside the cell, the new coccolith will "skate" on the cell surface bumping

into old coccoliths and changing their position until a stable position is achieved. The movement and positioning of coccoliths are reminiscent of bumper cars at carnivals, crashing into and bouncing off of one another.

Figure 10 illustrates the distribution of coccolith counts used to construct the curve in Figure 9. The mean values (Figure 9) and the modal distribution (Figure 10) correspond closely. It should be remembered that part of the variability of these data is superimposed on the diurnal cycle such that cells at one stage of the cell cycle may produce coccoliths faster than cells at other cell cycle stages.

Other environmental effects Table 2 shows some environmental factors which affect the coccolithogenic rate after EDTA treatment. Coccolithogenesis varies with the temperature showing a faster rate at the same temperature as optimal growth. There is an optimal light intensity for coccolithogenesis at approximately 7750 lux which also corresponds to optimal growth light intensity (Paasche, 1966b; Blankley, 1971). The s/v ratio shows that CO_2 exchange is important in coccolith production just as it is in growth. Factors which affect growth also affect coccolith production, and it has been impossible to alter one without also altering the other.

Morphology of regeneration Living cells treated with EDTA survive, have the coccolith rims removed and produce new coccoliths, and their surface morphology is compared in Figures 11-13. Figure 11 shows an untreated cell with calcified rims on the coccoliths. This untreated cell with few coccolithonets was selected to better view the areas normally obscured by the coccolithonets; adjacent cells do show coccolithonets. There are no radials or concentrics visible on the coccolith base even though the reticular material is absent. Figure 12 shows a cell at the end of the EDTA

Figure 10. Histogram of cell recovery from EDTA treatment showing the distribution of coccoliths per cell used in constructing Figure 9. The mean values and standard deviations are as follows for 0, 1, 2, 3, 4, 5, and 6 hours recovery, respectively: 0.1 coccolith/cell, S = 0.39; 1.7 coccoliths/hour = 2.79; 4.5 coccolith/cell, S = 4.14; 12.7 coccolith/cell, S = 6.36; 20.2 coccoliths/cell, S = 7.84; 28.7 coccoliths/cell, S = 8.4; 35.5 coccoliths/cell, S = 8.99

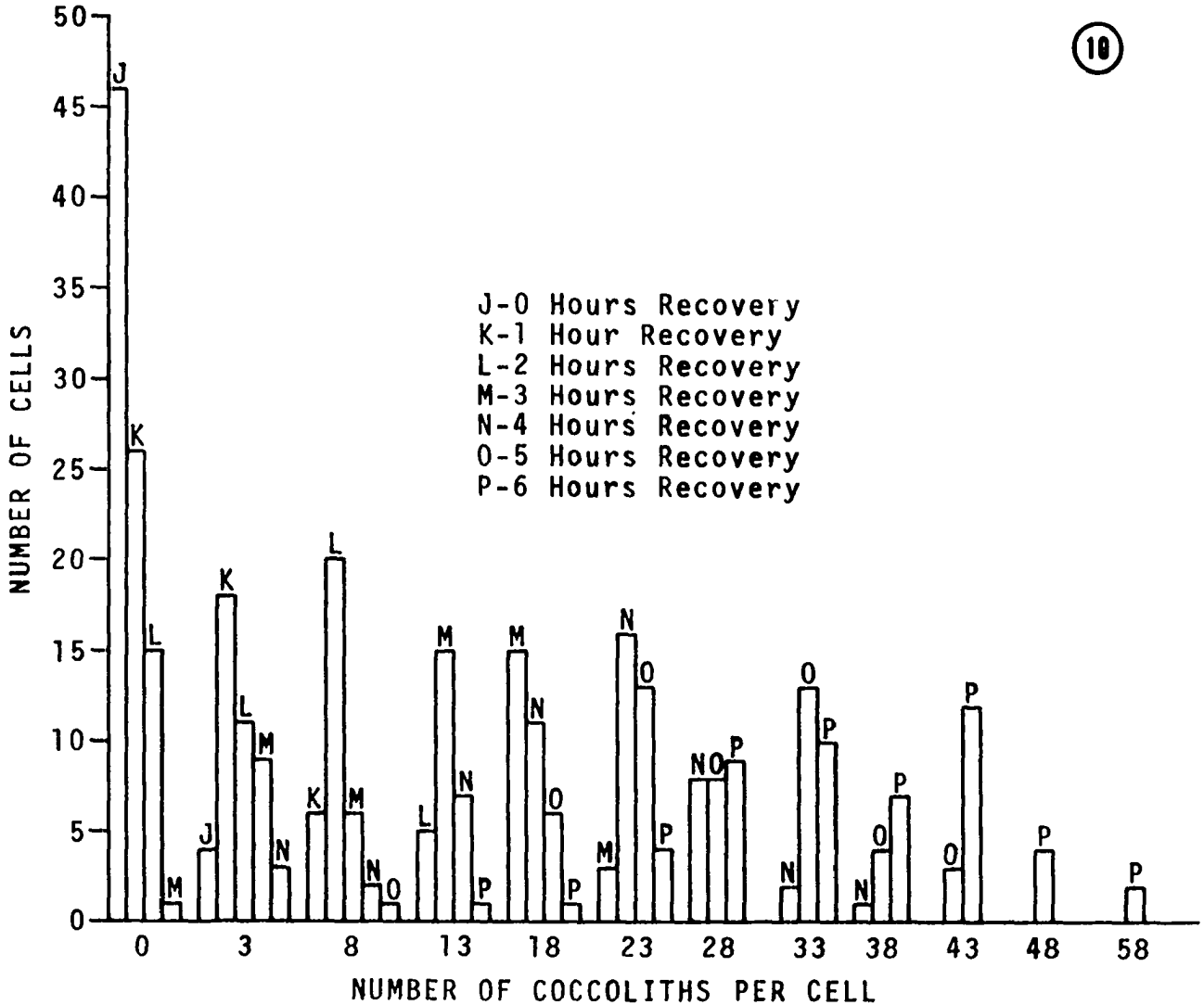
10
J-0 Hours Recovery
K-1 Hour Recovery
L-2 Hours Recovery
M-3 Hours Recovery
N-4 Hours Recovery
O-5 Hours Recovery
P-6 Hours Recovery
NUMBER OF CELLS
NUMBER OF COCCOLITHS PER CELL
0
5
10
15
20
25
30
35
40
45
50
0
3
8
13
18
23
28
33
38
43
48
58

Table 2. Environmental factors affecting the coccolithogenic rate following EDTA treatment

Factor	Coccolithogenic rate[a]
Light intensity	
4,300 lux	3.2
7,750 lux	7.5-8.0
16,100 lux	2.9
Temperature	
17-19°C	3.2
22-24°C	2.2
Surface to volume ratio	
9.6 cm^2/ml	3.0
22.1 cm^2/ml	5.4
62.3 cm^2/ml	7.5-8.0

[a]Rate units in coccoliths/cell/hour.

treatment. The calcified rims have been removed, but the curled edges of the bases are visible. No coccoliths are present. Figure 13 shows a cell recovery from EDTA treatment that has nine new coccoliths which are clustered in the anterior zone of the cell. Although not present in this cell, coccolithonets are visible in other cells at this stage of recovery. The new coccoliths are easily distinguishable from old coccolith bases, but it is impossible to determine if the new coccoliths are on top of old bases.

A comparison of the internal morphology for normal cells, EDTA treated cells, and cells recovering from EDTA treatment is presented in Figures 14-18. Figure 15 demonstrates the normal wall structure with the columnar material, scale layer, and characteristic coccolith morphology. Figure 14 shows the standard morphology of an internal coccolith at a mature stage of development in the Golgi. Coccolithosomes are also present. The coccolith

Figures 11-13. Scanning electron micrographs comparing untreated cells, EDTA treated cells, and cells recovering from EDTA treatments. X 9,000

Figure 11. An untreated cell with calcified coccolith rims present and no coccolithonets

Figure 12. A cell treated with 10 mM Na_2 EDTA for 40 minutes. Note the coccoliths possess only bases which are often curled at the edges (arrows). No coccolithonets are present

Figure 13. A cell recovering from 40 minutes of 10 mM Na_2 EDTA treatment. Note the difference between the old coccolith bases (o) and the nine new coccoliths (c) clustered at the anterior end

Figures 14-16. Transmission electron micrographs comparing the wall components and internal coccoliths of untreated and EDTA treated cells. X 36,000

Figure 14. A portion of a Golgi apparatus illustrating an internal coccolith (iC) at an advanced developmental stage and some coccolithosomes (CS)

Figure 15. The wall of an untreated cell showing the columnar material (cl), scale layer (S), and coccolith structure (c)

Figure 16. A calcified cell treated with 10 mM Na_2 EDTA for 40 minutes. Only remnants of matrix material remain on the coccolith base (arrows). The scales (S) and columnar material (Cl) are present on the wall. Internal coccoliths (iC) with some calcium and a distorted matrix and coccolithosomes are visible

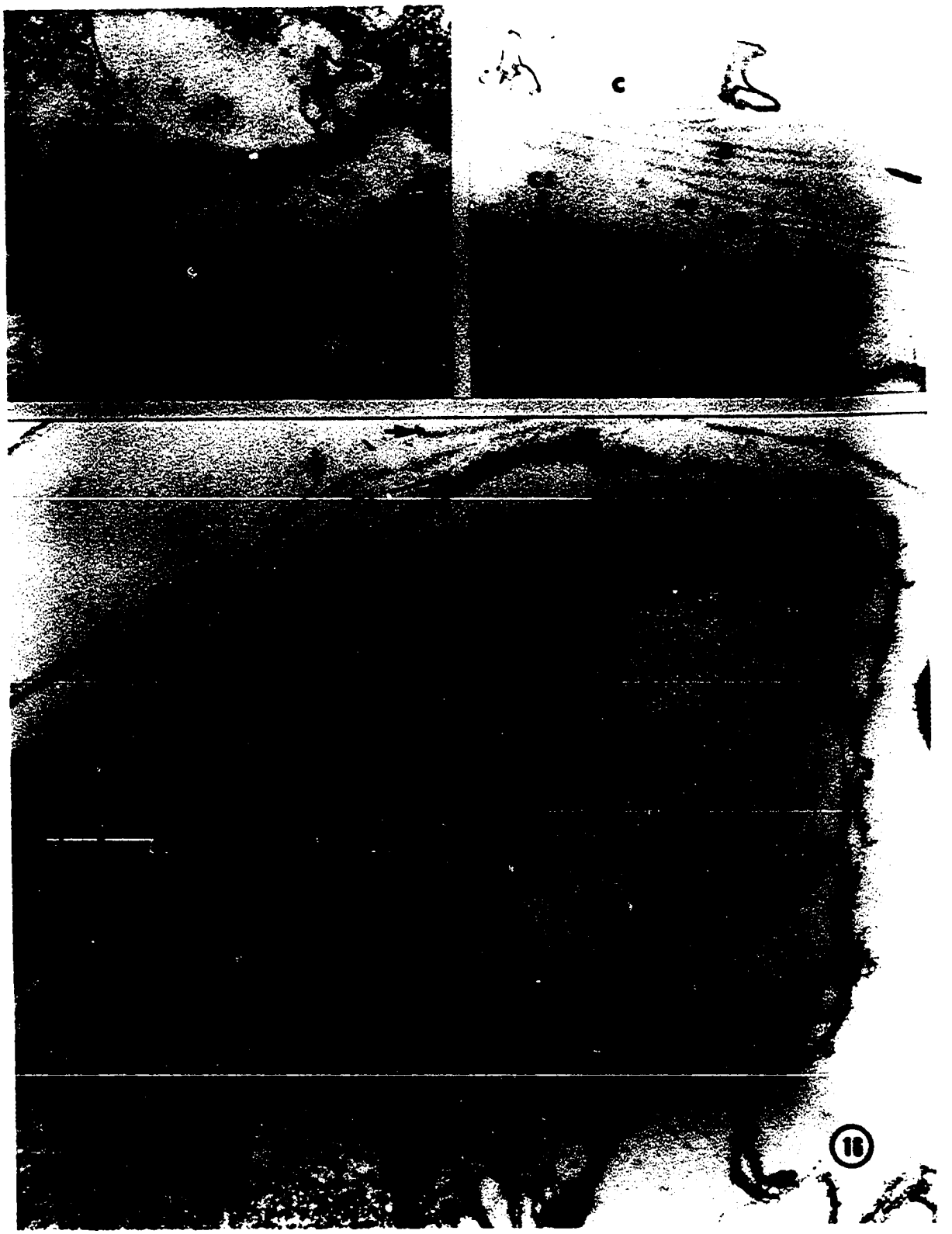
c
18

has its calcified rims removed from the EDTA treatment (Figure 16) and only remnants remain on the base. The scales are compressed tightly together indicating the extraction of some amorphous wall material. There is columnar material visible. The treatment leaves the internal coccoliths with some calcium and the matrix material intact, but some distortion is visible. The new coccoliths that are made during the recovery from the EDTA treatments (Figures 17 and 18) can be distinguished from the old coccoliths. In Figure 17, an old base is seen overlapping slightly another old base giving the impression of its being shoved off the cell. In Figure 18 an old coccolith base is being "squeezed" by two new coccoliths. During the recovery stages, old bases were never seen resting atop old bases nor were new coccoliths found on top of old bases. The old bases must restrict the movements of coccoliths on the cell surface bringing about their clustered arrangement in the anterior region.

Pattern of coccolithogenesis after treatment of cells with pronase

Coccolithogenesis Cells treated with 2.4 mg/ml of pronase in the dark for 12 hours exhibit a coccolith production rate of 1.5 to 2.5 coccoliths per hour during the first 25-30 hours of recovery (Figure 19). Some cells still have coccoliths at the end of the pronase treatment, but they are removed within the first 4 hours. Light microscope observations of recovery cells reveal that within 30 minutes after transfer to PMW_{II} the cells regenerate flagella and begin to vibrate without swimming. Coccoliths can be seen leaving the cell surface and becoming free in the medium. Initially the recovering cells are single (not clumped together as in EDTA treated cells); however, after 7-8 hours of recovery the cells begin to

Figures 17-18. Transmission electron micrographs of cells treated with 5 mM Na_2 EDTA for 20 minutes and allowed to recover in the light for 8 hours. The cells were decalcified following fixation

Figure 17. Old coccoliths (o) and new coccoliths (c) are distinguishable with one old base apparently being pushed from the cell surface (arrow). X 24,000

Figure 18. A higher resolution micrograph illustrating new coccoliths (c) will distribute themselves around and not on old coccoliths (o). X 36,000

17

18

Figures 19-20. Determination of normal coccolithogenic pattern following pronase treatment

Figure 19. Cells recovering from pronase treatment exhibit a coccolithogenic rate of about 1.5 coccoliths per hour. Note the drop in the number of coccoliths per cell after 2-3 hours of recovery (arrow)

Figure 20. Pronase treatment and recovery followed by EDTA treatment and recovery. Recovery is compared to cell growth during the 49 hours of recovery. Note that approximately 70% of the cells divided during each dark period

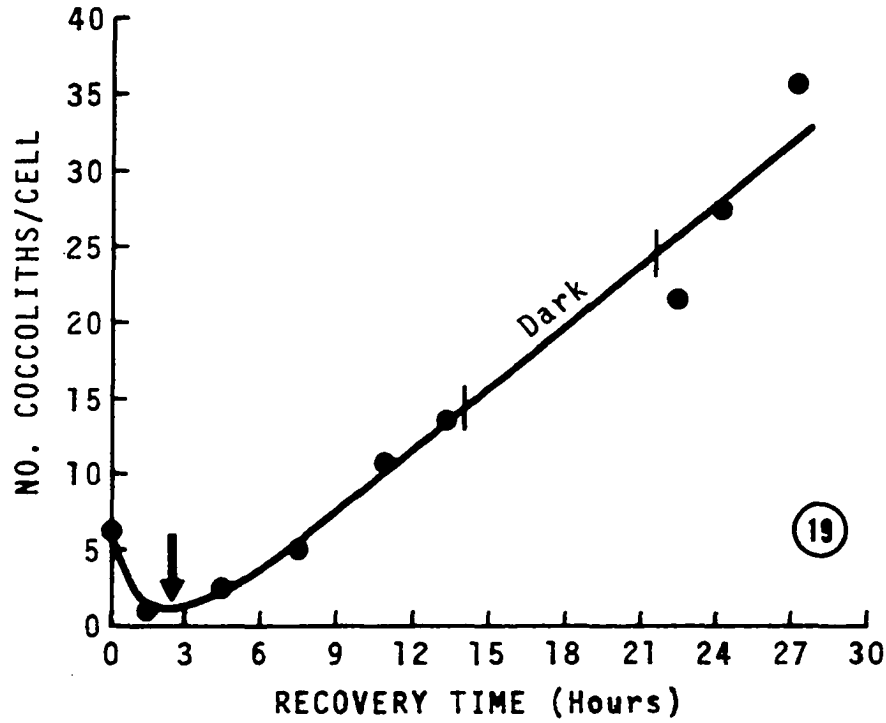
NO. COCCOLITHS/CELL
40
35
30
25
20
15
10
5
0
Dark
19
0 3 6 9 12 15 18 21 24 27 30
RECOVERY TIME (Hours)

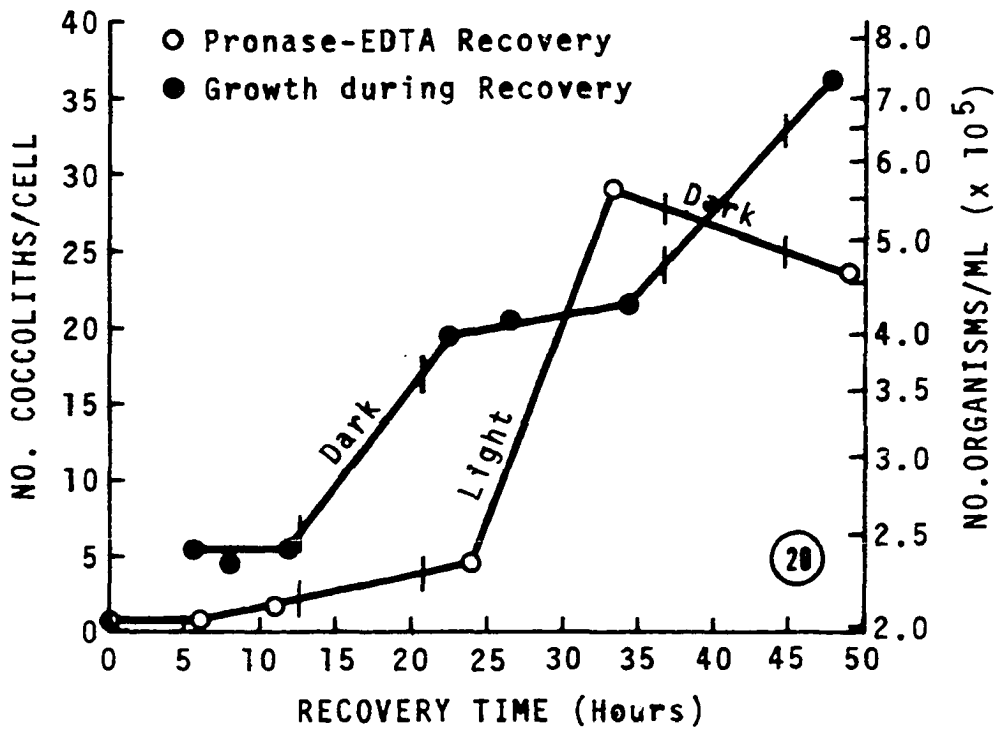
O Pronase-EDTA Recovery
● Growth during Recovery
NO. COCCOLITHS/CELL
NO.ORGANISMS/ML (x 10^5)
Dark
Light
Dark
20
0 5 10 15 20 25 30 35 40 45 50
RECOVERY TIME (Hours)

clump. After 4-6 hours new coccoliths start appearing on the cell surface and are randomly dispersed over the cell surface. When culture factors such as temperature, light intensity, and surface to volume ratios were varied as for the earlier EDTA treatments, the coccolithogenic rate following pronase treatment remained unchanged. The events of recovery from pronase are summarized and compared to the recovery events from EDTA in Table 3.

Table 3. Comparison of coccolithogenesis following EDTA or pronase treatment

Event compared	Recovery after EDTA treatment	Recovery after pronase treatment
0 time	no coccoliths visible	several coccoliths per cell
	cell structure together in clump	cells single
flagella	absent first 7 hours of recovery	regenerated within ½ hour
lag period	1-2 hours	4-6 hours
coccolith distribution	clustered	randomly dispersed
coccolithogenesis	varies with different culture conditions	remains constant under different culture conditions

When counting the coccoliths of cells recovering from the pronase treatment, it was impossible to distinguish between new coccoliths and the ones which were not removed by pronase. The presence of old coccoliths would inflate the counts and possibly alter the regeneration rate. To

eliminate this problem, cells recovering from pronase were removed at specified times, treated with EDTA for 20 minutes, and allowed to recover for four hours. The results are shown in Figure 20. Very few coccoliths (1-2 coccolith/cell/hr) are made during the first 24 hours of recovery, but a tremendous burst (10-13 coccoliths/cell/hr) occurred by 33 hours which subsides somewhat by 49 hours. A parallel experiment which measured cell growth during recovery shows that division occurs during both dark phases and that coccolith production increased following division and occurs maximally in the light. A certain percentage of cells (2-4%) did not recover enough to produce coccoliths following the pronase treatment.

Cells recovering from the pronase treatment do exhibit modal tendences as shown in Figure 21. The recovery of cells from pronase was not as uniform as with EDTA. Some cells had a harder time recoverying probably because of more cell damage from pronase. Some of this severity of effect might be attributed to permeability differences between cells at various cell cycle stages during the time of treatment which would allow the penetration of more pronase into the cells.

Concentration effects The most effective amount of pronase was determined by exposing cells to different concentrations of pronase for 12 hours and counting the number of coccoliths per cell. The results are plotted along the ordinate of Figure 22. The number of coccoliths per cell decreased as the pronase concentration increased. From these data the 10 mg/ml pronase concentration would be selected for standard treatments, but it was not because only 10-20% of these cells survived the treatment enough to produce coccoliths. Since 80-90% of the cells made coccoliths after 2-4 mg/ml pronase treatments, this concentration range was adopted.

Figure 21. Histogram of recovery from pronase treatment showing the distribution of coccolith per cell used in constructing Figure 19. The mean values and standard deviation (s) are as follows for 0, 1.5, 4.5, 7.5, 10.5, 13.5, 22.5, 24.5, and 26.5 hours, respectively: mean = 5.9 coccoliths/cell, s = 5.79; mean = 0.8 coccolith/cell, s = 2.42; mean = 3.1 coccolith/cell, s = 4.56; mean = 5.5 coccolith/cell, s = 6.46; mean = 12.6 coccolith/cell, s = 9.66; mean = 14.1 coccolith/cell, s = 11.12; mean = 22.3 coccolith/cell, s = 15.36; mean = 27.8 coccolith/cell, s = 14.01; mean = 35.0 coccolith/cell; s = 14.12

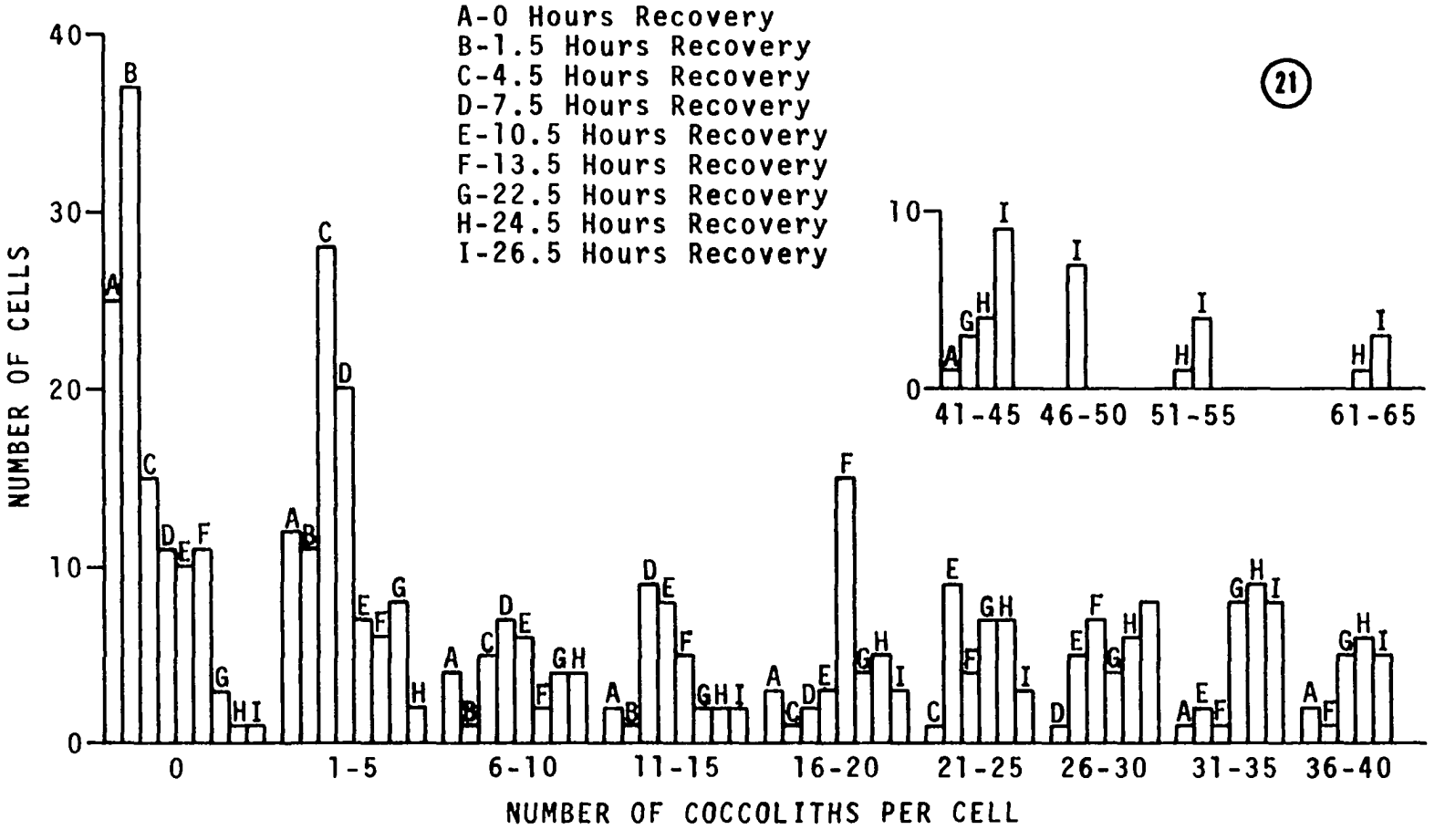
A-0 Hours Recovery
B-1.5 Hours Recovery
C-4.5 Hours Recovery
D-7.5 Hours Recovery
E-10.5 Hours Recovery
F-13.5 Hours Recovery
G-22.5 Hours Recovery
H-24.5 Hours Recovery
I-26.5 Hours Recovery
(21)
NUMBER OF CELLS
NUMBER OF COCCOLITHS PER CELL
0
1-5
6-10
11-15
16-20
21-25
26-30
31-35
36-40
41-45
46-50
51-55
61-65

Figure 22. Determination of the most effective pronase concentration. As the pronase concentration increases, the number of coccoliths per cell decreases. After five hours of recovery in the light, the number of coccoliths per cell has decreased even further (except in E)

A = 0 mg/ml pronase
B = 1 mg/ml pronase
C = 2 mg/ml pronase
D = 4 mg/ml pronase
E = 10 mg/ml pronase

Figure 23. Effect of varying the length of the pronase treatment on coccolithogenesis. See text for explanation

A = controls which include (1) cells on 16 hours of light and 8 hours of darkness, (2) cells incubated in darkness and no recovery, and (3) cells incubated in darkness with 4 hours recovery in light

B = cells incubated in darkness and pronase (2 mg/ml) with no recovery in light

C = cells incubated in darkness and pronase (2 mg/ml) with 4 hours recovery in light

D[1] = cells incubated in darkness, decalcified with EDTA, and allowed to recover in light for 4 hours

E = cells incubated in darkness and pronase, decalcified with EDTA, and allowed to recover in light for 4 hours

---

[1]Fifth data point remained in the EDTA for 90 minutes giving lower count.

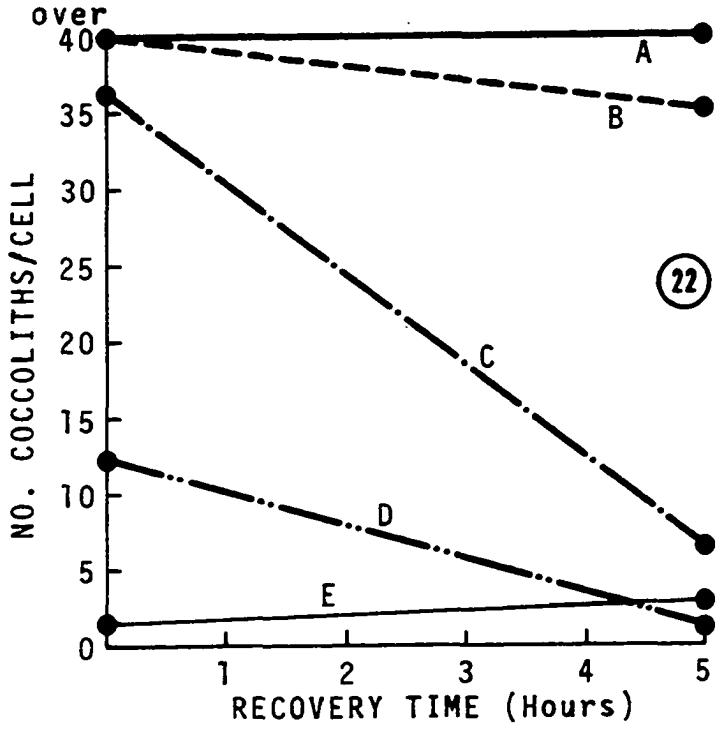
over
40
35
30
25
20
15
10
5
0
NO. COCCOLITHS/CELL
A
B
C
D
E
22
1
2
3
4
5
RECOVERY TIME (Hours)

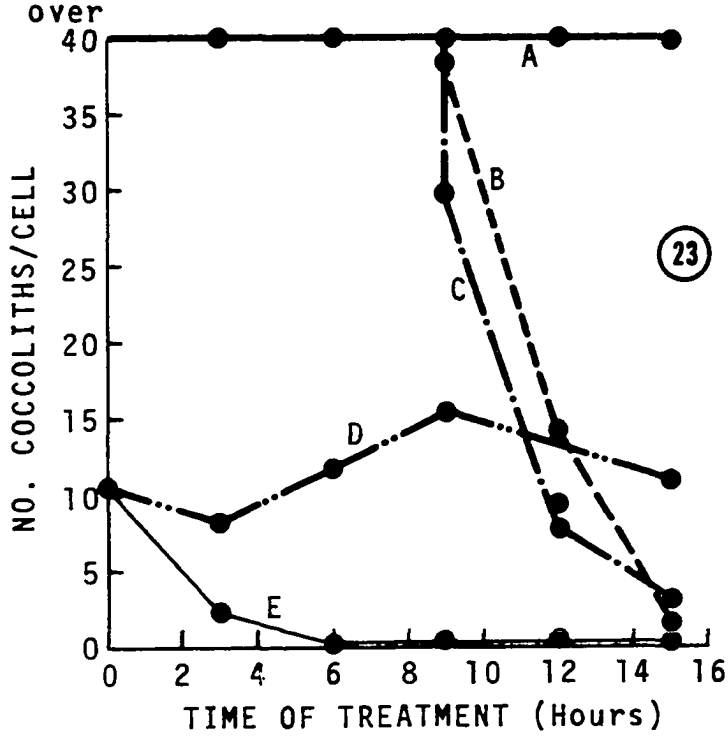
over
40
35
30
25
20
15
10
5
0
NO. COCCOLITHS/CELL
A
B
C
D
E
23
0
2
4
6
8
10
12
14
16
TIME OF TREATMENT (Hours)

The pronase concentration used varied with the lot number. If the cells were washed free of pronase and allowed to recover in the light for five hours (Figure 22), a reduction in coccolith number per cell was detected even in the 1 mg/ml sample.

Time effects How long must the cells remain in pronase before a measurable reduction in coccolith number can be observed? This was tested by placing live cells in a pronase medium in the dark and removing samples at three hour intervals. Each sample of cells was divided in half; the first half was fixed and the coccoliths counted (Figure 23, line B). The second half was washed and incubated in the light for four hours (Figure 23, line C). The four hour recovery time in the light was arbitrarily determined to provide sufficient time for any differences to develop. Line B (Figure 23) shows that it takes nine hours of pronase treatment to achieve a detectable reduction in coccoliths per cell. Line C shows that there is an additional reduction in coccoliths per cell during the four hour period in the light. The controls (line A) show that normal cells always possess more than 40 coccoliths.

There were many coccoliths on the cells during the first nine hours of the pronase treatment, and it was impossible to determine if cells were making new coccoliths during this time. To test this, two parallel experiments were conducted and compared. In the first instance cells were placed in the dark (Figure 23, line D), and in the second condition cells were placed in the dark with pronase added to the medium (Figure 23, line E). Samples were removed at three hour intervals, treated with EDTA to remove coccolith rims, washed, incubated in the light for four hours, and the number of coccoliths per cell counted. (Again the four hour light recovery

was thought to be a sufficient time for any differences to arise.) After three hours of incubation, the dark pronase treated cells (line E) make fewer coccoliths than the dark cells do (line D). By six hours of incubation, dark pronase treated cells did not make any coccoliths, but dark cells made more than they did at three hours. Pronase has shut down the manufacture of coccoliths.

Diurnal cycle effects An additional question is whether a "clock" controls biochemical responses or whether light and energy production can explain the effects of coccolithogenesis. The diurnal cycle has an effect on the rate at which cells manufacture coccoliths. For example, line D of Figure 23 shows that coccolith production varies depending on the length of time the cells are in the dark. The greatest production occurs after 9 hours in the dark which corresponds to the end of the 8 hour dark period of the normal diurnal cycle. The low coccolith production at 0 and 3 hours indicates a slowing of coccolithogenesis during the nonphotosynthetic part of the diurnal cycle. Subsequent samples taken at various times during the light period show a maximum during the first 4-8 hours followed by a graduate decline. Coccolith production during the dark period is known to be only 2-3 coccoliths per hour (Williams, 1972, 1974).

Morphology of regeneration Scanning electron microscopy of the pronase treated cells (Figure 24) reveals an essentially naked surface with a smooth to somewhat "lumpy" appearance and occasionally valleys and pockets. There are very few coccoliths on the cell; they remain free and appear unaffected by the pronase. In this micrograph, favorable views of the apparently normal coccoliths show that the lower (proximal) surfaces of the coccolith bases are smooth, while on edge they show the groove formed

Figure 24. SEM of pronase treatment showing the pronase effects on the cells and coccoliths. Note the smooth, lower (proximal) surface of coccolith bases (arrows) and the grooves in the coccolith rims (arrowhead). X 5,800

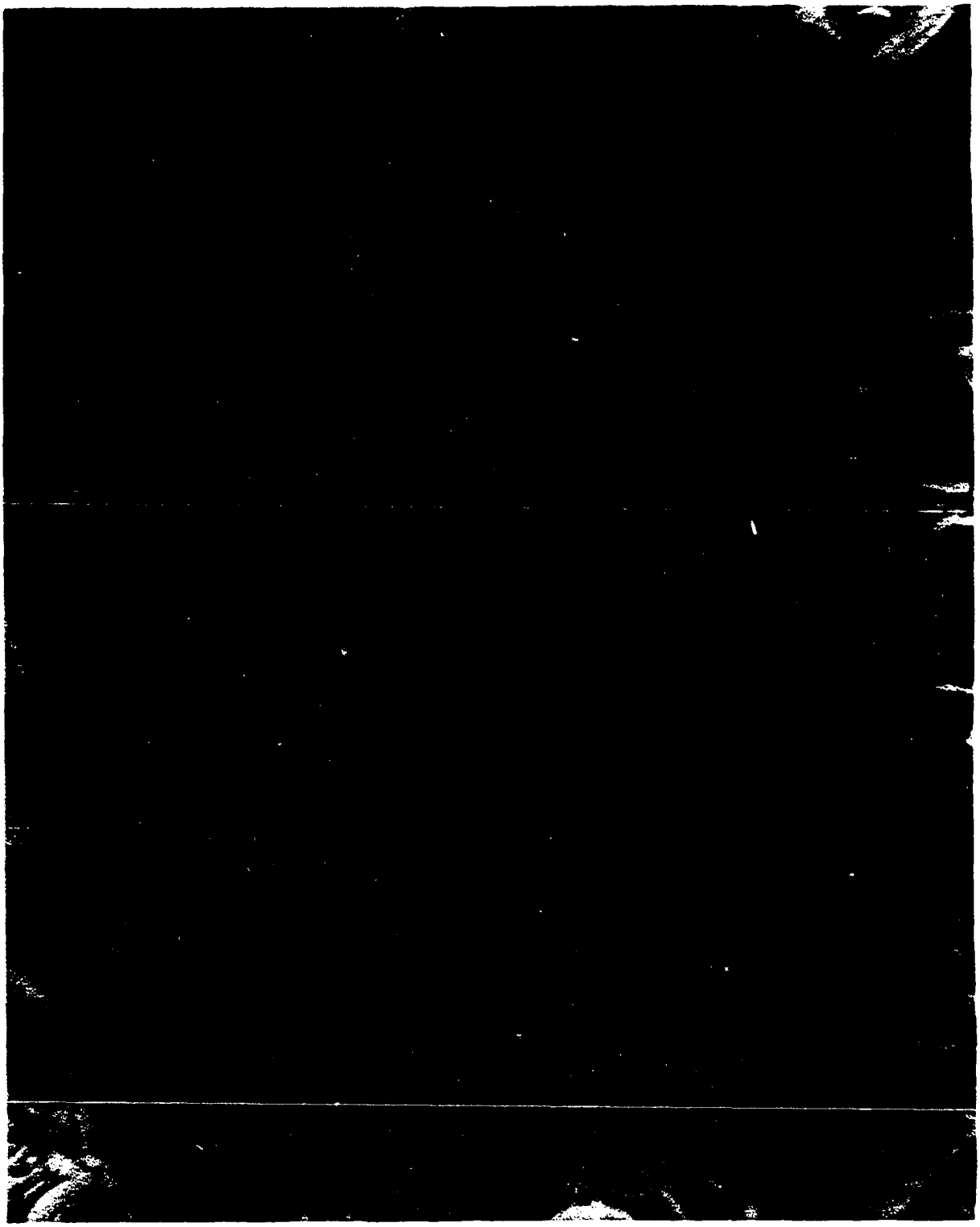

by the alternating A and B elements fitted around the base. Coccoliths show some variation in size (diameters of the bases) which is unrelated to the pronase treatment. Although not visible here, coccolithonets are found on the cells following the pronase treatment.

Ultrastructural alterations from the pronase treatment were assessed from thin sections of the treated material (Figures 25-27). Inside the cell (Figure 25), the Golgi apparatus shows unusual amounts of membranes lying in dilated cisternae or vacuoles both proximally (arrows) and distally (arrowheads). Even the medial Golgi region seems unusual with scales and coccolithosomes apparently randomly distributed. From this and other micrographs, it appears that, at the least, the normal Golgi processing for export has been disrupted. No enzymatic damage is evident in the scales or coccolith rims and bases (Figures 26 and 27); even crossbridging is present between the radials of scales and bases (Figure 27). In Figure 26 the wall of the cell is discontinuous (arrowheads) no doubt owing to the removal of coccoliths and many of the scales, although some of the latter remain on the surface. There is no columnar material present on the cells.

After four hours of recovery from the pronase treatment, the cell is a protoplast (Figure 28). There are no outside scales, coccoliths, or columnar material. The Golgi apparatus is in an abnormal state with expanded cisternae. Coccolithosomes and scales are present but rarely are internal coccoliths seen at this recovery stage.

An example of a cell at 12 hours of recovery after pronase treatment is shown in Figure 29a. The cell has formed a single ring of scales and synthesized some columnar material. Several coccoliths have been deposited on the cell surface; note their random distribution. None of the coccolith

Figures 25-27. Thin sections of pronase treated material demonstrating pronase effects

Figure 25. Section showing Golgi region. Present are membranous whorls (arrows), scales (S), and coccolithosomes (Co). X 20,000

Figure 26. Cross section of coccoliths removed by pronase. Note the reduced scale layer and absence of columnar material. Also note the base-to-base configuration (arrow). X 36,000

Figure 27. Oblique section through a coccolith and some scales. No digestion is evident in the scales, rims, or bases. Note the cross-bridging in the scales and base (arrows). X 72,000

25

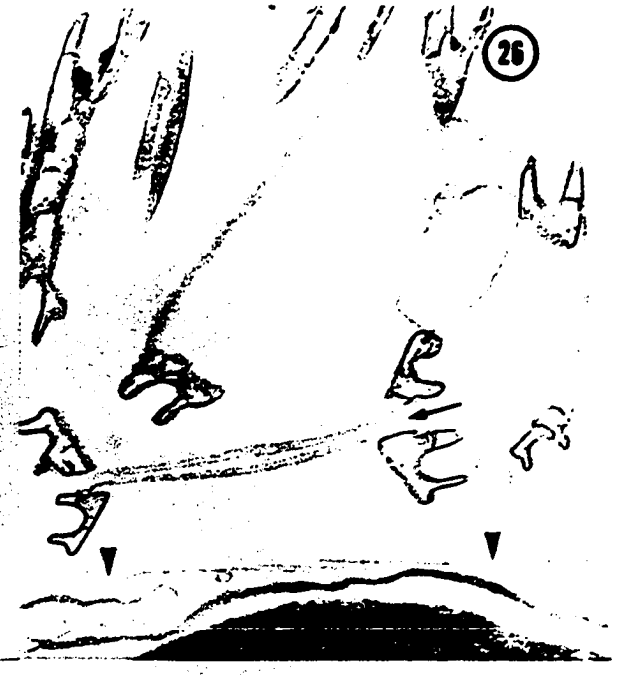

26

27

Figure 28. Cell after four hours recovery in the light from a 12 hour pronase treatment. The cell wall is absent. Present are chloroplasts (Ch), mitochondria (M), and an abnormal Golgi (G) with scales (S) and coccolithosomes. X 20,000


S
S
Co
28

Figure 29. A cell at 12 hours recovery from pronase treatment

Figure 29a. Present are a nucleus (N), Golgi (G), vacuoles (V), chloroplasts (Ch), layer of scales (S), and some coccoliths (C). Note the section through the haptonema (H). X 20,000

Figure 29b. Enlargement of the internal coccolith. Note the inverted arrangement of the A element on the base (arrow). X 72,000


S
A

rims are normal in shape (see Figures 14, 17, 18, and 26 for examples of characteristic rim morphology). The enlarged internal coccolith (Figure 29b) illustrates an A element that has been added to the base upside down. This kind of abnormality is interpreted to suggest that morphogenetic elements located in the cisternal membranes have become disoriented (the cause) resulting in either an unusual rim or an unusual peripheral membrane/anvil relationship or both (the effect) (see Discussion).

The bizarre nature of the coccoliths made by cells after 12 hours of recovery is illustrated in Figure 30. The coccolith rims have atypical shapes and internal vesicular material (arrows). The bases are irregularly "wavy" and of varying thickness with poorly formed edges (no "notch" is present at arrowhead). (See Figures 26 and 27 for a comparison of coccoliths after pronase treatment.) A major increase in new wall production occurs in the second interfission period after removal from pronase (see Figure 20); thus it seems that the occurrence of the first cytokinesis marks the return to a normal or near normal synthetic pattern.

Cells after 24 hours recovery from pronase show a wall with its parts in the proper places (Figure 31). The columnar material is more evident, the scales have formed a layer at least one scale thick, and some normal coccoliths have appeared (Figure 33), although aberrant coccoliths are still present (Figure 31). The Golgi apparatus has a more normal appearance with increased numbers of cisternae (Figures 32 and 33). Some Golgi seem to be producing mostly scales (Figure 32), while others show only coccolith assembly (Figure 33). Some peculiar membrane profiles still exist in association with the Golgi which are interpreted as still representing effects of and perhaps recovery stages from pronase treatment.

Figure 30. TEM micrograph illustrating the peculiar shapes of the coccoliths on cells after 12 hours of recovery from pronase treatment. Note the "wavy" bases, the absence of a "notch" on the edge of one coccolith (arrowhead), and vesicular material inside the rims (arrow). Columnar material (Cl) is beginning to appear. X 55,800

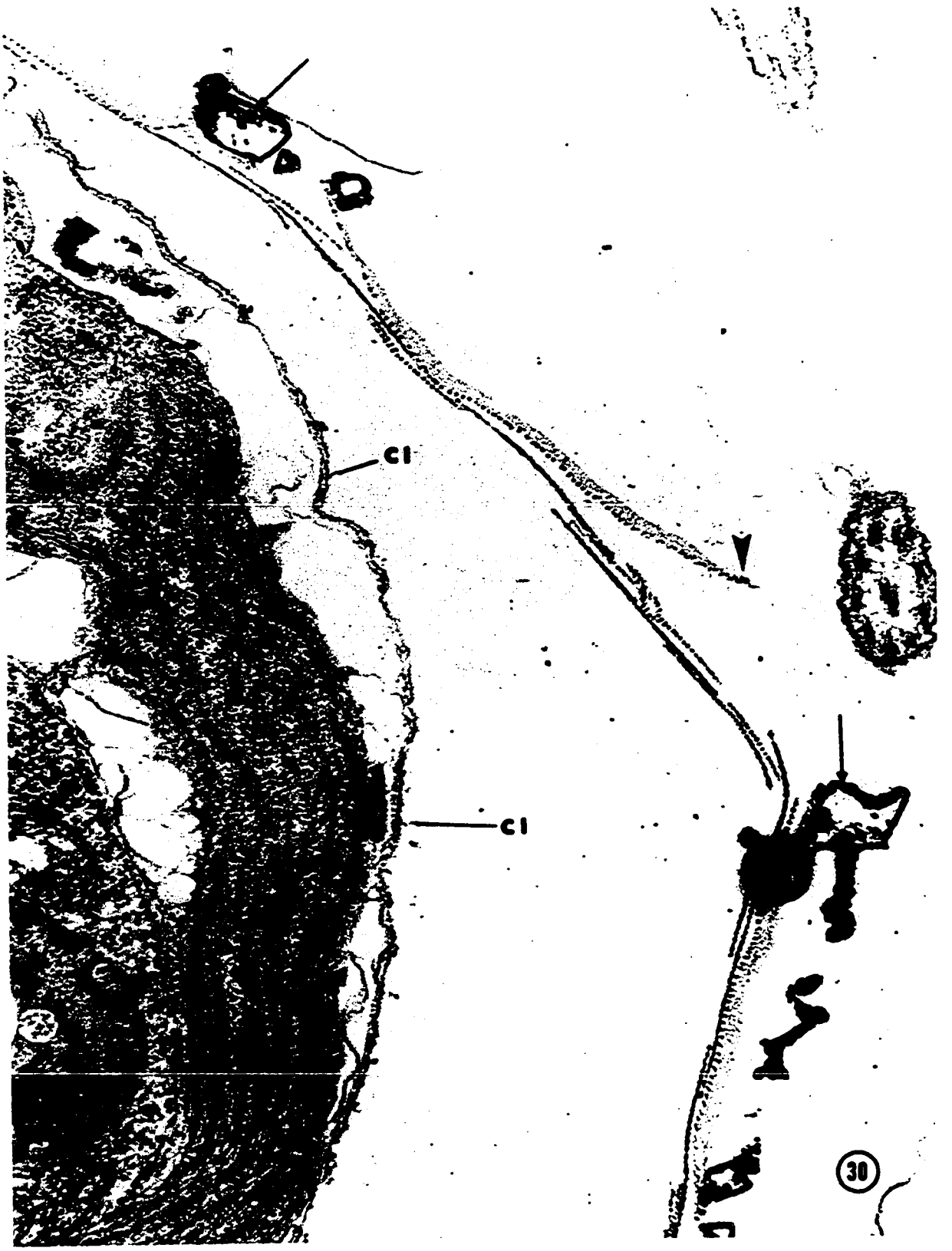
C1
C1
30

Figures 31-33. Cells from 24 hours of recovery from pronase treatment

Figure 31. The cell wall has columnar material (Cl), a layer of scales, and coccoliths. Note the vesicular, aberrant nature of the coccolith rims (R). X 72,000

Figure 32. The Golgi apparatus (G) is producing mainly scales, although some coccolithosomes (Co) are present. Note the unusual membrane proliferation in the lateral earpockets and distal cisternae (arrows). X 20,000

Figure 33. New internal coccoliths (iC) are visible within Golgi cisternae and the unusual kinds of membrane profiles resembling those shown in Figure 32 are present again (arrows). X 27,500

The Chemistry of the Cell Wall

Disassembly and reassembly of the wall

Fractionation Cells proved to be difficult to homogenize and still maintain nearly complete exoskeletons and intact cell organelles. Efforts to find optimal homogenization conditions centered around the selection of a suitable homogenizer, the development of a satisfactory homogenization medium, and the separation of the desired cell components from the undesired fractions.

Several kinds of ground-glass hand homogenizers or Teflon-glass homogenizers of the Potter-Elvehjem type were tried, but they failed to break up more than 20% of the cells. A French press at 1300-1400 lbs/in^2 provides homogenates with aggregates containing 10-15% whole cells. The Servall Omni-Mixer yields similar results to the French press and was used in the experiments reported here because it was more convenient. None of these homogenization procedures gave intact exoskeletons.

The choice of homogenization medium depended on the fraction of the cell desired. If cell walls were needed, the PMW_{III} solution (see Materials and Methods) provides a greater yield of wall material. If internal components like the Golgi apparatus, endoplasmic reticulum, or other membranous organelles were desired, Morre's buffer (MHM) for rat liver fractionation (Morre et al., 1969) was used.

Attempts to fractionate the cell into different membrane fractions on discontinuous sucrose gradients yielded enzymatic and morphological patterns which were unusual compared to liver, for example, and it was difficult to decide whether such results arose through experimental errors or represented membrane systems which were quite different from the usual

plant and animal tissues (or perhaps both). In hindsight, the latter explanation seems the more probable based on the cytochemical evidence to be discussed later.

Frozen and unfrozen cells gave identical results for the cell wall studies that I conducted with the exception that less pigment contamination was obtained with fresh cells; that is, the fresh cells provided milky, white walls and frozen cells yielded green walls.

Dissociation In order to obtain wall components for chemical analysis and other studies, a procedure was needed to separate the scales and coccoliths from the "glue" with which they are embedded and attached to the wall. Two such methods were familiar to us. First Triton X-100, a mild, nonionic detergent, had been used by us for isolating coccoliths and scales from Hymenomonas (Kuratana, 1974). Secondly, an extracellular enzyme preparation associated with a seawater wash of agar plates after zoospore release (Brown et al., 1970) had been used to obtain scales from Pleurochrysis, a probable alternate life cycle form of Hymenomonas. Both of these procedures yielded little information about the "glue" or other non-scale coccolith components. An alternative method utilizing the chaotropic agents, lithium chloride and sodium perchlorate, had been used successfully with Chlamydomonas (Hills, 1973) to obtain a reversible dissociation of the cell wall; it was tested and is reported here for Hymenomonas.

The effects of 10 M LiCl are shown in a sample taken from the supernatant of a cell homogenate (see Material and Methods, page 38) as seen in Figure 34. While still in LiCl, the scales and coccoliths were dispersed from the wall. Fibrous material with finger-like projections is seen free and associated with the coccoliths and scales. The material tends to bind

Figure 34. Walls from homogenized cells in 10 M LiCl. Coccoliths and scales are released from the glue, and fibrous subunits appear which laterally associate with each other and form end-on associations with the coccoliths and scales (arrows). Small spherosomes are occasionally visible (arrowheads). Note that the underside of a coccolith is visible (CU). 1% ammonium molybdate staining. X 10,800

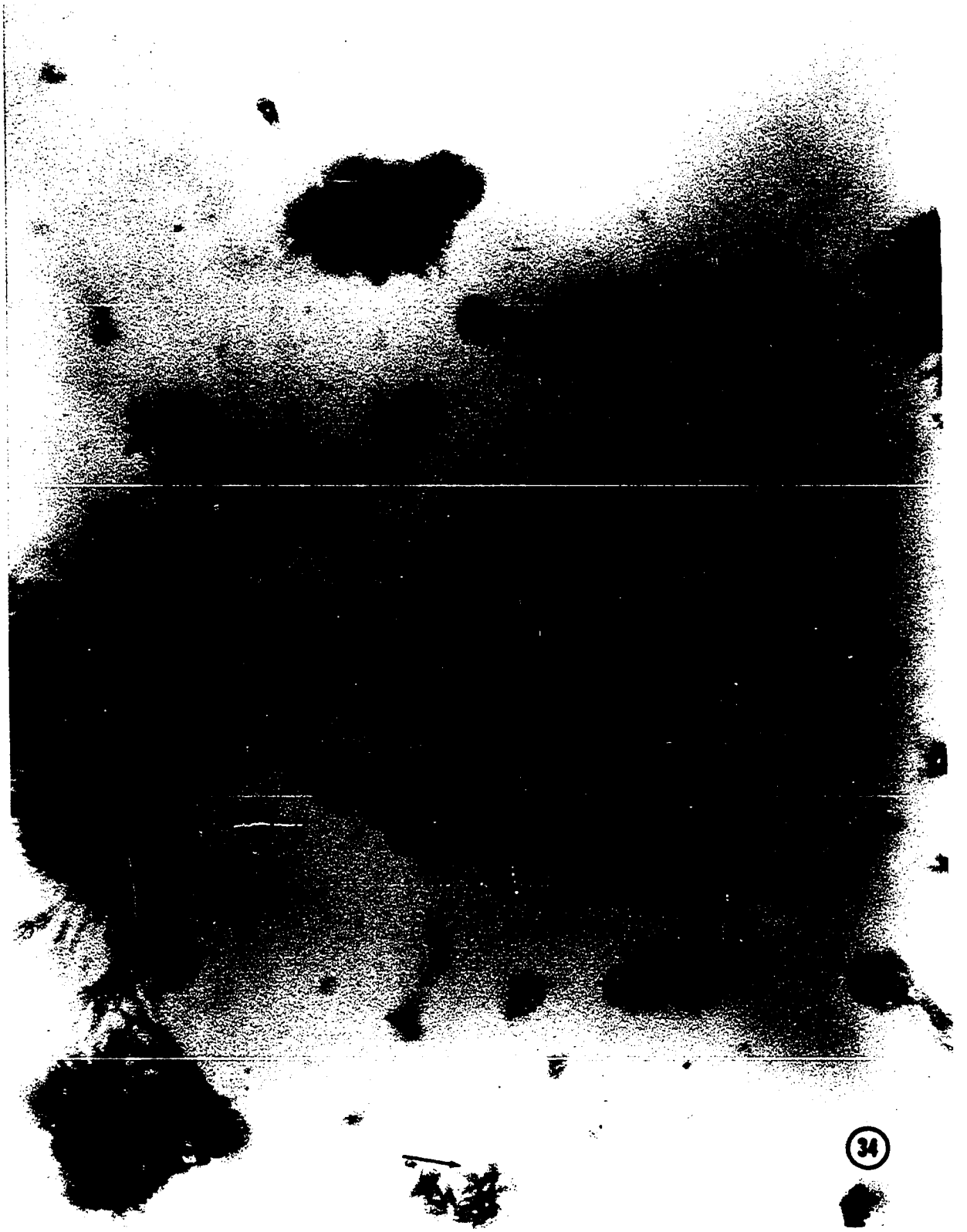
34

laterally with itself and have end-on associations with the coccoliths and scales (arrows). Subunits of the fibrous material range in length from 210 nm to 860 nm with an average length of 510 nm and range in width from 50 nm to 72 nm. Coccolithonets, by comparison, range in length from 43 nm to 670 nm with an average length of 230 nm and range in width from 20 nm to 35 nm. The walls of homogenized cells that are untreated with LiCl are so electron dense that a 100 kv electron beam can't penetrate them. This fibrous material is tentatively identified as the electron-transparent wall "glue" of sectioned material.

The coccolith bases and scales have no obvious defects from the 10 M LiCl (Figure 35). The calcified rims are still intact as are concentrics and radials of both coccolith bases and scales. Figure 36 shows a haptonemal scale also with no apparent damage.

Small "fuzzy" spheres with 80-110 nm diameters are released during LiCl solubilization. These spherosomes look "membranous" and, based on their size and morphology, are tentatively identified as the membrane spheres found distal to the plasma membrane and proximal to the scales (for example, see Figure 17).

If 6 M $NaClO_4$ is substituted for 10 M LiCl, the cell wall dissociates in a similar manner. However, the treatment does considerably greater damage to the coccolith rims (Figure 38), although the coccolith bases and scales appear relatively normal (Figures 38 and 39). Plainly visible are radials and concentrics. Spherosomes are sometimes present (Figure 39) and seem to be associated with material ramifying (arrow) from the edge of the scale.

Figure 35. A coccolith and some scales in 10 M LiCl showing little damage to scales and coccolith bases with some degradation of anvil elements. 1% ammonium molybdate staining. X 52,800

Figure 36. A haptonemal scale in 10 M LiCl with no structural damage. 1% ammonium molybdate staining. X 123,000

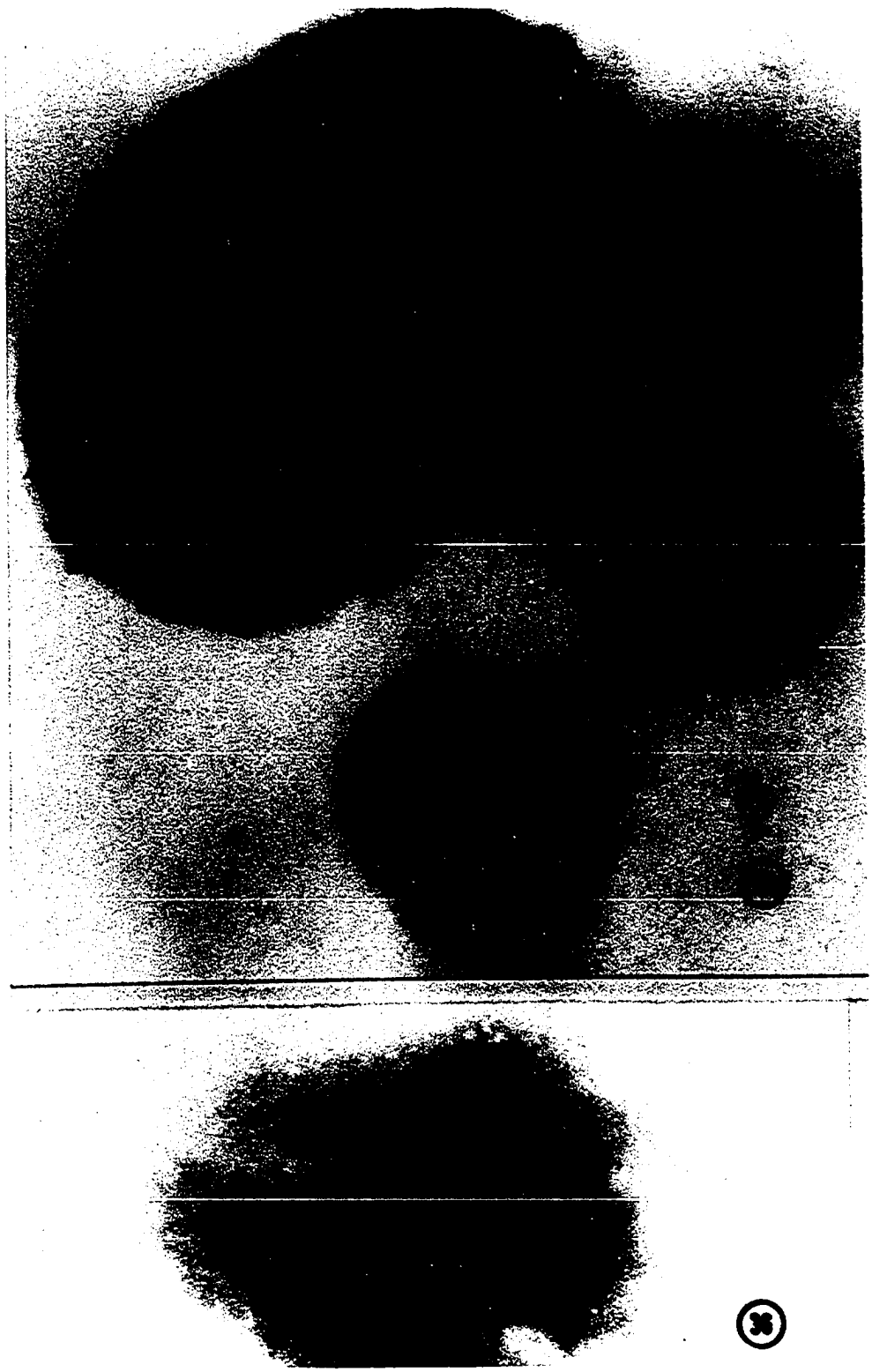

Figure 37. Spherosomes released in the presence of 10 M LiCl. Note their "fuzzy" appearance. 1% ammonium molybdate staining. X 123,000

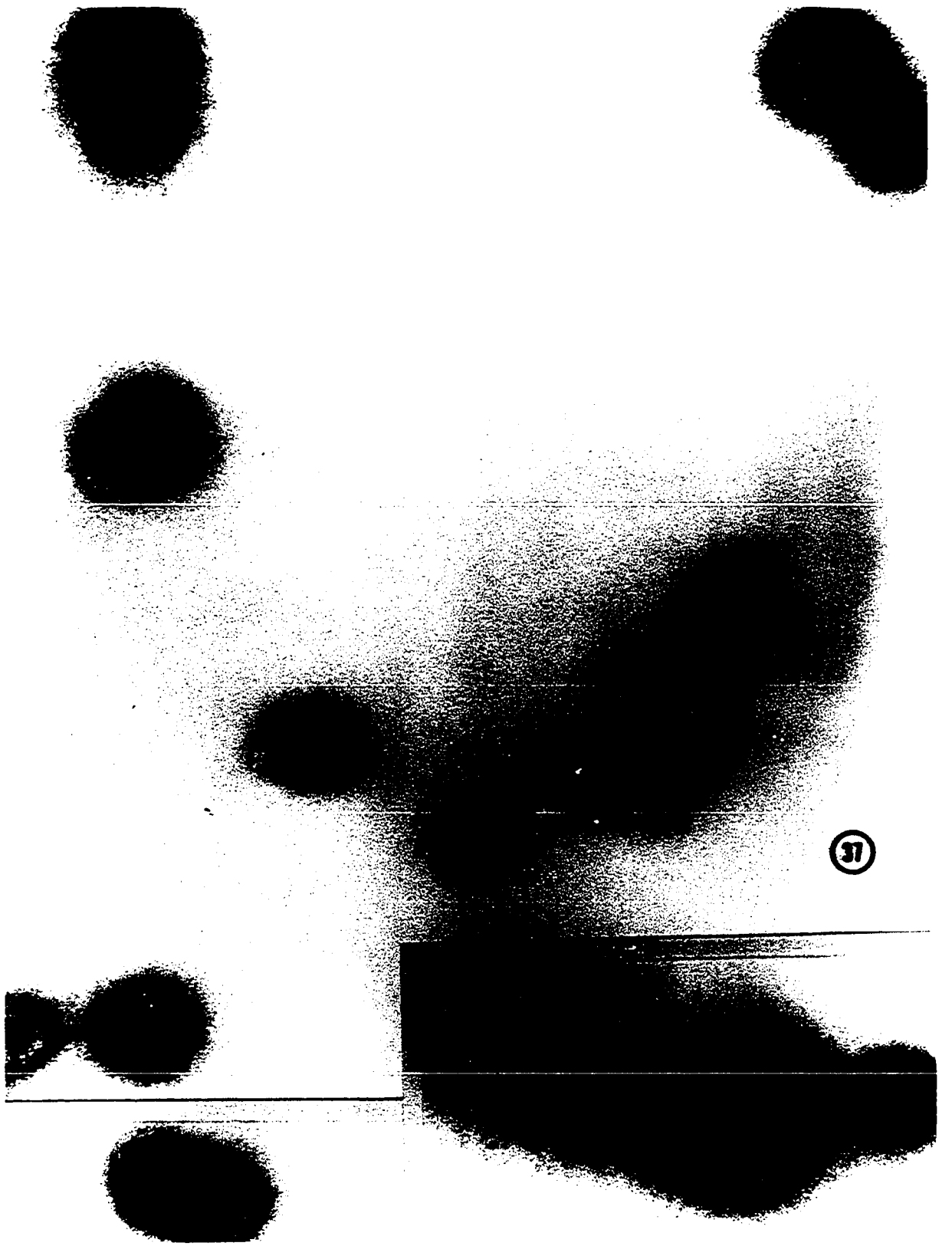
37

Figures 38-39. Cell walls from homogenized cells in 6 M $NaClO_4$. 1% ammonium molybdate staining. X 78,400

Figure 38. The coccolith rims show structured damage, but concentrics are visible in the base. Concentrics and radials are present in the scales

Figure 39. Concentrics (Cc) and radials are seen on the scales. Note the spherosome (arrow)

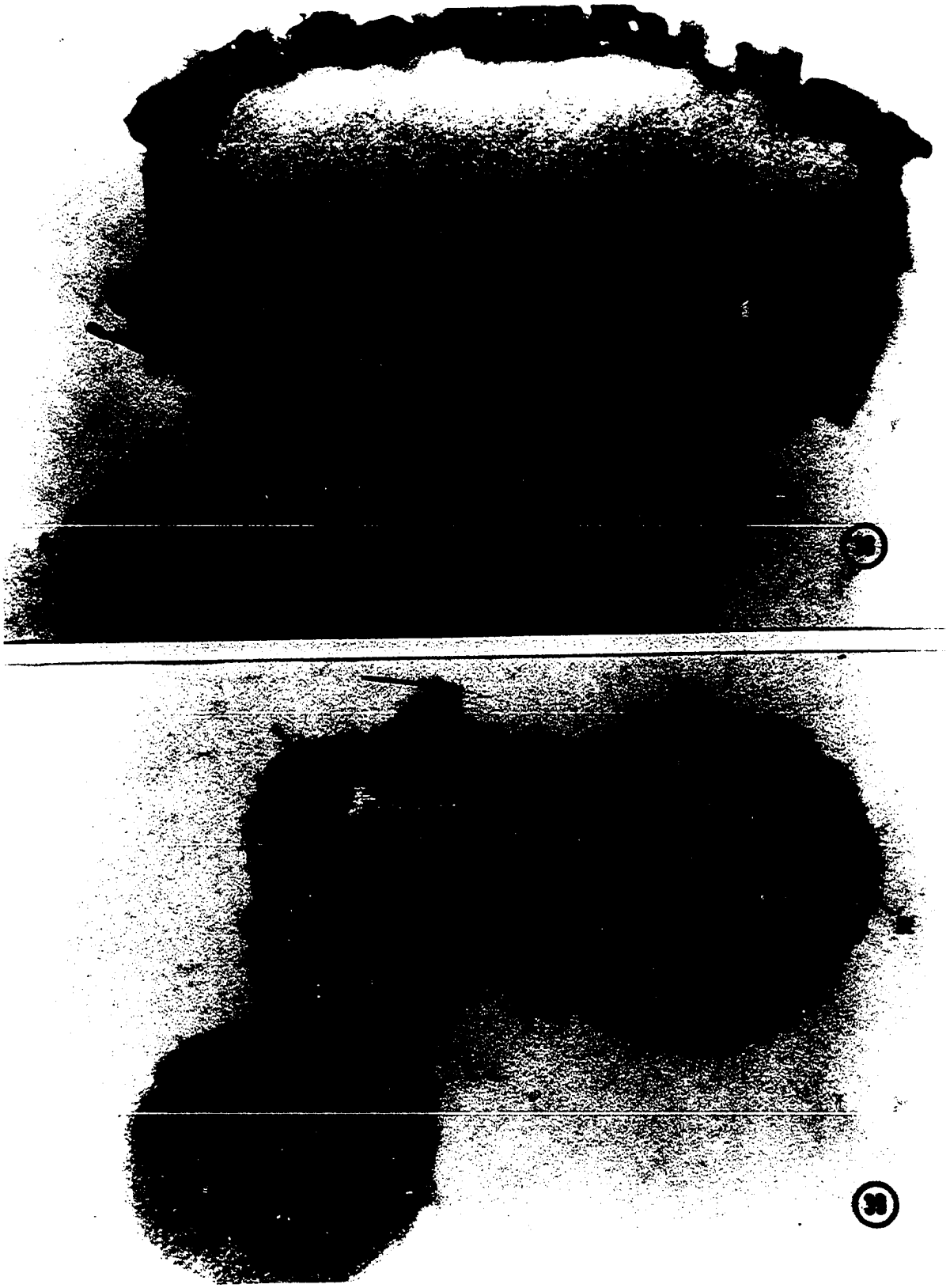

Reassociation When LiCl dissociated cell walls are placed in a dialysis bag and dialyzed against water, a reassociation of the material results that is easily visible with the naked eye. The appearance of the dissociated and reassociated material is shown in Figure 40. The extent of reassociation depends on the source of the walls. If whole cells are placed in LiCl and reassociated, a large ball or clump forms; if walls from homogenized cells are used and reassociated, several small clumps form. No reassociation occurs when LiCl material is spun at 7000 g for 30 minutes and that supernatant dialyzed against water. Finally the walls from homogenized cells are much better for TEM observations.

Figure 41 shows an electron micrograph of the reassociated walls of homogenized cells after 10 M LiCl solubilization. The major portion of this reaggregate is fibrous material with greater lateral association than in Figure 35 and is often so thick that the electron beam can't penetrate it. Subunits are not readily identifiable. The 6 M $NaClO_4$ treated walls reaggregate into long strands similar to the LiCl treated material, but, in $NaClO_4$, subunits are more evident (Figure 42). This is another indication that $NaClO_4$ has a somewhat different effect on wall components than LiCl. In balance, less structural damage seemed to occur with LiCl, and it was, therefore, used for most future experiments.

In order to test the effects of various factors on reaggregation, a means of obtaining solubilized walls that did not reaggregate was needed and is summarized in the flow sheet in Figure 43a. Whole cells or walls from homogenized cells are placed in 10 M LiCl for two hours, and unbroken cells are spun out by centrifugation for 5000 g min (1000 g for 5 minutes). The supernatant is placed in a dialysis bag, LiCl is removed, replaced with

Figure 40. Picture of LiCl dissociated and reassociated wall material before and after dialysis

Before Dialysis

After Dialysis

Figure 41. Reassociated wall material after 10 M LiCl treatment of walls from homogenized cells. Note the fibrous nature of the reassociated product and the variation in fiber density presumably due to differences in lateral association of subunits. 1% ammonium molybdate staining. X 36,000

Figure 42. Reassociated wall material after 6 M $NaClO_4$ treatment of walls from homogenized cells. Note the less dense fibers and more obvious subunits. 1% ammonium molybdate staining. X 20,000

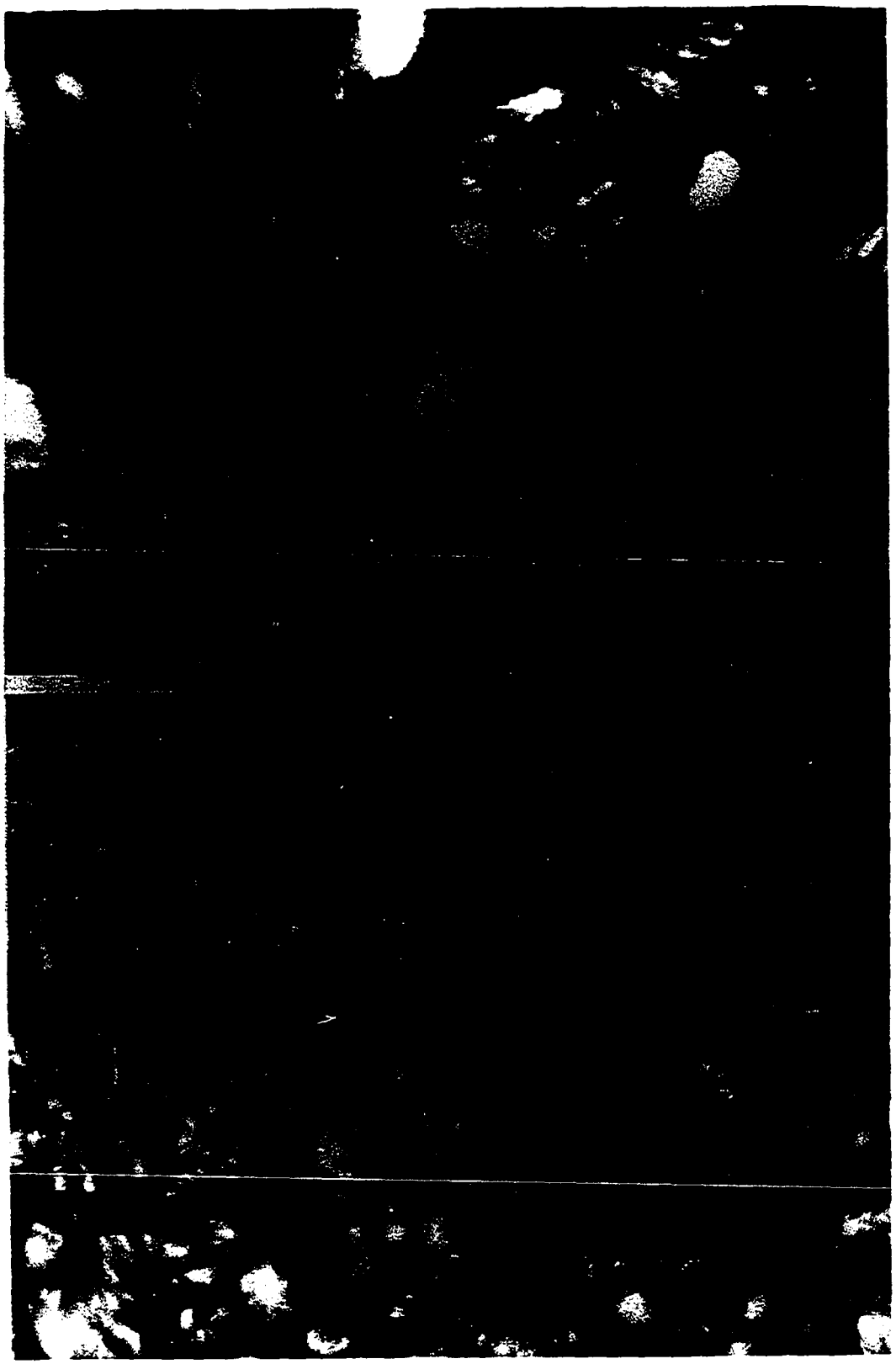

Figure 43. A flow sheet for the biochemical analysis of solubilized cell wall factions

Figure 43a. Flow sheet for the analysis of reaggregation following LiCl solubilization

Figure 43b. Flow sheet for the analysis of reaggregation following EDTA solubilization

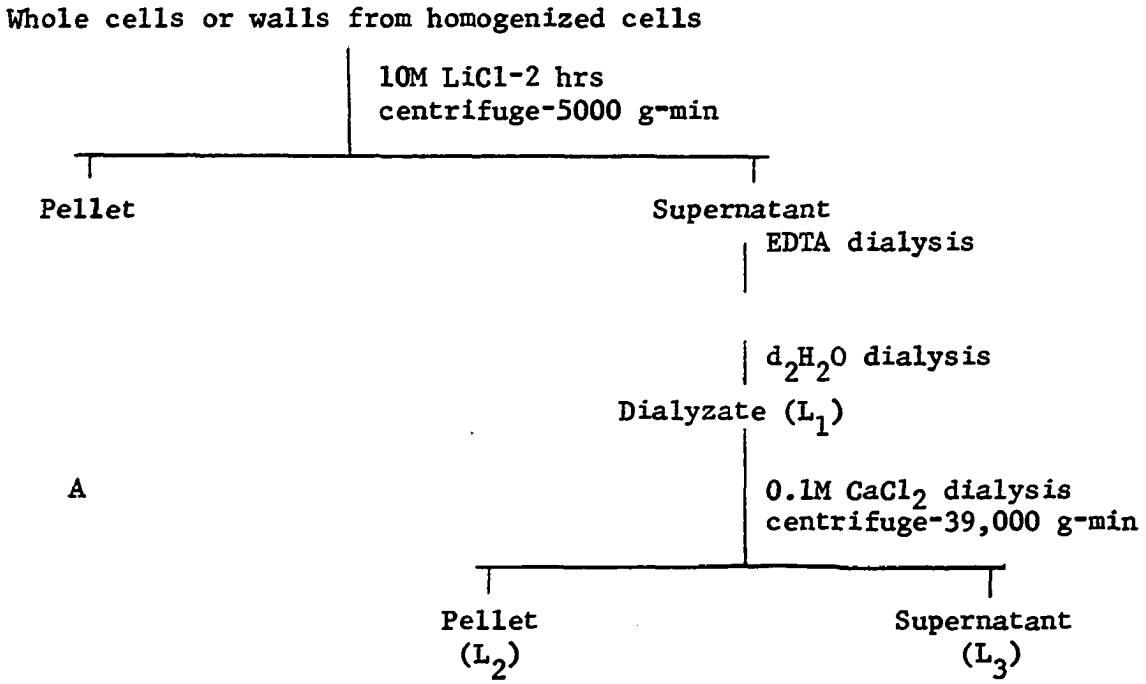
Whole cells or walls from homogenized cells
10M LiCl-2 hrs
centrifuge-5000 g-min
Pellet
Supernatant
EDTA dialysis
d_2H_2O dialysis
Dialyzate (L_1)
A
0.1M $CaCl_2$ dialysis
centrifuge-39,000 g-min
Pellet
(L_2)
Supernatant
(L_3)

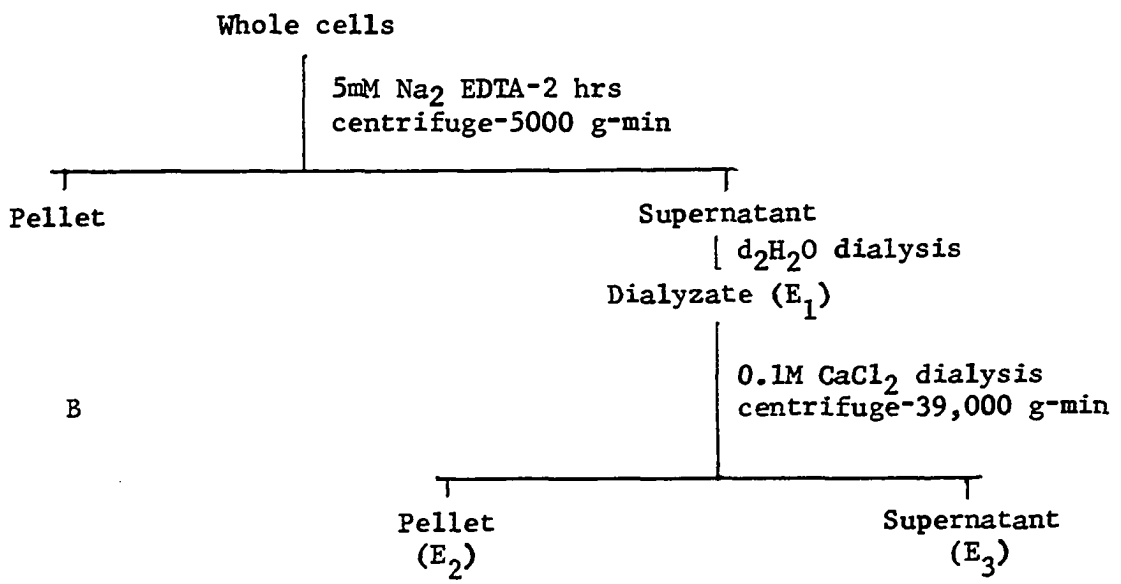
Whole cells
5mM Na_2 EDTA-2 hrs
centrifuge-5000 g-min
Pellet
Supernatant
d_2H_2O dialysis
Dialyzate (E_1)
B
0.1M $CaCl_2$ dialysis
centrifuge-39,000 g-min
Pellet
(E_2)
Supernatant
(E_3)

EDTA and no reaggregation occurs. Presumably the EDTA dialysis results in the chelation of cations that would otherwise induce reassociation. For removal of the EDTA, the dialysis bag is next transferred to double distilled water. After dialysis, reaggregation still has not occurred. Factors responsible for reaggregation can be tested; the fraction in the dialysis bag is the dialyzate (L_1).

A limited number of ions was tested for their ability to elicit a reaggregation response. The results are given in Table 4. Calcium ions provide the most rapid reassociation rate, and the reassociation rate varies with its concentration. Magnesium ions substitute for calcium ions but the rate is slower. The monovalent cations, Na^+ and K^+, did not bring reaggregation within two hours. For anions, the nitrate ion could be substituted for the chloride ion and the sulfate ion inhibited. Thus, a calcium dependency for reaggregation seems established, with some substitution by magnesium ions possible.

Figure 44 shows the effect of pH on reaggregation. The optimum pH is approximately 7.5, and no reaggregation occurs below pH 4.5 or above pH 11.8. The line is only approximate above pH 10 which is beyond the physiological range anyway. There now is established a pH dependency as well as a divalent cation dependency for reaggregation.

Biochemical analysis The material extracted from live cells by 5 mM Na_2 EDTA was analyzed for protein and carbohydrate using the Lowry and phenol-sulfuric acid methods, respectively; results are presented in Table 5. After two hours, EDTA extracts 4.8% of the cell's carbohydrate and 0.7% of the cell's protein. After 7 hours of extraction, 17.7% of the cell's carbohydrate content and 6.5% of the cell's protein content are

Table 4. The effect of ions on the aggregation process

Compound tested	Ionic strength of the solution[a]	Relative rate of response
$CaCl_2$	0.90[c]	++++[b]
$CaCl_2$	0.30[c]	+++
$Ca(NO_3)_2$	0.90[c]	++++
$CaSO_4$	0.04[c]	++
$MgCl_2$	0.90	++
$MgSO_4$	1.20	+
NaCl	0.30	-
Na_2SO_4	0.90	-
KCl	0.30	-

[a]Ionic strength calculated according to the following formula: $\mu = \frac{1}{2} \Sigma mZ^2$ where μ = ionic strength, m = molarity of the ion, Z = charge of the ion, and Σ = summation of mZ^2 for all ions (White *et al.*, 1968).

[b]Relative units based on approximate time for reaggregation to be visualized: ++++ = 2-4 minutes, + = approximately 30 minutes, and - = no reaggregation within 2 hours.

[c]Molarity of solution was 0.01 M; all others were 0.3 M.

removed. The third extraction indicates that prolonged EDTA treatment results in nonspecific extraction which is probably due to cell injury and death. Any future experiments must consider eliminating lengthy EDTA treatment of whole cells to reduce this nonspecific extraction.

Using the fractionation schemes in Figure 43, the dissociated and reassociated walls were analyzed by disc-gel electrophoresis. The dialyzate (L_1), the reaggregated pellet (L_2), and the supernatant (L_3) were stained using Coomassie blue for proteins and PAS for carbohydrates. In Figure 45 carbohydrate staining of the fractions reveals a single band near the bottom of the gel in L_1 and L_2, but nothing appeared in L_3. If EDTA

Figure 44. Graph showing the effect of pH on reaggregation

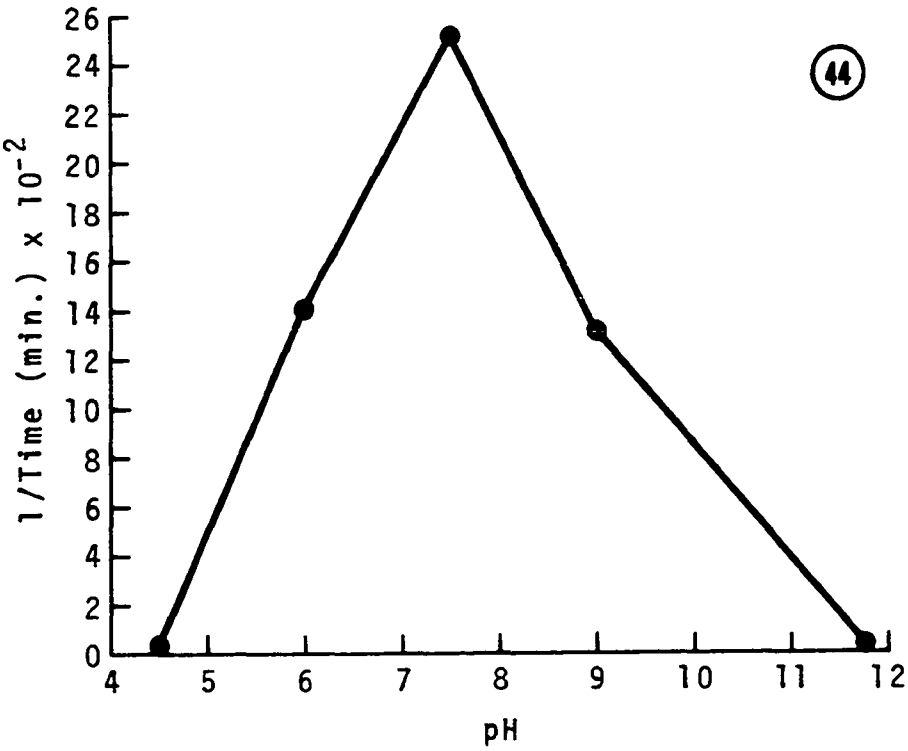
26
24
22
20
18
16
14
12
10
8
6
4
2
0
1/Time (min.) x 10^{-2}
4
5
6
7
8
9
10
11
12
pH
44

Table 5. Lowry and phenol-sulfuric acid analysis of live cells treated with 5 mM EDTA

	Extraction time (hours)	Carbohydrate		Protein	
		Amount extracted (μg/ml)[a]	% extracted	Amount extracted (μg/ml)[a]	% extracted
Extraction No. 1	2	81	4.8	23	0.7
Extraction No. 2	2	70	4.1	13	0.4
Extraction No. 3	3	148	8.8	192	5.4
Cell pellet		1490		3300	
Total	7	1689	17.7	3528	6.5

[a]Average of 3 separate samples.

and no LiCl were used to solubilize the walls (Figure 43b), similar electrophoretic results are obtained for the dialyzate (E_1), reaggregated pellet (E_2), and the supernatant (E_3) when stained for carbohydrate (Figure 45), i.e., the same single band appears and disappears.

If protein staining of the same fractions is carried out (Figures 46 and 47), no corresponding band migrates to the position of the carbohydrate and must be less than 20,000 daltons because of its migration at or ahead of the tracking dye. A comparison of the protein bands obtained with LiCl and EDTA solubilization (Figure 47) shows the number and migration position to be nearly identical. There is one additional protein band (arrowhead) after EDTA treatment. Also there are two bands near the bottom of the gels which appear to undergo some modification since they seem altered in density and width. The function, if any, of these proteins in reaggregation

Figure 45. Disc gel electrophoresis of LiCl and EDTA dissociated and reassociated fractions stained for carbohydrates with PAS reagent. Note the single band near the bottom of the gel for L_1, L_2, E_1, and E_2 and no band in L_3 nor E_3 (arrow). (See Figure 43 for sample identification)

Figure 46. Disc gel electrophoresis of LiCl dissociated and reassociated fractions compared for corresponding bands from protein (CB) and carbohydrate (PAS) staining of the gels. There is no protein band corresponding to the PAS positive band (arrow).

Figure 47. Disc gel electrophoresis of LiCl and EDTA dissociated and reassociated fractions comparing their protein bands. Note the band difference for L_2 and L_3 (arrowhead)

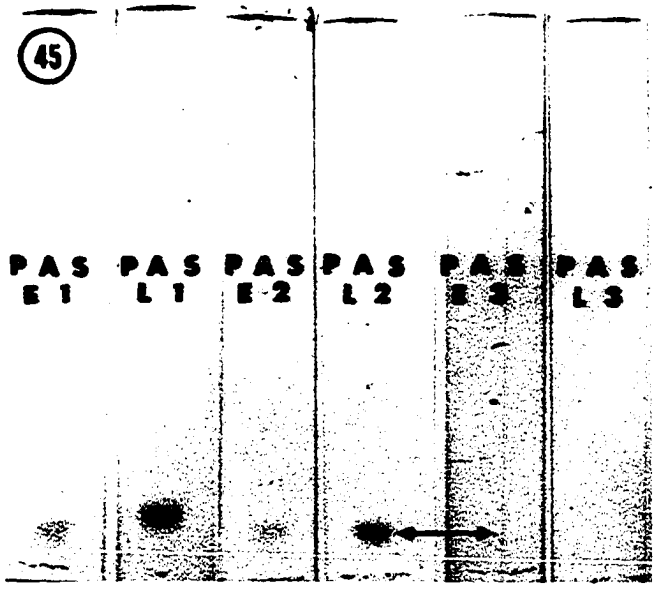
45
PAS E1
PAS L1
PAS E2
PAS L2
PAS E3
PAS L3

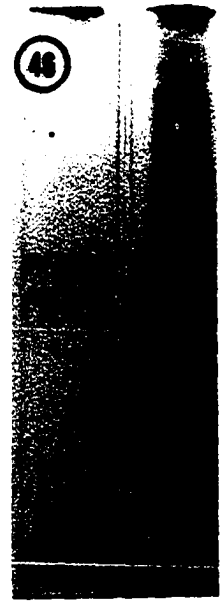
46

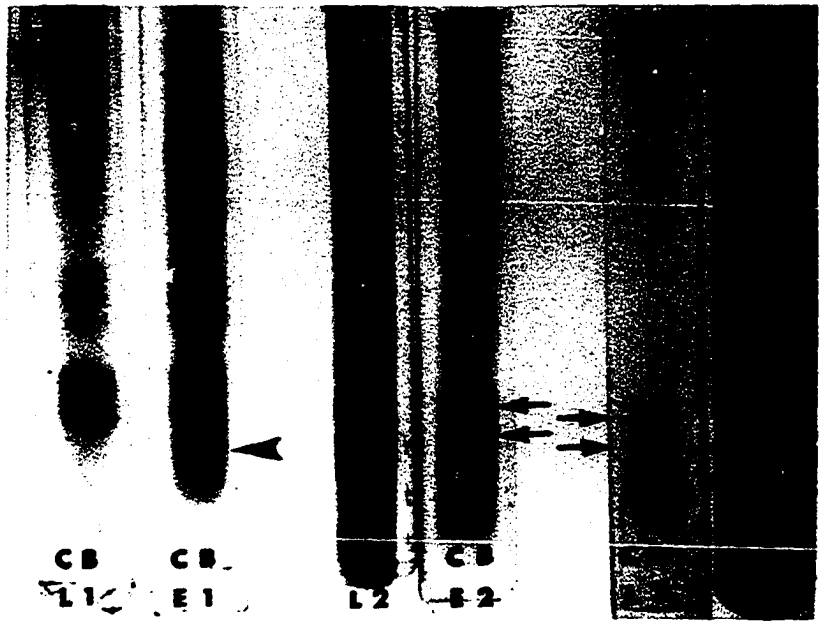
CB L1
CB E1
L2
CB E2

is not clear. The only apparent difference between LiCl and EDTA solubilization of the wall is that a faster and more extensive wall dissociation occurs when LiCl is used.

Ionic interactions of the wall with cationized ferritin

Binding in normal cells The role of negatively charged molecules in the cell walls of Hymenomonas was investigated with cationized ferritin as an electron dense molecule. Cationized ferritin is horse spleen ferritin which has had its carboxyl groups cationized to tertiary amines with the nucleophile, N,N-dimethyl-1,3-propanediamine (Danon, 1972). The iron-containing molecule is 11.0 nm in diameter with 12-24 identical peptide chains per molecule and a molecular weight of approximately 750,000 d. In physiological pH ranges, 50-60% of the carboxyl groups are cationized and, as such, the molecule will form ionic interactions with negatively charged molecules. The presence of electron-dense iron makes it a particularly useful marker for electron microscopy.

The cell walls of cells maintained on the normal diurnal cycle bind cationized ferritin (Figure 48). The granular ferritin deposits are found on columnar material, the top and bottom of scales, and the proximal (bottom) surface of the coccolith base. Bound ferritin is absent from the distal (top) surface of the coccoliths including the rim elements. Intramural spherosomes lack ferritin deposits. The ferritin appears to associate with and thereby accentuate the appearance of the columnar material. Thus the kind of preparation illustrated in Figure 48 provides the evidence for the role of columnar material as connecting links between the plasma membrane and the scales. For comparison in control cells (Figure 49) not exposed to

Figure 48. Cationized ferritin treated cell maintained on the normal 8 hour dark-16 hour light diurnal cycle. The distinct electron dense granules in the wall are ferritin deposits. Note that ferritin binds to the bottom surface of the coccolith and not to the top (arrows). Also note the intramural spherosome (arrowhead). X 72,000

Figure 49. A control cell showing wall components. Note the linear polymer (columnar material) running from the plasma membrane to the base of the scale. X 72,000

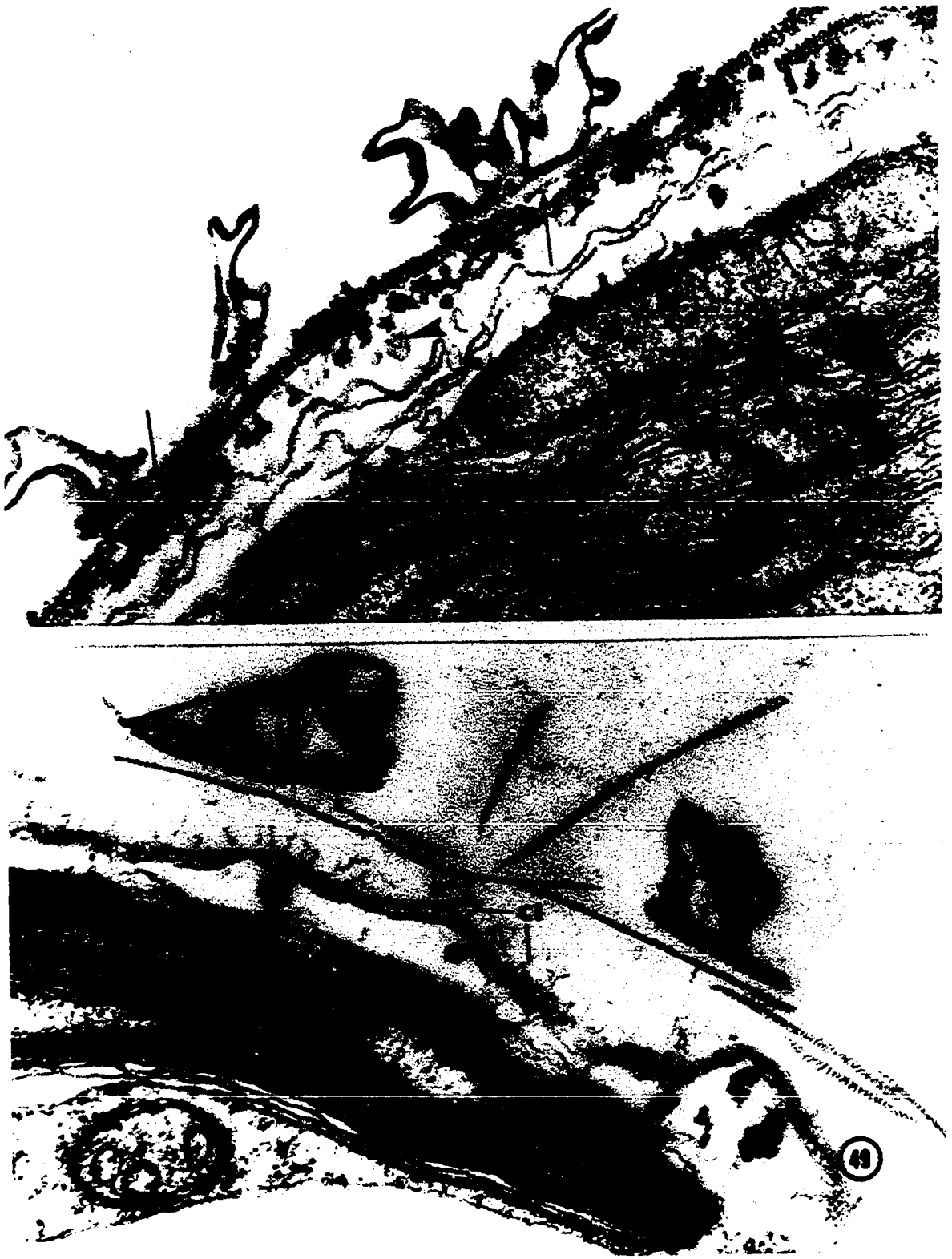

ferritin, no granular deposits that could be confused with ferritin granules are seen associated with the columnar material, scales, or bases.

The cationized ferritin does not enter the cell (Figure 50) as is evidenced by a lack of ferritin binding to the internal coccoliths. The only electron dense granules in the Golgi region are coccolithosomes and not ferritin. There are numerous examples shown in Figure 50 of ferritin binding to the bottom surface of the coccoliths and not the top.

Binding in dark-incubated cells The laying down of new wall material in relationship to the old wall can be followed in cells treated with ferritin, washed, placed in the dark for 12 hours, and incubated in the light for seven hours. Figure 51 demonstrates that areas of new wall are interspersed within the old wall. The columnar material must be synthesized at the level of the plasmalemma because ferritin can be seen at the distal end of one "column" and not at the proximal end (arrow).

Cells incubated in the dark, ferritin treated, washed, and incubated in the light (Figure 52) show a pattern similar to those treated with ferritin before being placed in the dark. The new scales are inserted at intermittent points beneath the old wall. Columnar material with bound ferritin is in close association with the plasma membrane (arrows). The appearance of a few molecules of ferritin associated with new scales, in this intermediate case between control and the early application of ferritin (Figures 50, 51) is intriguing.

Binding in pronase treatment cells Cells incubated with pronase in the dark for 12 hours, treated with cationized ferritin, and recoverd for seven hours in the light have less ferritin bound to their coccolith bases and scales (Figure 53). This indicates that pronase is digesting something

Figure 50. A cationized ferritin treated cell on normal diurnal cycle showing no ferritin deposits inside the cell. Present are Golgi apparatus (G), coccolithosomes (Co), nucleus (N), chloroplast (Ch), and microtubule bundles (Mb). Note the ferritin binding to bottom surface only of coccoliths (arrows). X 20,000

Figure 51. Cells treated with ferritin, incubated 12 hours in the dark, and finally incubated in the light for seven hours illustrating the old and new wall relationships. Note the new scales (arrowhead) surrounded by the old wall. Also note the distance that the bound ferritin on the columnar material is from the plasma membrane. X 39,600

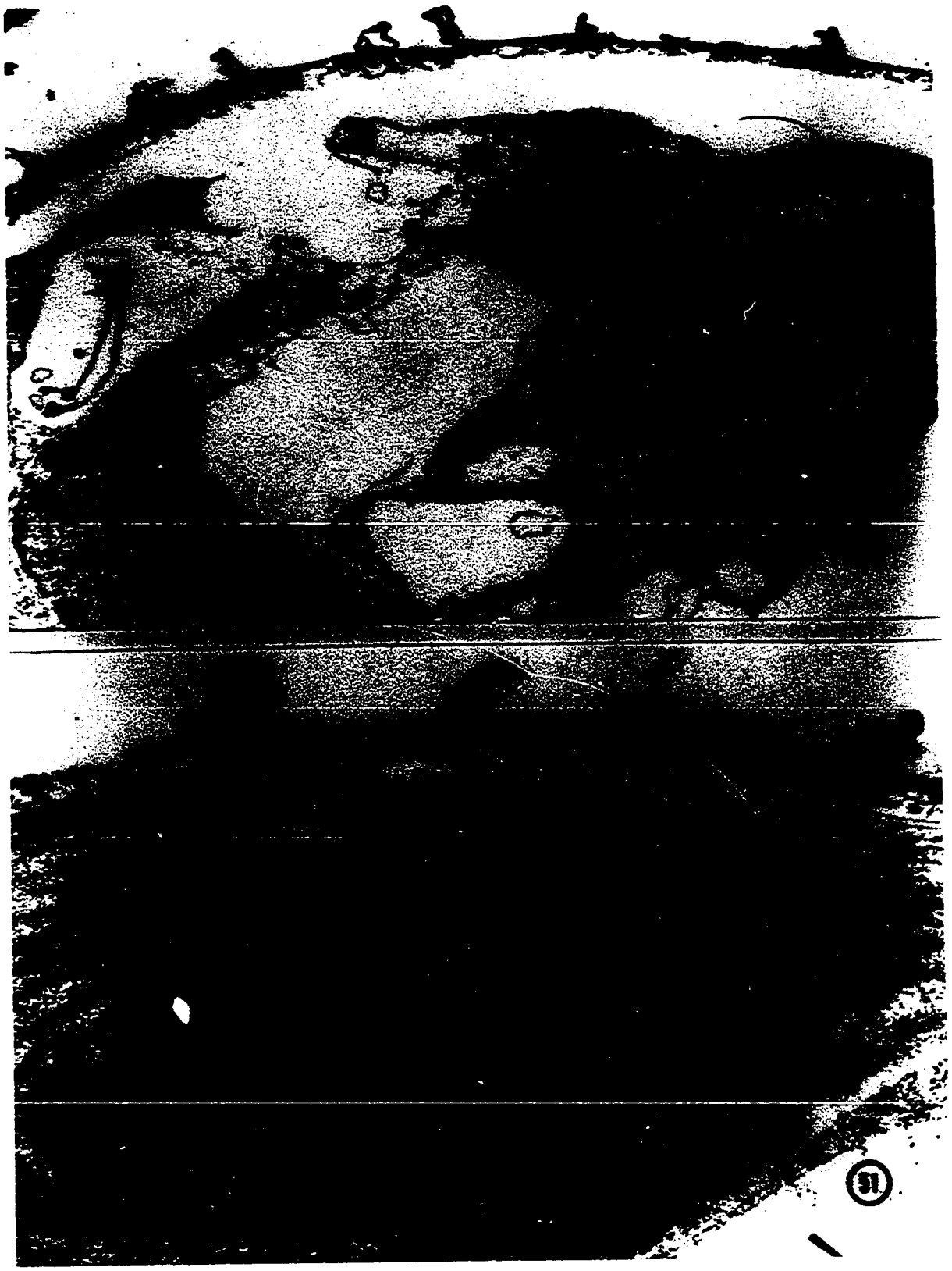

Figure 52. Cell, incubated in the dark for 12 hours, treated with cationized ferritin, and incubated in the light for seven hours, exhibiting old and new cell wall relationships. Observe the new scale insertion (arrowhead) and spherosome (Sp) without ferritin. X 36,000

Figure 53. Cell, incubated in the dark for 12 hours with pronase, treated with cationized ferritin and recovered in the light for seven hours, showing the effects of pronase or ferritin binding. Observe the reduced ferritin binding to scales and coccoliths and the reduced number of coccoliths on the cell surface. X 36,000

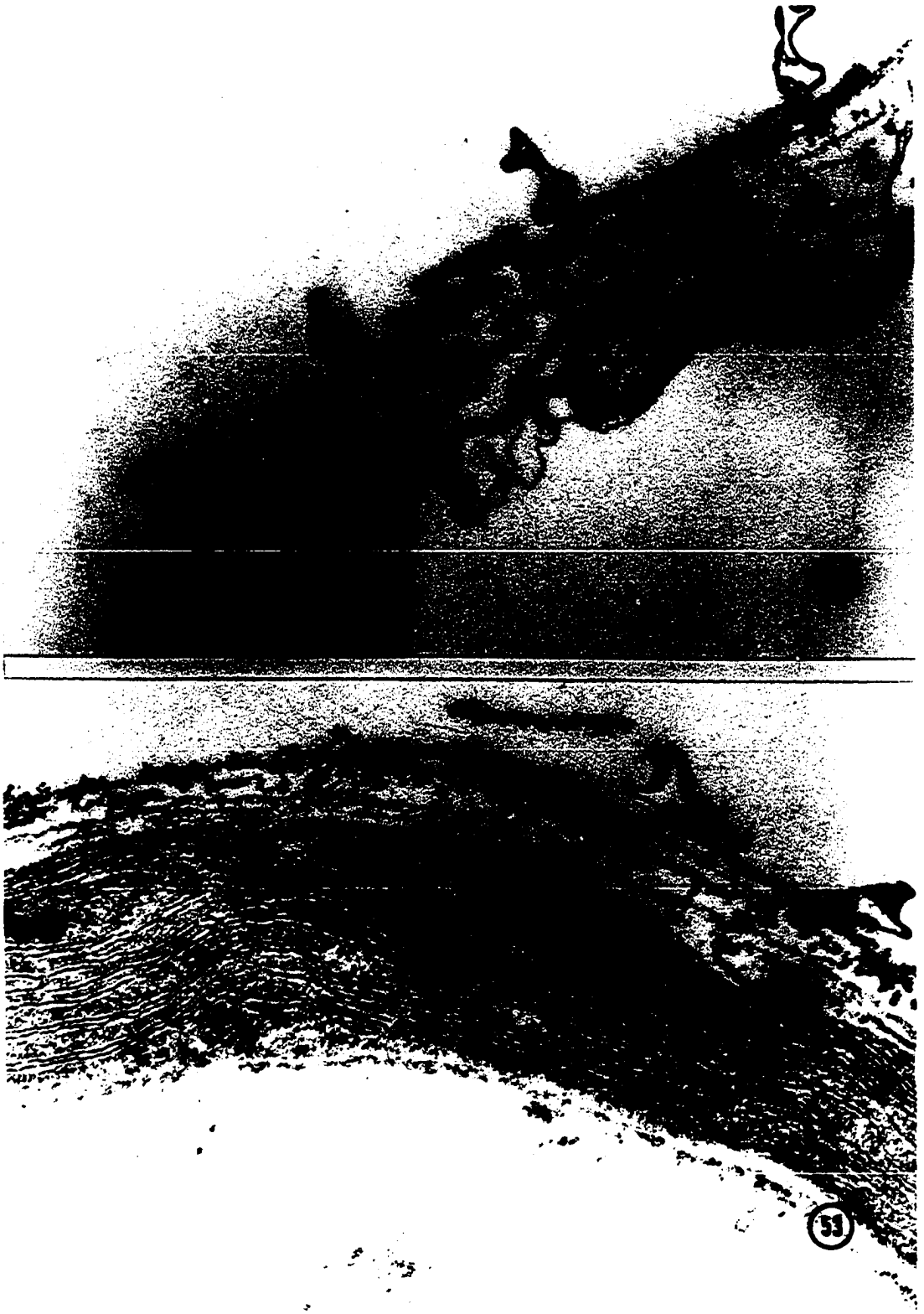
53

from the bases and scales which may be required to hold them on the cell, hence, their reduced numbers during pronase treatment. A marked reduction in coccolith number on the cell surface is evident in both Figures 53 and 54. After pronase treatment the columnar material with bound ferritin is usually not in close association with the plasma membrane. Numerous areas of new scale additions are seen without any old columnar material attached proximal to them (Figure 54). The pronase must cleave the columnar material at the plasma membrane surface.

The presence of a nearly intact old wall after pronase treatment was not expected (Figures 53 and 54). In pronase treated cells allowed to recover in the light before adding the ferritin (Figure 55) or pronase treated cells not treated with ferritin (Figures 26 and 28), the walls are removed. The ferritin must stabilize the wall sufficiently to prevent its dissociation (see Discussion).

Cells treated with pronase for 12 hours in the dark, allowed to recover in the light, and incubated with ferritin show randomly distributed columnar material which binds ferritin (Figure 55). Our interpretation is that the cell was a protoplast and is now resynthesizing its cell wall. There is one scale on the cell which has columnar material between it and the plasma membrane.

The Biological Degradation of the Cell Wall

Multiple scale and coccolith containing vesicles and hydrolytic enzymes

Structure During the course of observing pronase treated cells, membrane bound vesicles which contain a large number of bases and scales are located inside the cell. Figure 56 demonstrates an extreme example of

Figure 54. Cell treated with pronase in the dark for 12 hours, incubated with cationized ferritin, and recovered for seven hours in the light demonstrating a lack of association between the plasma membrane and columnar material with bound ferritin (arrow). Note that internally in the tonoplast (T) fibrils with bound ferritin are visible (arrowheads). X 20,000

Figure 55. Cells treated with pronase in the dark for 12 hours, recovered in the light for seven hours, and incubated with cationized ferritin illustrating the loss of the cell wall. Note the cationized ferritin binding to columnar material (arrows) at random points around the cell


55

Figure 56. Cell treated for 24 hours in pronase illustrating the appearance of multiple scale and coccolith containing vesicles (MSCV). Present are mitochondria (M) and chloroplast (Ch). Note the large accumulations of rough endoplasmic reticulum (arrow) and the absence of columnar material on the plasma membrane (P). X 20,000

Figure 57. Cell from normal diurnal cycle showing the localization of aryl sulfatase in the MSCV's (arrows). Unstained X 20,000

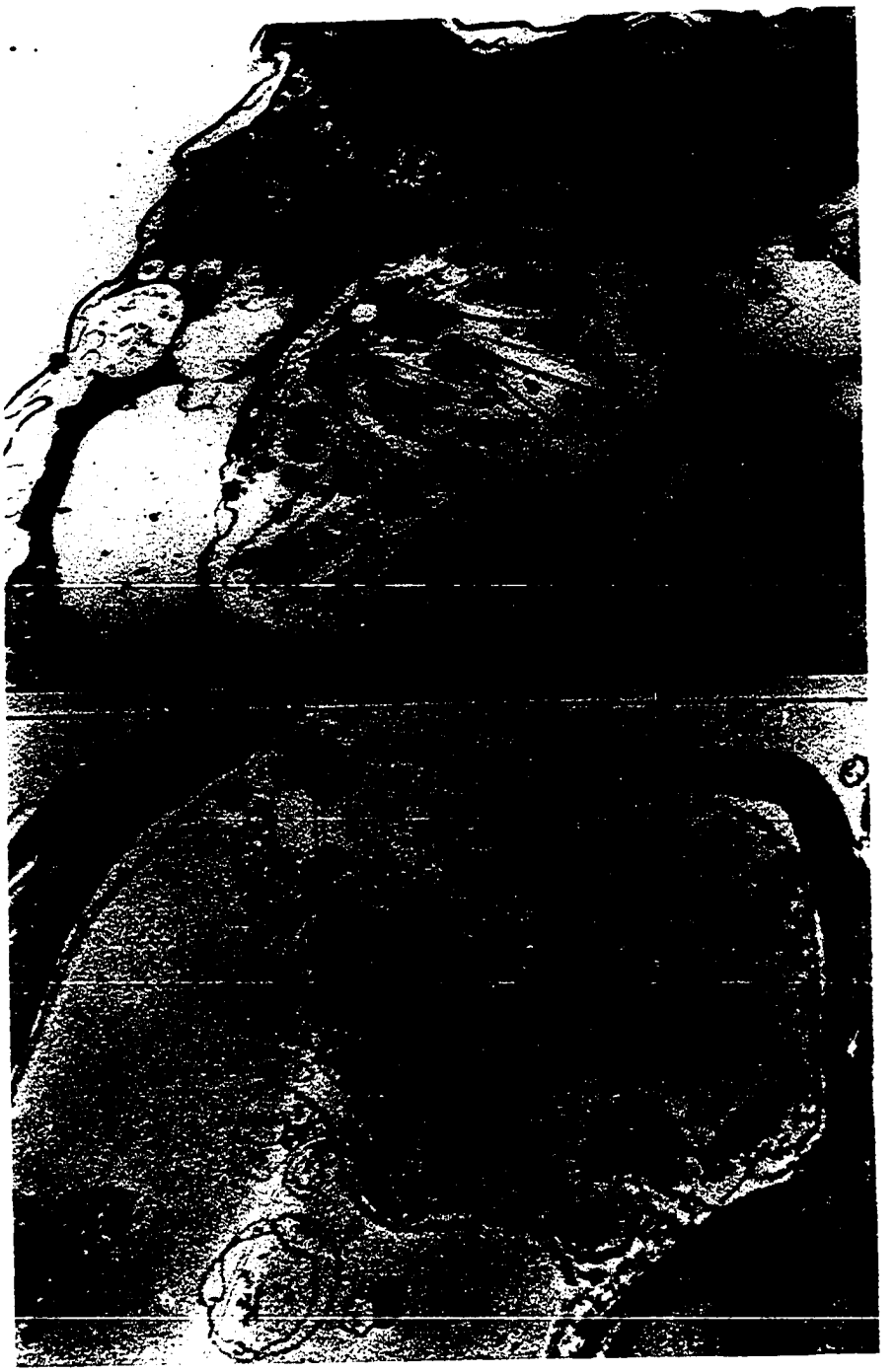

this with 28 bases and scales are enclosed within one membrane. I will refer to these vesicles as multiple scale and coccolith containing vesicles (MSCV's). The degraded appearance of the coccoliths suggested that they were lysosomes or lytic compartments which should contain hydrolytic enzymes. In addition to the MSCV's in Figure 56, there is no columnar material on the plasma membrane and the mitochondria look poor.

Enzyme localization To test the hypothesis that MSCV's were lysosomes, two common lysosomal hydrolases, aryl sulfatase and acid phosphatase, were localized cytochemically. Aryl sulfatase with ρ-nitrocatechol sulfate as the substrate is localized in the MSCV's (Figure 57); the lead deposits are slight. A substrateless control (Figure 58) for aryl sulfatase and acid phosphatase showed no electron dense particles in the Golgi (again coccolithosomes are identifiable), tonoplast, MSCV's, or cell wall. For this test, it is important to eliminate divalent cations like manganese which are normal cofactors in the incubation medium, so that nonspecific deposits do not appear.

Acid phosphatase with β-glycerophosphate as the substrate yielded lead deposited in the MSCV's and tonoplast (Figure 59). The deposits generally were associated with the membranes. In addition to the substrateless control (Figure 58), the acid phosphatase enzyme was inhibited specifically by sodium fluoride (Figure 60). No electron dense particles are seen in the tonoplast, Golgi apparatus, or cell wall. The electron dense granules in the Golgi are coccolithosomes. No lead deposits are present in MSCV's either (Figure 61). Besides acid phosphatase localization in the MSCV's and tonoplasts, acid phosphatase positive deposits are seen in the distal cisternae of the Golgi apparatus (Figure 62), but they are not associated

Figure 58. Substrateless control cell for aryl sulfatase and acid phosphatase showing no lead deposits in the MSCV's, tonoplast (T), Golgi apparatus (G), or cell wall. Unstained X

Figure 59. Cell from normal diurnal cycle showing acid phosphatase localization (arrows) in the MSCV's and tonoplast. Note the lead deposits are membrane associated. Unstained X 20,000

Figure 60. Sodium fluoride inhibited control for acid phosphatase in a cell on normal diurnal cycle illustrating an absence of lead deposits in the Golgi apparatus (G) and tonoplast (T). Unstained X 20,000


T
MSCV
T

Figure 61. NaF inhibited control showing no lead deposits in MSCV's. Unstained. X 36,000

Figure 62. Cell on normal diurnal cycle demonstrating acid phosphatase localization in the distal Golgi cisternae (arrows). Unstained. X 36,000

with cisternae containing coccolith precursors or scales. The MSCV's are, therefore, lytic compartments with hydrolytic enzyme activity.

Enzyme activity of homogenates To determine if the hydrolytic activities fall within normal limits established for other similar cell types, cell homogenates were assayed for three enzymes, acid phosphatase with ρ-nitrophenyl phosphate as the substrate, aryl sulfates with ρ-nitrophenyl sulfate as the substrate and cathepsin D with hemoglobin as the substrate. Their specific activities were 0.766 mM Pi/mg protein/hour, 0.009 μM ρ-nitrophenyl/mg/protein/hour, and 0.845 μM tyrosine/mg protein/hour, respectively. The aryl sulfatase activity is low, but other values were within expected limits.

Neutral red staining vesicles Neutral red is a compound which develops a red color in the acid pH range (Stadelmann and Kinzel, 1972) and can be used to locate vesicles of high hydrogen ion concentration within the cell. Neutral red can exist in several ionic states depending on the pH of its environment. At pH 7.8, it has no charge (carbenium form) and is free to migrate into and out of the cell and its organelles; however, when it enters a compartment of low pH, it becomes positively charged, can no longer pass through the membrane, and is trapped. As the compound becomes concentrated, a red color results. Figure 63 shows the size, distribution, and location of neutral red staining vesicles (NRV's). The tonoplast and vesicles at the cell posterior concentrate the dye, but staining is absent from the Golgi region. The stain is not reliable with fixed or dead cells; thus counting of the NRV's was done with living cells.

The number of NRV's for cells grown under the usual diurnal cycle increases during the light period and decreases during the dark period

Figure 63. Light micrograph of neutral red staining vesicles of cells on a normal diurnal cycle illustrating their size, distribution, and location. X 3,000

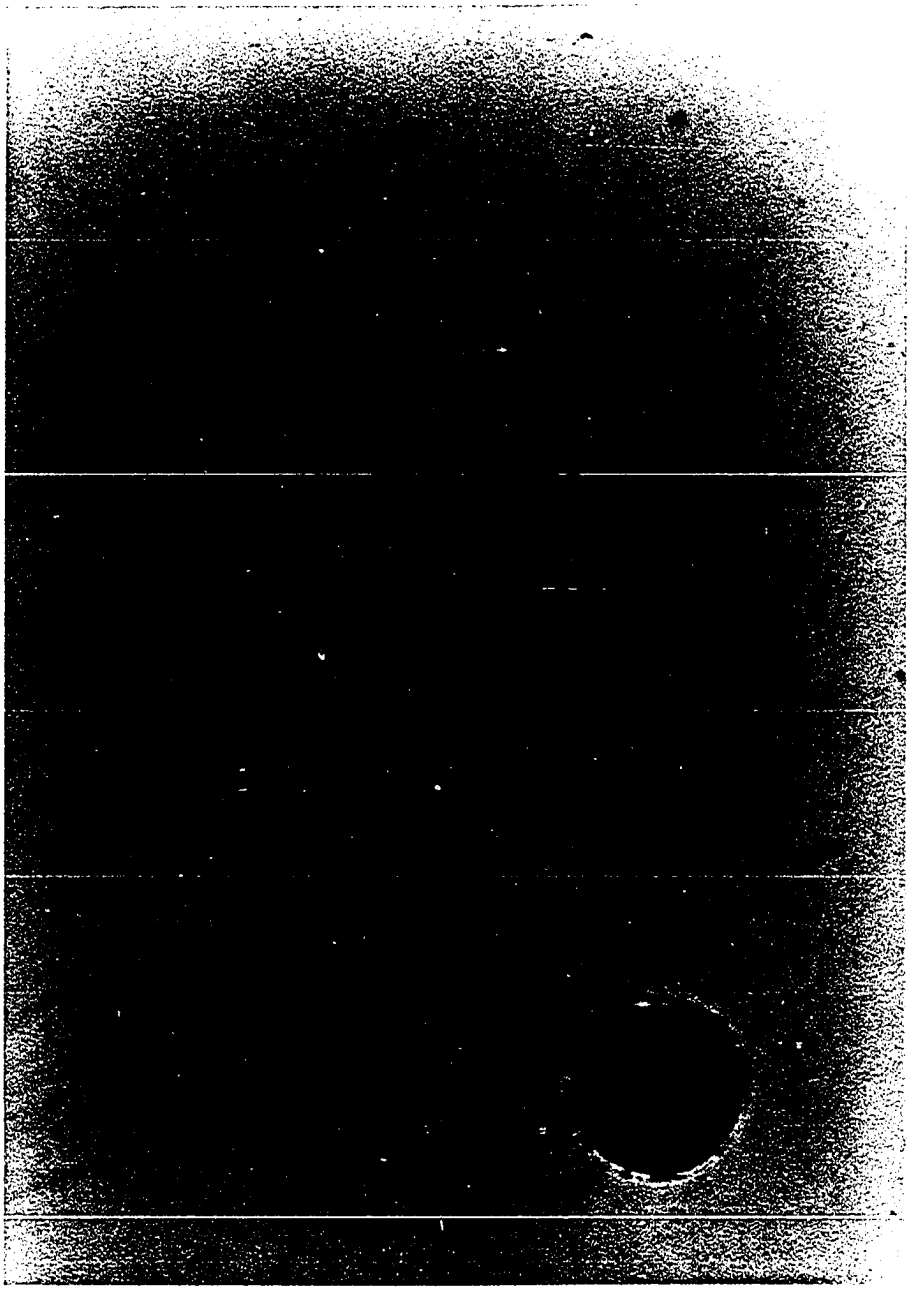

(Figure 64). Staining of the large vacule or tonoplast is most common in the early light hours. The number of NRV's remains constant during the first five to six hours of light and is followed by a rapid increase. A parallel experiment was to compare cells treated with pronase (in the dark) with controls (also in the dark). These were then compared with control cells on the normal light-dark cycle. There was no indication that pronase treated cells exhibited any unusual NRV behavior.

Evidence for cell wall resorption A possible origin for the MSCV's was that they were formed by phagocytosis. Cells were allowed to grow for several hours after being treated with cationized ferritin; any uptake of ferritin into the MSVS's would indicate cell wall phagocytosis. Figure 65 shows a cell treated with cationized ferritin, incubated in the dark, and placed in the light. In the tonoplast, columnar material with bound ferritin is seen. This same kind of uptake is present in Figure 54. Also present in Figure 63 are some gray vesicles which are likely candidates for neutral red staining vesicles. No ferritin-like granules are seen in the tonoplast of control cells like the one shown in Figure 66. Again, presumptive neutral red staining vesicles are shown.

Figure 64. A graph showing the diurnal fluctuations in the number of neutral red staining vesicles (NRV's) in cells grown on 16 hours light-8 hours dark

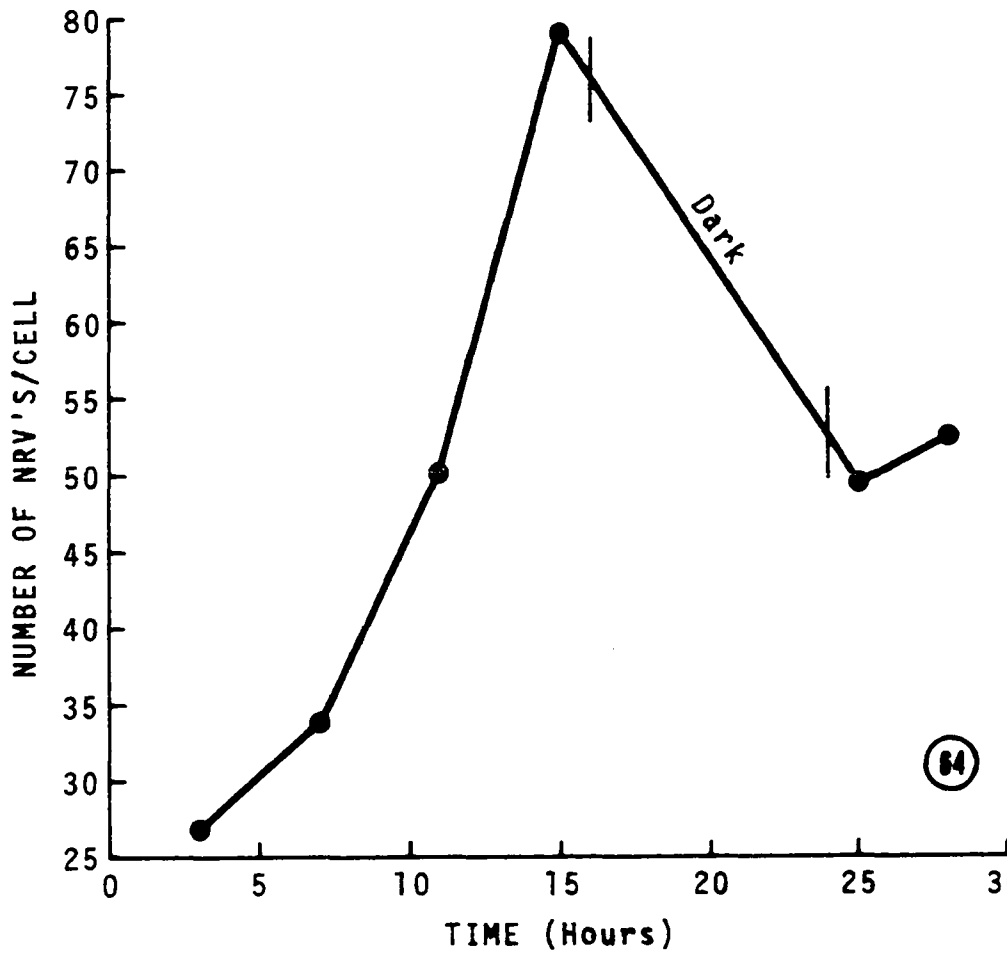
80
75
70
65
60
55
50
45
40
35
30
25
0
5
10
15
20
25
30
NUMBER OF NRV'S/CELL
TIME (Hours)
Dark
64

Figure 65. Cell treated with ferritin, incubated in the dark for 12 hours, and placed in the light for seven hours showing the uptake of ferritin (arrows) into the tonoplast. Observe the gray vesicles. X 20,000

Figure 66. Control cell with ferritin treatment showing no ferritin-like granules in the tonoplast. Observe the gray vesicles. X 20,000

DISCUSSION

A characteristic feature of most plant cells is the presence of a cellulose-containing cell wall. The wall is a kind of exoskeleton that is chemically complex and morphologically diverse, assuming quite different forms in different plants and even within the same plant, i.e., differentiation of plant parts is often emphatically emphasized by the diversity of the walls in the leaves, roots, etc.

The ability to synthesize cellulose is limited to a few prokaryotes and most plant eukaryotes; its near ubiquity in the latter suggests that it evolved early, perhaps in ancient seas and probably in unicells. Without belaboring the point, we think that Hymenomonas represents a prototype which produced cellulose in discrete and movable packages which could be manipulated by the cell, and yet, which could be used as a kind of exoskeleton--a sort of chain mail armor to which pieces could be added to allow for growth, and which could be separated into halves to allow for division. The coccolith was an evolutionary sophistication clearly evolved from the smaller scale which served as the layer below. Its function was probably protective, resisting wave action and other kinds of mechanical injury. The success of the coccolithophorid group is well-documented in the fossil record.

Cell Wall Biosynthesis

One of the purposes of this investigation was to determine the morphological relationship between coccolithogenesis and the other cell wall components of Hymenomonas in regard to their intracellular synthesis and

deposition onto or into the cell wall. It seemed possible that chemical agents should exist which could selectively extract one or more cell wall components without destroying cell viability. In this report, two such agents met these specifications--EDTA and pronase. EDTA decalcified the cells leaving behind the old coccolith base and allowed a distinction to be made between old and new coccoliths on the cell surface. The old coccolith bases impeded the movement of new coccoliths; this resulted in clustered arrangements of coccoliths. In a similar study by Williams (1972, 1974) using an acidic pH of 5.5 for decalcification, an identical polarization of coccoliths was found; however, his investigation of recovery from the pH treatment was limited primarily to light microscopy with EM observations confined to those cells at the end of the acidic incubation. The coccolithogenic rate of approximately 8 coccoliths per cell per hour was somewhat below the 10-12 coccoliths per cell per hour of Williams (1972, 1974); nevertheless, the recovery of cells from EDTA was more than adequate to allow for the discrimination of experimental variables and was, in my hands, easier to manipulate. On morphological grounds, the extraction of additional cell wall was suspected when the subsurface scales were more closely appressed following EDTA extraction (Figure 17); these suspicions were confirmed when the biochemical analyses showed that both carbohydrates and proteins were released during EDTA chelation. Whether any of these same carbohydrates and proteins are released under the acidic decalcification procedures of Williams (1972, 1974) is unknown since no biochemical examination was carried out; however, it does appear likely from the data on the effect of pH on reaggregation (Figure 44) that substantial amounts

of wall material would not be dislodged from the cell at pH 5.5.

The enzymatic degradation of the cell wall of Hymenomonas results in protoplast or wall-less cell formation (Figure 28). From these protoplasts the distinct morphological units of the cell wall, the columnar material, the subsurface scales, and the coccoliths, can be followed intra- and extracellularly during their synthesis and deposition. The columnar material is synthesized randomly at the plasma membrane level (Figures 51 and 55). Simultaneously the Golgi apparatus begins the synthesis and manufacture of scales which are attached to the cell surface ionically via the columnar material (Figure 55). After a single layer of scales is laid down, coccoliths begin to be synthesized and deposited on the cell exterior. The newly deposited coccoliths "skate" around on the smooth cell surface created from the subsurface scales and the electron transparent, amorphous "glue". The site of intracellular biosynthesis of "glue" material is apparently in the same Golgi cisternae as the scales because Brown and his coworkers (Brown et al., 1973; Brown and Romanovicz, 1976) have shown cytochemically that polysaccharide positive material is present together with scales in the Golgi of Pleurochrysis. After a single layer of scales is made, additional layers can be added by inserting new scales from underneath and shoving the old scales outward (Figures 51 and 52). The movement of scales, coccoliths and their precursors from the endoplasmic reticulum through the Golgi apparatus to the cell wall supports the endomembrane concept of Morre and Mollenhauer (1974). In addition, the synthesis of many cell wall polysaccharides in the Golgi is common among all plant cells (Chrispeels, 1976; Karr, 1976; Westafer and Brown, 1976).

This work also supports the developmental sequence for coccolith production developed by Outka and Williams (1971) and others (Dorigan and Wilbur, 1973; Pienaar, 1971a; Williams, 1972).

Protoplast production from the enzymic action of pronase in Hymenomonas is an important discovery since protoplast formation in algae is far from commonplace with only a few other reported examples. The enzymes employed in obtaining higher plant cell protoplasts (Cocking, 1972), the cellulases, hemicellulases, and pectinases, have been successful only with the green alga, chlorella (Braun and Aach, 1975). An enzyme produced by Chlamydomonas reinhardii gametes called autolysine removes the walls of vegetative cells (Schlosser et al., 1976). Pronase has been successful in removing 6 of the 7 wall layers of Chlamydomonas (Forster, 1975) and, from bacteria, a portion of the wall of Bacillus subtilis (Reeve and Mendelson, 1973). The wall of Hymenomonas carterae can now be added to this list. In the aforementioned examples, cell wall formation studies were not conducted and would not be good models for its study because their walls have poorly defined morphologies; this is not true with Hymenomonas. The coccoliths and scales are readily followed as they are synthesized and deposited.

The action of pronase on the cell wall was twofold: (1) the pronase cleaved the columnar material at the plasma membrane level (Figures 26, 54, 56) and some component of the coccolith bases and scales were digested away because less cationized ferritin was bound to them (Figures 53 and 54). The coccolith and scale numbers should be reduced during pronase attack and they are. If the columnar material is cleaved, the cell wall

and the plasma membrane are no longer attached to one another and if a hole were to develop in the wall, the protoplast could easily slip out. This could help explain how gametes and zoospores can emerge from algal cells. If the cells were to produce an enzyme which could detach the cell wall from the plasma membrane and a second enzyme which could digest or soften the wall, the gametes and zoospores would be released. Enzymes such as this do exist for Pleurochrysis (Brown et al., 1970) and Chlamydomonas (Schlosser et al., 1976).

Pronase must enter the cell because the damage done during the construction of the coccoliths following recovery from pronase was plainly shown (Figures 29-31). Support for protease enzymes entering the cells comes from a study of tritiated trypsin and conjugated fluorescent antibodies to trypsin (Hodges et al., 1973) where the trypsin was evident for up to 48 hours in Hela and baby mouse kidney cells and pronase is known to contain trypsin and chymotrypsin-like enzymes (Jurasek, et al., 1974; Russin et al., 1974). A question arises as to the purity of the pronase used here as compared to commercial enzyme preparations used for producing higher plant cell protoplasts which are probably a mixture of several enzymes. Pronase, Grade B, is electrophoretically pure, according to Calbiochem, and yields only one band on SDS gels in our hands. The fact that Hymenomonas recovers slowly and with considerable evidence of damage suggests that proteolytic in the crude commercial enzymes could be a reason for failure of higher plant protoplasts to grow and divide.

The penetration of pronase into the cells provides a possible mechanism for why coccolith biosynthesis is shut down during enzymatic treatment.

The microtubules are made of protein which could easily be degraded by pronase enzymes and microtubules are needed for coccolith secretion (Williams, 1972). This possibility was not actively pursued but a re-evaluation of additional micrographs might provide some valuable information. An alternative explanation might be that protein synthesis or mitochondrial and chloroplast activity have been affected by the enzyme treatment either directly or indirectly because in trypsin treated macrophages, protein synthesis was inhibited and glucose oxidation and ATP content were decreased (Ulrich, 1976). These explanations are speculative but an examination of how pronase affects coccolithogenesis is a natural extension and it could shed some light on other controls involved with cell wall biosynthesis.

Previous studies of coccolithogenesis have focused on coccolith production in the light versus in the dark (Blankley, 1971; Crenshaw, 1964; Dorigan and Wilbur, 1973; Paasche, 1964, 1966a; Williams, 1972, 1974). Most of these investigators found coccolith production to occur at reduced rates in the dark. None of these investigators tried to determine if coccolithogenesis was controlled by a "clock" or rhythm. The results presented here do indicate that coccoliths are not produced at the same rate throughout the light-dark cycle (Figure 23). The question is do these fluctuations correlate with the number of coccoliths required to maintain the normal complement of 100-200 coccoliths per cell or, in other words, can the cell make about 100 coccoliths per day? If one calculates on the basis of (1) the minimum time for maximum coccolith production, i.e., 8 coccoliths per hour for four hours, (2) an average rate of 4 coccoliths per

hour for the remaining 12 hours of light, and (3) 2 coccoliths per hour during the dark (Williams, 1972, 1974), the cell could make 96 coccoliths per day (one division cycle) which easily falls within the 75-100 coccoliths/cell/day necessary to sustain the cells at these high coccolith levels. Thus the fluctuations meet the cell's demand for coccoliths and it is assured that the fluctuations must be under genetic control because no evidence is available that their production can be stimulated. Any future experimentation comparing coccolithogenic rates must involve cells taken from the same time or else experimental variation may actually be reflecting different synthetic rates during the diurnal cycle.

Future experiments relating to cell wall biosynthesis in Hymenomonas might involve a determination of the role of microtubules in this process which would involve colchicine inhibition of the protoplasts. Some additional cytochemical staining for polysaccharides might visualize molecular arrangements in the electron transparent "glue" as it has for Roland et al. (1975) and Roland et al. (1977). Along with these investigations, parallel biochemical studies should be conducted.

Cell Wall Chemistry

The extraction of cell wall material usually involves drastic procedures which result in a heterogeneous mixture of molecules within each fraction. Often these extractions may also result in the breakage of covalent linkages thus obtaining only parts of whole molecules. In the investigation reported here, a method of obtaining molecules and cell wall fractions without breaking covalent bonding was demonstrated through the employment of LiCl to solubilize the cell wall of Hymenomonas carterae.

The practice of Brown et al. (1970, 1973) to use an enzyme mix from the cell medium to obtain scales for biochemical analysis opens the door to the question--has there been something chemically linked to the scales which is not being analyzed? The action of chaotropic agents like LiCl is to break up hydrogen bonding and hydrophobic interactions. From unreported results, preliminary indications are that cells, coccoliths, scales, and amorphous "glue" could be separated from one another by combinations of differential and density gradient centrifugation techniques; thus, isolation would allow biochemical analysis to be carried out on the various components.

The spherical vesicles released during LiCl dissociation were tentatively identified as spherosomes. A more correct term is probably paramural body; this designation is given to vesicles found within the cell wall as defined by Marchant and Robards (Roland, 1973). The paramural bodies are of two main types: lomasomes, which are vesicles derived primarily from intracellular membranes with subsequent fusion with the plasma membrane and released into the wall, and plasmalemmasomes, which are vesicles formed directly from the plasmalemma; the function of paramural bodies is not known. At least some of the paramural bodies of Hymenomomas could be classified as lomasomes (Figure 54); whether there is heterogeneity of Hymenomonas paramural bodies is not known. Paramural bodies have been reported in fungi (Moore and McAlear, 1961) and higher plants (Roland, 1973; Westafer and Brown, 1976). The fact that the paramural bodies can be released by LiCl provides a means for their biochemical characterization which could lead to a determination of their function within the cell wall.

The reassociation of dissociated cell wall material from Hymenomonas or other coccolithophorids has never been reported before. Brown et al. (1973) briefly mentioned that they could precipitate alkali-extracted radial microfibrils from Pleurochrysis scales with calcium and ethanol but no further details were available. The work completed here would suggest that it is highly unlikely that the reaggregated material contained any free radial microfibrils; rather it consisted of the amorphous, electron transparent "glue" used to cement the scales in the wall. The reassociation of Hymenomonas wall components behaves similarly to the alginate of brown algae in that they both require calcium or magnesium ions to reaggregate (Haug, 1974) and remain soluble in the presence of monovalent cations. The red algae possess a galactan polysaccharide called carrageenan which requires monovalent cations for gel formation and are unaffected by divalent cations (Haug, 1974). Even green algae have some ion requirements; for example, Nitella cell walls will harden the most with trivalent aluminum (Métraux and Tais, 1977). A glycoprotein from Chlamydomonas, a green alga, will self-assemble in the absence of any cations (Catt et al., 1976; Hills, 1973; Hills et al., 1975; Roberts and Hills, 1976); the glycoprotein has a molecular weight of 300,000 d. with high levels of hydroxyproline (Catt et al., 1976). Even with limited biochemical information about the reaggregation product of Hymenomonas, the Chlamydomonas glycoprotein and the Hymenomonas reassociated product are apparently not the same type of molecules because crystalline structures are formed after the glycoprotein reassembles (Hills et al., 1975)

and the reaggregation of Hymenomonas produces fibres. A biochemical analysis of the carbohydrate and amino acid monomers of the Hymenomonas reassociation product would be helpful in assigning any resemblance of this product to the red and brown algae. Finally in higher plants Roland et al. (1977) suggest a self-assembly process for molecular arrangements within the wall because the extracted and precipitated wall polysaccharides have the same appearance as was shown by native wall material. An identical approach with Hymenomonas using LiCl extractions produced similar results, i.e., wall material was solubilized from homogenates and then reprecipitated; the latter resembled the pattern obtained more directly from whole cells. The involvement of calcium in the cell wall reaggregation of Hymenomonas is not surprising since calcium is known to play an important role in lectin binding (Albersheim and Anderson-Prouty, 1975; Kauss, 1976) and animal cell aggregations (Neely et al., 1976). The Hymenomonas system stands in sharp contrast with an investigation recently reported (Morris et al., 1977) where plant galactomannans and an extracellular bacterial polysaccharide group known collectively as xanthans will form associated products only when they are present together and the galactomannans need only be present in small amounts for precipitation to proceed.

The identification of the carbohydrate band obtained from SDS gel electrophoresis (Figure 45) and its correlation with a specific wall structure is complicated; however, one would like to think that the molecules comprising this band are intimately involved in the reassociation process. This band is tentatively assigned as equivalent to the amorphous "glue"

based on the following: (1) the treatment of whole cells with LiCl causes scales and coccoliths to come off the cell, i.e., they become "unglued". (2) Careful EM observations of the supernatant which contains scales and coccoliths show no identifiable differences between native and LiCl removed scales and coccoliths. These scales and coccoliths had fibrous strands attached which had specific widths (50-72 nm) and lengths (510 nm) and, furthermore, the fibers attach to the undersurface of the coccoliths and not to the top (Figure 34). (3) During dialysis of the supernatant from (1) against water, a massive aggregation of cells, scales, coccoliths and "glue" occurred. This aggregation, when placed on a grid, was too thick to get a beam through. However, light microscopy of the aggregate showed many cells and coccoliths and fibers up to 1-2 millimeters in width and several centimeters in length. (4) Treatment of homogenates, as in 1-3 above, resulted in identical aggregates except that whole cells were missing and the ultimate size and thickness of the entire aggregates were less (compare Figures 34, 41, 42). The sizes of the individual fibers, scales, and coccoliths was the same in all preparations. In some preparations, the coccoliths and scales were not bound to the reassociated fibers; this is apparently because increasing concentrations of calcium result in stronger gels which do not allow binding of coccoliths or scales to occur. (5) EM observations of thin-sectioned, EDTA-treated material shows the loss of amorphous material between and around the scales, the calcite, and most of the matrix from the anvils; SEM observations revealed that coccolithonets were removed by EDTA treatment. We believe that the EDTA treatment is essentially a mild form of the LiCl treatment. (6) The amount of

total carbohydrate (6%) removed from the cell by EDTA is too high to be accounted for by the matrix material of the coccoliths alone. (7) The molecule comprising the carbohydrate band is different from the low molecular weight glycoprotein obtained by Kuratana (1974) because the molecule here is a carbohydrate not a glycoprotein. We, therefore, conclude that the amorphous material, the coccolithonets and the carbohydrate molecules are the same thing and are the primary constituents of the reassociating material.

The cell wall of Hymenomonas is held together primarily by the ionic interactions of its component parts which has been explicitly demonstrated with the cationized ferritin binding differentially to the columnar material, the entire periphery of the scales, and the proximal surface of the coccoliths (Figures 48, 50-55, 65, 66). The results for cationized ferritin binding to columnar material and scales are identical to those found by Brown and Romanovicz (1976) for Pleurochrysis; however, Pleurochrysis has no coccoliths for ferritin to bind. This establishes a chemical difference between coccoliths and scales and, equally as important, it reveals a function for coccoliths; namely, coccoliths prevent cells from sticking or clumping together. It also explains why cells stick together after EDTA and pronase treatments (Table 3). When EDTA removes the calcified rims from the coccoliths, the cells are able to come in closer contact with one another and the sticky "glue" of separate cells come in contact resulting in cell adhesion. Immediately following pronase digestion, the cells have no walls or very little wall material but as the cell synthesizes a new wall, cell contact will bring about clumping. In both

cases single cells are released from the clumps when sufficient coccoliths are made to pry the cells apart. The ionic association between the scales and the columnar material supports Manton and Leedale's (1969) suggestion that columnar material is involved in holding the cell wall to the cell membrane. The demonstration of polyanionic groups on cell surfaces is not uncommon; a recent study using cationized ferritin on human fibroblasts has found that polyanionic groups are randomly dispersed on the cell surface (Basu et al., 1977) just as was shown for Hymenomonas during columnar material synthesis (Figure 55). The binding of cationized ferritin in the cell walls must be quite strong because under conditions that normally remove the wall, i.e., pronase digestion, the wall is not dismantled when ferritin is present (Figures 53-54). Also from unreported results, normal cells treated with ferritin have had coccoliths lying proximal to the cationized ferritin bound wall and distal to the plasmalemma, which indicates that coccoliths can't pass through the cationized ferritin bound wall. The cationized ferritin must make crosslinkages ordinarily not possible thus stabilizing a normally more flexible wall.

The biochemical characterization of the cell wall of Hymenomonas is not well-understood but with the aid of cell wall solubilization by LiCl, the wall components could be separated and analyzed. In addition with the employment of cationized ferritin before, during, and after dissociation and reassociation, a great deal could be learned about the identity and interaction of the cell wall's component parts.

Biological Cell Wall Degradation

The appearance of membrane-bound vesicles containing numerous scales and coccoliths (called here MSCV's) in Hymenomonas has been reported by several authors (Blankenship and Wilbur, 1975; Flesch and Outka, 1976; Isenberg and Lavine, 1973; Isenberg et al., 1966; Pienaar, 1969b, 1971a; Wilbur and Watabe, 1963). They were thought to be part of the calcification and biosynthetic pathway for coccolithogenesis (Isenberg and Lavine, 1973; Isenberg et al., 1966; Pienaar, 1969b; Wilbur and Watabe, 1963). Evidence presented in this dissertation clearly showed that these vesicles contained hydrolytic enzymes and should be classified as secondary lysosomes. This would support the suggestions of Pienaar (1971a) who actually localized acid phosphatase in these structures; however, he failed to report any controls for his localizations and a great deal of nonspecific lead deposits were present in his micrographs. The results reported here have shown that two hydrolytic enzymes, arylsulfatase and acid phosphatase, were located within the MSCV's and that whole cells contain at least three hydrolytic enzymes, acid phosphatase, arylsulfatase, and cathepsin D. Thus, this report identifies these MSCV's as secondary lysosomes; according to the criteria used by Novikoff and Holtzman (1976) tentative determination that a cytoplasmic particle is a lysosome is as follows: (1) if electron microscopy shows the structure to be membrane delimited and (2) if cytochemistry shows it to have one or more of the hydrolase activities found in biochemically studied lysosomes. Final identification depends on cytochemical and biochemical studies on isolated organelles. The first two criteria have been met for MSCV's; the last has not been

possible as yet. In addition, acid phosphatase localizations should use sodium fluoride (NaF) inhibited controls because NaF inhibits lysosomal phosphatases (Holtzman, 1976). With plant cells, acid phosphatase localizations have been questioned as a marker enzyme for lysosomes (Matile, 1975; Washitani and Sato, 1976) because there is a lack of specificity of these enzymes in plants, but in reviewing the literature, very few investigators use NaF inhibited controls (see for example, Washitani and Sato, 1976). In most plant systems, vacuoles have been equated with lysosomes (Gahan, 1973; Matile, 1975, 1976); the localization of acid phosphatase and arylsulfatase in the tonoplast of Hymenomonas would support this idea also.

MSCV's probably originate in one of two ways: (1) Golgi cisternae could fuse with the tonoplast membrane forming autophagic vacuoles or (2) the cell wall could undergo phagocytosis or be resorbed to form the secondary lysosome; the latter was suggested by Flesch and Outka (1976). The appearance of cationized ferritin in the tonoplast supports this latter hypothesis (Figures 54 and 65). In Pleurochrysis, Brown and Romanovicz (1976) were not able to show any uptake of ferritin into the cell. An interesting observation was made by Parke and Adams (1960) who reported the uptake of bacteria into Hymenomonas carterae. If bacteria could be phagocytosed, it seems likely that cell wall material could be taken in with the bacteria or by itself. Probably both pathways exist, as in most plant cells, and particular needs would dictate which of the two pathways the cell would take.

Acid phosphatase localization was also found in the distal Golgi

cisternae which agrees with the results of Brown and Romanovicz (1976) using Pleurochrysis; however, there was no localization of arylsulfatase activity anywhere in the Golgi while Brown and Romanovicz (1976) found numerous localizations there. Whether this discrepancy is methodological, i.e., due to a difference in copper capture (Brown and Romanovicz, 1976) versus lead capture as performed by us, or whether there is a difference in the two life cycle stages cannot be determined at this time. If arylsulfatase is present primarily when the scales are being synthesized as suggested by Brown and Romanovicz (1976), one would expect to find arylsulfatase during the recovery from pronase but, from unreported results, the arylsulfatase localizations were absent from cells after 8 hours of recovery when Golgi vesicles were actively making scales. Even if positive arylsulfatase localizations would have been found in the Golgi, we would have interpreted them to mean just as we interpret the acid phosphatase presence in the Golgi, namely, that these cisternae represent formative stages in tonoplast and vacuole formation. The involvement of the Golgi apparatus in the formation of lysosomes is a well-established fact in animal systems (Holtzman, 1976; Novikoff and Holtzman, 1976) and is the proposed and generally accepted mechanism for vacuole and tonoplast formation in plant cells (Gahan, 1973; Matile, 1975, 1976; Wilson, 1973). The hydrolytic enzymes of lysosomes digest denatured material and have no known function in synthetic reactions, even though such a hypothesis was proposed by Brown and Romanovicz (1976). Also, just because the enzymes are localized in a given cell organelle does not necessarily mean they are active there, i.e., proper substrates etc. may not be present.

The neutral red staining information indicates that Hymenomonas has a cyclic turnover of vesicles of low pH. Whether or not these NRV's are actually lysosomes is difficult to assess, but in numerous plant cells, vacuoles concentrate the stain (Stadelmann and Kinzel, 1972). Neutral red certainly could be used to distinguish between live and dead cells since only live cells concentrate the stain which constitutes the dye's principal usefulness in animal cell work (Filman et al., 1975). The role of NRV's in the cell and the reason for their cyclic behavior should be the subject of future research.

Hypothetical Cell Wall Model of Hymenomonas

To help summarize, a hypothetical model of the cell wall of Hymenomonas carterae is presented in Figure 67. The model is based primarily on morphological and cytochemical evidence since little biochemical information is available. The model emphasizes the ionic interactions which exist between the cell components. At the plasma membrane, the negatively-charged columnar material is synthesized by the addition of carbohydrate units embedded in the membrane forming a glycoprotein. A scale, which has been synthesized within the Golgi apparatus along with some amorphous polysaccharide, is secreted near a free strand of columnar material and the two become linked together by a calcium-polysaccharide bridge. The newly synthesized scale is attached to the next outer scale layer by several calcium-polysaccharide bridges which subsequently are linked to the third scale layer with similar bridges. The coccolith now passes from the Golgi through the wall and attaches to the cell via calcium-polysaccharide

Figure 67. Hypothetical cell wall model for Hymenomonas

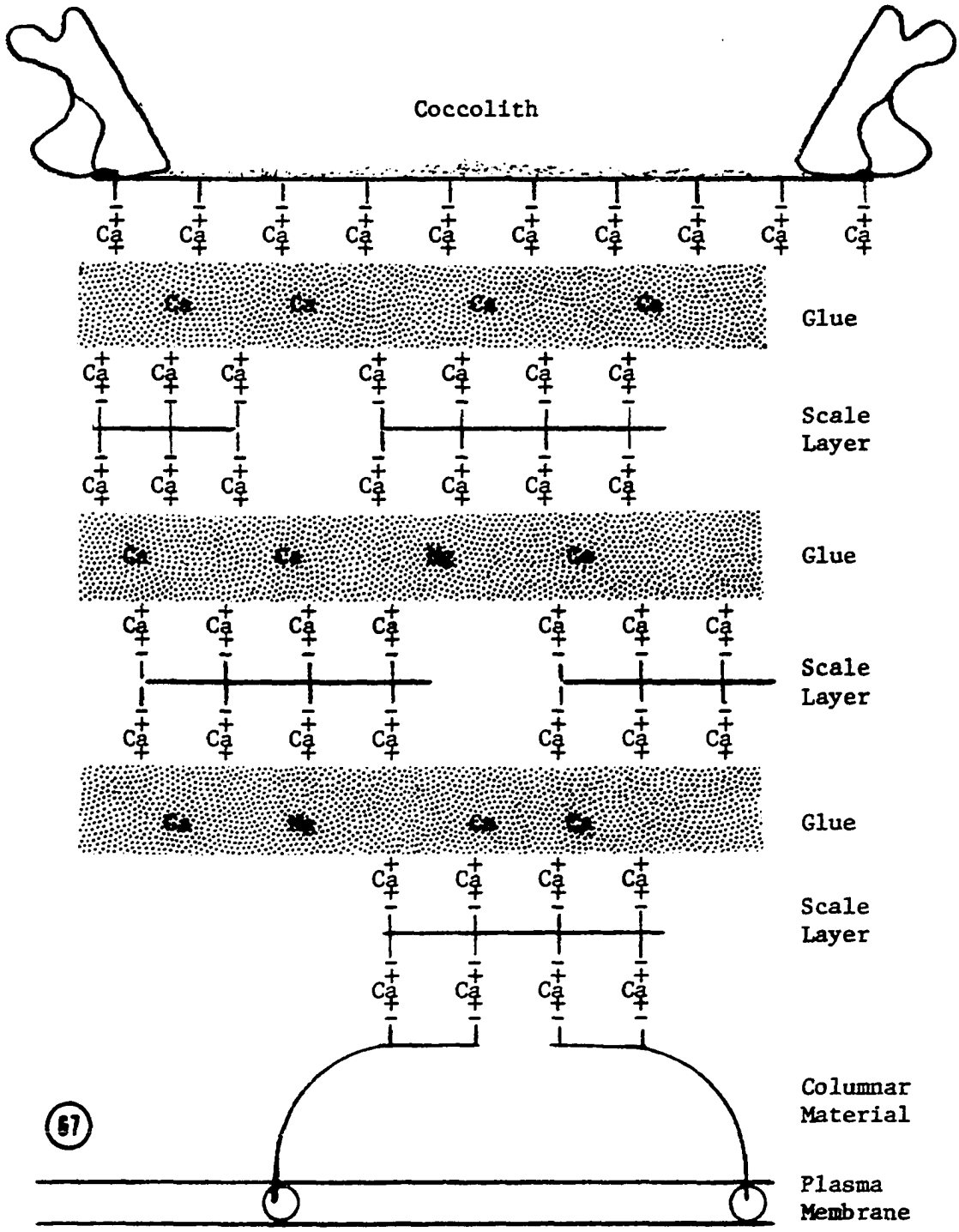
Coccolith
Glue
Scale Layer
Glue
Scale Layer
Glue
Scale Layer
Columnar Material
Plasma Membrane
57

bridges from the outer scale layer. The coccolith maintains its orientation of calcified rims projecting outward because the outer surface carries no charged groups and the undersurface has negatively charged moieties. The ionic charges of the molecules were indicated by the binding of cationized ferritin; however, the cationized ferritin does not discriminate between kinds of negatively charged groups so that specific ions possessing negative charges could be different among the columnar material, scales, coccolith bases, and amorphous "glue". From alcian blue staining of Pleurochrysis (Romanovicz and Brown, 1976) and Hymenomonas (Spicer et al., 1967), it is known that both sulfate and carboxyl groups are present. It is also known that cationized ferritin will bind to the scale radials (Romanovicz and Brown, 1976). The reassociation of the amorphous glue with calcium or magnesium indicates that ionic groups in the "glue" are different from those of scales and coccoliths because the scales and coccoliths were often absent from the reassociated fibres. The glycoprotein nature of the columnar material is indicated by its cleavage from the plasma membrane by pronase without the destruction of the cleaved portion and as indicated by ferritin binding following pronase treatment. There may be some ionic bridges that do not involve calcium as an intermediate. This model is very tentative and as more biochemical information is obtained modifications will necessarily result. However, the use of ionic interconnections between the wall components appears sound.

Conclusion

The discrete morphological markers, especially coccoliths, of Hymenomonas carterae provided an excellent model system for the study of cell wall biosynthesis and assembly. The ability to experimentally manipulate the cell was a decided advantage in understanding how the cell wall components come together and separate. While protoplast formation is common in the plant world, no protoplast system so explicitly demonstrates the biosynthetic machinations that transpire as the cell controls, via its genome to its membranes and its enzymes, the synthesis of coccoliths, scales, and the other cell wall components. Once the materials are synthesized, in essence, the entire wall self-assembles through the ionic interactions inherent within the molecules themselves. The capacity to separate the wall superstructure into its constitutents allows future investigations to pursue the molecular composition of these construction units. Because of its distinct morphology, the coccolith and its precursors, provide a morphological assay system for the evaluation of various effectors on the cell's control systems for cell wall synthesis and assembly.

BIBLIOGRAPHY

Albersheim, P. 1975. The walls of growing plant cells. Sci. Am. 232: 80-95.

Albersheim, P. 1976. The primary cell wall. Pages 225-274 in J. Bonner and J. E. Varner, eds. Plant Biochemistry. Academic Press, New York.

Albersheim, P. and A. J. Anderson-Prouty. 1975. Carbohydrates, proteins, cell surfaces, and the biochemistry of pathogenesis. Ann. Rev. Plant Physiol. 26: 31-52.

Anson, J. L. 1939. The purification of cathepsin. J. Gen. Physiol. 23: 695-704.

Baddiley, J. 1975. Mechanism and control of cell wall synthesis in bacteria. Pure Appl. Chem. 42: 417-429.

Bateman, D. F. and H. G. Basham. 1976. Degredation of plant cell walls and membranes by microbial enzymes. Pages 316-355 in R. Heitifuss and P. H. Williams. eds. Physiological Plant Pathology. Volume 4. Encyclopedia of Plant Physiology. Springer-Verlag, Berlin.

Basu, S. K., R. G. W. Anderson, J. L. Goldstein, and M. S. Brown. 1977. Metabolism of cationized lipoproteins by human fibroblasts. Biochemical and morphologic correlations. J. Cell Biol. 74: 119-135.

Bauer, W. D., K. W. Talmadge, K. Keegstra, and P. Albersheim. 1973. The structure of plant cell walls. II. The hemicellulose of the walls of suspension-cultured sycamore cells. Plant Physiol. 51: 174-187.

Black, M. 1962. The fine structure of the mineral parts of coccolithophoridae. Proc. Linn. Soc., London 174: 41-46.

Blackwelder, P. L., R. E. Weiss, and K. M. Wilbur. 1976. Effects of calcium, strontium, and magnesium on the coccolithophorid Cricosphaera (Hymenomonas) carterae I. Calcification. Mar. Biol. 34: 11-16.

Blankenship, M. L. and K. M. Wilbur. 1975. Cobalt effects on cell division and calcium uptake in the coccolithophorid Cricosphaera carterae (Haptophyceae). J. Phycol. 11: 211-219.

Blankley, W. 1971. Auxotrophic and heterotrophic growth and calcification in coccolithophorids. Ph.D. Thesis. University of California, San Diego (Lib. Congr. Card No. Mic. 71-22,618). 186 pp. Univ. Microfilms, Ann Arbor, Michigan.

Blankley, W. F. and R. A. Lewin. 1976. Temperature responses of a coccolithophorid, Cricosphaera carterae, measured in a simple and inexpensive thermal gradient device. Limnol. Oceanogr. 21: 457-462.

Braarud, T., G. DeFlandre, P. Halldal, and E. Kamptner. 1955. Terminology, nomenclature, and systematics of the Coccolithophoridae. Micropaleontology 1: 157-159.

Bracker, C. E., J. Ruiz-Herrera, and S. Bartnicki-Garcia. 1976. Structure and transformation of Chitin synthetase particles (chitosomes) during microfibril synthesis in vitro. Proc. Natl. Acad. Sci. USA 73: 4570-4574.

Braun, E. and H. G. Aach. 1975. Enzymatic degradation of the cell wall of Chlorella. Planta 126: 181-185.

Bricas, E. 1973. Survey of synthetic work in the field of the bacterial cell wall peptides. Pages 205-235 in P. G. Katsoyannis, ed. The Chemistry of Polypeptides. Plenum Press, New York.

Brody, S. 1973. Metabolism, cell walls, and morphogenesis. Pages 107-154 in S. J. Cowand, ed. Developmental Regulation Aspects of Cell Differentiation. Academic Press, New York.

Brown, R. M., Jr. 1969. Observations on the relationships of the Golgi apparatus in the marine chrysophycean alga, Pleurochysis scherffelii Pringsheim. J. Cell Biol. 41: 109-123.

Brown, R. M., Jr. and D. Montezinos, 1976. Cellulose microfibril: Visualization of biosynthesis and orienting complexes in association with the plasma membrane. Proc. Natl. Acad. Sci. USA 73: 143-147.

Brown, R. M., Jr. and D. K. Romanovicz. 1976. Biogenesis and structure of Golgi derived cellulosic scales in Pleurochrysis. I. Role of the endomembrane system in scale assembly and exocytosis. Appl. Poly. Symp. 28: 587-610.

Brown, R. M., Jr., W. W. Franke, H. Kleinig, H. Falk, and P. Sitte. 1970. Scale formation in chrysophycean algae I. Cellulosic and noncellulosic wall components made by the Golgi apparatus. J. Cell Biol. 45: 246-271.

Brown, R. M., Jr., W. Herth, W. W. Franke, and D. Romanovicz. 1973. The role of the Golgi apparatus in the biosynthesis and secretion of a cellulosic glycoprotein in Pleurochrysis: A model system for the synthesis of structural polysaccharides. Pages 207-257 in F. Loewus, ed. Biogenesis of Plant Cell Wall Polysaccharides. Academic Press, New York.

Brown, R. M., Jr., J. H. M. Willison, and C. L. Richardson. 1976. Cellulose biosynthesis in Acetobacter xylinum: Visualization of the site of synthesis and direct measurement of the in vivo process. Proc. Natl. Acad. Sci. USA 73: 4565-4569.

Burgess, J. and E. R. Fleming. 1974. Ultrastructural observations of cell wall regeneration around isolated tobacco protoplasts. J. Cell Sci. 14: 439-449.

Burgess, J. and P. J. Linstead. 1977. Coumarin inhibition of microfibril formation of cultural protoplasts. Planta 133: 267-273.

Cabib, E. 1975. Molecular aspects of yeast morphogenesis. Ann. Rev. Microbiol. 29: 191-214.

Catt, J. W., G. J. Hills, and K. Roberts. 1976. A structural glycoprotein, containing hydroxyproline, isolated from the cell wall of Chlamydomonas reinhardii. Planta 131: 165-171.

Chrispeels, M. J. 1976. Biosynthesis, intracellular transport, and secretion of extracellular macromolecules. Ann. Rev. Plant Physiol. 27: 19-38.

Cocking, E. C. 1972. Plant cell protoplasts-isolation and development. Ann. Rev. Plant Physiol. 23: 29-50.

Cohen, A. L. 1974. Critical Point Drying. Pages 44-112 in M. A. Hayat, ed. Principles and Techniques of Scanning Electron Microscopy Vol. 1. Biological Applications. Van Nostrand Reinhold Company, New York.

Cook, G. M. W. and R. W. Stoddart. 1973. Surface carbohydrates of the eukaryotic cell. Academic Press, London. 346 pp.

Crenshaw, M. 1964. Coccolith form by two marine coccolithophorids, coccolithus huxleyi and Hymenomonas. Ph.D. Thesis. Duke Univ. (Lib. Congr. Card No. Mic. 65-3972). 74 pp. Univ. Microfilms, Ann Arbor, Michigan.

Dalessandro, G. and D. H. Northcote. 1977. Possible control sites of polysaccharide synthesis during cell growth and wall expansion of pea seedlings (Pisium sativum L.). Planta 134: 39-44.

Danon, D. 1972. Use of cationized ferritin as a label of negative charges on cell surfaces. Ultrastruct. Res. 38: 500-510.

Darley, W. M., D. Porter, and M. S. Fuller. 1973. Cell wall composition and synthesis via Golgi-directed scale formation in the marine eukaryote, Schizochytrium aggregatum, with a note on Thraustochytrium sp. Arch. Mikrobiol. 90: 89-106.

Davies, D. R. and V. Lyall. 1973. The assembly of a highly ordered component of the cell wall: The role of heritable factors and of physical structure. Mol. Gen. Genet. 124: 21-34.

Dorigan, J. L. and K. M. Wilbur. 1973. Calcification and its inhibition in coccolithophorids. J. Phycol. 9: 450-456.

Douglas, S. D., H. D. Isenberg, L. S. Lavine, and S. S. Spicer. 1967. Correlation between the presence of sulfated polysaccharides and mineralization in a marine coccolithophorid protozoan: Histochemical and autoradiographic studies. J. Histochem. Cytochem. 15: 285-291.

Drews, G. 1974. Special cytology: Cytology and morphogenesis of the prokaryotic cell. Fortschr. Bot. 36: 21-29.

Ebersold, W. T. 1963. Heterozygous diploid strains of Chlamydomonas reinhardii. Genetics 48: 888.

Ebersold, W. T. 1967. Chlamydomonas reinhardii heterozygous diploid strains. Science 157: 447-449.

Elder, J. H., C. A. Lembi, L. Anderson, and D. J. Morre. 1972. Scale calcification in a chrysophycean alga. A test system for the effects of DDT on biological calcification. Proc. Indiana Acad. Sci. 81: 106-113.

Engels, F. M. 1974. Function of Golgi vesicles in relation to cell wall synthesis in germinating Petunia pollen. IV. Identification of cellulose in pollen tube walls and Golgi vesicles by x-ray diffraction. Acta Bot. Neerl. 23: 209-215.

Evans, L. L. and M. E. Callow. 1976. Secretory processes in seaweeds. Pages 487-499 in N. Sunderland, ed. Perspectives in Experimental Biology. Vol. 2. Botany. Pergamon Press, Oxford.

Filman, D. J., R. J. Brawn, and W. B. Dandliker. 1975. Intracellular supravital stain delocalization as an assay for antibody-dependent complement-mediated cell damage. J. Immunol. Methods 6: 189-207.

Flesch, D. C. and D. Outka. 1976. Cell wall resorption and re-formation after pronase treatment in the unicellular alga, Hymenomonas carterae. J. Cell Biol. 70: 180a.

Forster, G. F. 1975. Attempts at cell fusion in Chlamydomonas. Bot. Soc. Edinb. Trans. 42: 357.

Franke, W. W., U. Scheer, and W. Herth. 1974. General and Molecular Cytology. Fortschr. Bot. 36: 1-20.

Gaarder, K. R. and B. R. Heimdal. 1977. A revision of the genus Syracosphaera Lohmann (coccolithineae). "Meteor" Forsch. Ergebn. D. No. 24: 54-71.

Gahan, P. B. 1973. Plant Lysosomes. Pages 69-85 in J. T. Dingle, ed. Lysosomes in Biology and Pathology. Volume 3. American Elsevier Publishing Company, Inc., New York.

Gander, J. E. 1974. Fungal cell wall glycoproteins and peptido-polysaccharides. Ann. Rev. Microbiol. 28: 103-119.

Glaser, L. 1973. Bacterial cell surface polysaccharides. Ann. Rev. Biochem. 42: 91-112.

Green, J. C. and D. H. Jennings. 1967. A physical and chemical investigation of the scales produced by the Golgi apparatus within and found on the surface of the cells of Chrysochromulina chiton Parke et Manton. J. Exp. Bot. 18: 359-370.

Grimm, I., H. Sachs, and D. G. Robinson. 1976. Structure, synthesis, and orientation of microfibrils. II. The effect of colchicine on the wall of Oocystis solitaria. Cytobiology 14: 61-74.

Hanke, D. E. and D. H. Northcote. 1974. Cell wall formation by soybean callus protoplasts. J. Cell Sci. 14: 29-50.

Hara, M., N. Umetsu, C. Miyamoto, and K. Tamari. 1973. Inhibition of the synthesis of plant cell wall materials, especially cellulose biosynthesis by coumarin. Plant Cell Physiol. 14: 11-28.

Haug, A. 1974. Chemistry and biochemistry of algal cell-wall polysaccharides. Pages 51-88 in D. H. Northcote, ed. MTP International Review of Science. Biochemistry Series One. Volume 11. Plant Biochemistry. University Park Press, Baltimore.

Helsper, J. P. F. G., J. H. Veerkamp, and M. M. A. Saasen. 1977. β-glucan synthetase activity in Golgi vesicles of Petunia hydrida. Planta 133: 303-308.

Herth, W., W. W. Franke, J. Stadler, H. Bittiger, G. Keilich, and R. M. Brown. 1972. Further characterization of the alkali-stable material from the scales of pleurochrysis scherfelii: A cellulosic glycoprotein. Planta 105: 79-92.

Herth, W., A. Kuppel, W. W. Franke, and R. M. Brown. 1975. The ultrastructures of the scale cellulose from Pleurochrysis scherffelii under various experimental conditions. Cytobiology 10: 268-284.

Hills, G. J. 1973. Cell wall assembly in vitro from Chlamydomonas reinhardii. Planta 115: 17-23.

Hills, G. J., J. M. Phillips, M. R. Gay, and K. Roberts. 1975. Self-assembly of a plant cell wall in vitro. J. Mol. Biol. 96: 431-441.

Hodge, J. E. and B. T. Hofreiter. 1962. Determination of reducing sugars and carbohydrates. Meth. Carbohydr. Chem. 1: 380.

Hodges, G. M., D. C. Livingston, and L. M. Franks. 1973. The localization of trypsin in cultured mammaliam cells. J. Cell Sci. 12: 887-902.

Holtzman, E. 1976. Lysosomes: A survey. Springer-Verlag, Wien. 298 pp.

Hopsu-Havu, V. K., A. U. Arstila, H. J. Helminer, H. O. Kalimo, and G. G. Glenner. 1967. Improvements in the method for the electron microscopic localization of aryl sulfatase activity. Histochemie 8: 54-64.

Isenberg, H. D. and L. S. Lavine. 1973. Protozoan calcification. Pages 649-686 in I. Zipkin, ed. Biological Mineralization. John Wiley and Sons, Inc., New York.

Isenberg, H. D., L. S. Lavine, M. C. Moss, D. Kupferstein, and P. E. Lear. 1963a. Calcification in a marine coccolithophorid. Ann. N.Y. Acad. Sci. 109: 49-64.

Isenberg, H. D., L. S. Lavine, and H. Weissfellner. 1963b. The suppression of mineralization in a coccolithophorid by an inhibitor of carbonic anhydrase. J. Protozool. 10: 477-479.

Isenberg, H. D., S. D. Douglas, L. S. Lavine, S. S. Spicer, and H. Weissfellner. 1966. A protozoan model of hard tissue formation. Ann. N.Y. Acad. Sci. 136: 155-170.

Ivatt, R. J. and C. Gilvarg. 1977. Structural relationship after teichuronic acid and peptidoglycan of Bacillus megaterium. Biochemistry 16: 2436-2440.

Jurasek, L., M. R. Carpenter, L. B. Smillie, A. Gertler, S. Levy, and L. H. Ericsson. 1974. Amino acid sequence of Streptomyces griseus protease B, a major component of pronase. Biochem. Biophys. Res. Commun. 61: 1095-1100.

Karr, A. L. 1976. Cell wall biosynthesis. Pages 405-426 in J. Bonner and J. E. Varner, eds. Plant Biochemistry. 3rd ed. Academic Press, New York.

Kauss, H. 1976. Plant Lectins (Phytohemagglutinins). Pages 58-70 in H. Ellenberg, ed. Progress in Botany. Volume 38. Morphology, Physiology, Genetics, Taxinomy, Geobotany. Springer-Verlag, Berlin.

Keegstra, K., K. W. Talmadge, W. D. Bauer, and P. Albersheim. 1973. The structure of plant cell walls. III. A model of the walls of suspension-cultured sycamore cells based on the interconnections of the macromolecular components. Plant Physiol. 51: 188-196.

Kiermayer, O. and B. Dobberstein. 1973. Membrankomplexe dictyosomaler herkuzft als matrizen fur die extraplasmatische synthese und orientierung von mikrofibrillen. Protoplasma 77: 437-451.

Klaveness, D. 1972. Coccolithus huxleyi (Lohmann) Kamptner. I. Morphological investigations on the vegetative cell and the process of coccolith formation. Protistologica 8: 335-346.

Klaveness, D. 1976. Emiliania huxley: (Lohmann). Hay and Mohler. III. Mineral deposition and the origin of the matrix during coccolith formation. Protistologica 12: 217-224.

Kuratana, A. 1974. The isolation and preliminary characterization of the coccoliths of Hymenomonas carterae. Master's Thesis. Iowa State University. 69 pp.

Lamport, D. T. A. 1969. The isolation and partial characterization of hydroxyproline-rich glycopeptides by enzymic degradation of primary cell walls. Biochemistry 8: 1155-1163.

Lamport, D. T. A. 1970. Cell wall metabolism. Ann. Rev. Plant Physiol. 21: 235-270.

Lamport, D. T. A. 1973. Is the primary cell wall a protein-glycan network? Pages 28-40 in M. B. Ephrussi, ed. Protoplastes et fusion de cellules somatiques vegetales. Institut National de la Recherche Agronomique, Paris.

Leadbeater, B. S. C. 1970. Preliminary observations on differences of scale morphology at various stages in the life cycle of Apistonema-Syracosphaera sensu von Stosch. Br. Phycol. J. 5: 57-69.

Leadbeater, B. S. C. 1971. Observations on the life history of the haptophycean alga Pleurochrysis scherffelii with special reference to the microanatomy of the different types of motile cells. Ann. Bot. 35: 429-439.

Lefort, F. 1971. Sur l'appartenance a une seule et meme espece de deux Coccolithophoracees, Cricosphaera carterae et Ochrosphaera verrucosa. Comp. Rend., D. 272: 2540-2543.

Levine, R. P. and W. T. Ebersold. 1960. The genetics and cytology of Chlamydomonas. Ann. Rev. Microbiol. 14: 197-216.

Loewus, F., Editor. 1973. Biogenesis of plant cell wall polysaccharides. Academic Press, New York. 379 pp.

Lowry, O. H., N. J. Rosebrough, A. L. Farr, and R. J. Randall. 1951. Protein measurement with the folin phenol reagent. J. Biol. Chem. 193: 265-275.

Luben, R. A., J. K. Sherman, and C. L. Wadkins. 1973. Studies of the mechanism of biological calcification. IV. Ultrastructural analysis of calcifying tendon matrix. Calc. Tiss. Res. 11: 39-55.

Manocha, M. S. and M. Shaw. 1964. Occurrence of lomasomes in mesophyll cuts of Khapli wheat. Nature (London) 203: 1402-1403.

Manton, I. 1966. Observations on scale production in Prymnesium parvum. J. Cell Sci. 1: 375-380.

Manton, I. 1967a. Further observations on the fine structure of Chryschromulina chiton with special reference to the haptonema, "peculiar" Golgi structure and scale production. J. Cell Sci. 2: 265-272.

Manton, I. 1967b. Further observations on scale formation in Chrysochromulina chiton. J. Cell Sci. 2: 411-418.

Manton, I. 1968. Further observations on the microanatomy of the haptonena in Chrysochromulina chiton and Prymnesium parvum. Protoplasma 66: 35-53.

Manton, I. and G. F. Leedale. 1969. Observations on the microanatomy of Coccolithus pelagicus and Cricosphaera carterae, with special reference to the origin and nature of coccoliths and scales. J. Mar. Biol. Assoc. U.K. 49: 1-16.

Manton, I. and L. S. Peterfi. 1969. Observations on the fine structure of coccoliths, scales, and the protoplast of a freshwater coccolithophorid, Hymenomonas roseola Stein, with supplementary observations on the protoplast of Cricosphaera carterae. Roy. Soc. (London) Proc. B.

Matile, P. 1975. The lytic compartment of plant cells. Springer-Verlag, New York. 183 pp.

Matile, P. 1976. Vacuoles. Pages 189-224 in J. Bonner and J. E. Varner, eds. Plant Biochemistry. 3rd ed. Academic Press, New York.

Métraux, J.-P. and L. Taiz. 1977. Cell wall extension in Nitella as influenced by acids and ions. Proc. Natl. Acad. Sci. U.S.A. 74: 1565-1569.

Miller, D. H., D. T. A. Lamport, and M. Miller. 1972. Hydroxyproline heterooligosaccharides in Chlamydomonas. Science 176: 918-920.

Miller, D. H., I. S. Mellman, D. T. A. Lamport, and M. Miller. 1974. The chemical composition of the cell wall of Chlamydomonas gymnogama and the concept of a plant cell wall protein. J. Cell Biol. 63: 420-429.

Mills, J. T. 1975. Hymenomonas coronato sp. Nov., A new coccolithophorid from the Texas coast. J. Phycol. 11: 149-154.

Monro, J. A., D. Penny, and R. W. Bailey. 1976. The organization and growth of primary cell walls of lupin hypocotyl. Phytochemistry 15: 1193-1198.

Montreuil, J. 1975. Recent data on the structure of the carbohydrate moiety of glycoproteins. Metabolic and biological implications. Pure Appl. Chem. 42: 431-477.

Moore, R. T. and J. H. McAlear. 1961. Fine structure of mycota. V. Lomasome-Previously uncharacterized hyphal structures. Mycologia 53: 194-200.

Morre, D. J. and H. H. Mollenhauer. 1974. The endomembrane concept: A functional integration of endoplasmic reticulum and Golgi apparatus. Pages 84-137 in A. W. Robards, ed. Dynamic Aspects of Plant Ultrastructure. McGraw-Hill, London.

Morre, D. J., R. L. Hamilton, H. H. Mollenhauer, R. W. Mahley, W. P. Cunningham, R. D. Cheetham, and V. S. Lequire. 1969. Isolation of a Golgi apparatus-rich fraction from rat liver. J. Cell Biol. 44: 484-491.

Morris, E. R., D. A. Rees, G. Young, M. D. Walkin Shaw, and A. Darke. 1977. Order-disorder transition for a bacterial polysaccharide in solution. A role for polysaccharide conformation in recognition between Xanthomonas pathogen and its plant host. J. Mol. Biol. 110: 1-16.

Mueller, S. C., R. M. Brown, Jr., and T. K. Scott. 1976. Cellulosic microfibrils: Nascent stages of synthesis in a higher plant cell. Science 194: 949-951.

Neely, A. N., J. V. Sitzmann, and J. H. Kersey. 1976. EGTA and proteinase reversal of cellular aggregation of activated lymphocytes. Nature 264: 770-771.

Neville, A. C., D. C. Gubb, and R. M. Crawford. 1976. A new model for cellulose architecture in some plant cell walls. Protoplasma 90: 307-317.

Northcote, D. H. 1972. Chemistry of the plant cell wall. Ann. Rev. Plant Physiol. 23: 113-132.

Novikoff, A. B. and E. Holtzman. 1976. Cells and organelles. 2nd ed. Holt, Rinehart, and Winston, New York. 400 pp.

O'Brien, T. P. 1972. The cytology of cell wall formation in some eukaryotic cells. Bot. Rev. 38: 87-118.

Olson, R. A., W. H. Jennings, and M. B. Allen. 1967. Spectral properties of a pigmental body in Hymenomonas sp: An extra-chloroplast organelle containing chlorophyll. J. Cell Physiol. 70: 133-140.

Outka, D. E. and D. C. Williams. 1971. Sequential coccolith morphogenesis in Hymenomonas carterae. J. Protozool. 18(2): 285-297.

Paasche, E. 1962. Coccolith formation. Nature 93: 1094-1095.

Paasche, E. 1964. A tracer study of inorganic carbon uptake during coccolith formation and photosynthesis in the coccolithophorid Coccolithus huxleyi. Physiol. Plant Suppl. 111: 1-82.

Paasche, E. 1966a. Adjustment to light and dark rates of coccolith formation. Physiol. Plant 19: 271-278.

Paasche, E. 1966b. Action spectrum of coccolith formation. Physiol. Plant 19: 770-779.

Paasche, E. 1967. Marine plankton algae grown with light-dark cycles. I. Coccolithus huxleyi. Physiol. Plant 20: 946-956.

Paasche, E. 1968. Biology and physiology of coccolithophorids. Ann. Rev. Microbiol. 22: 71-86.

Packard, M. J. and S. M. Stack. 1976. The preprophase band: Possible involvement in the formation of the cell wall. J. Cell Sci. 22: 403-411.

Paddock, T. B. B. 1968. A possible aid to survival of the marine coccolithophorid Cricosphaera and similar organisms. Br. Physiol. Bull. 3: 519-523.

Palevitz, B. A. and P. K. Hepler. 1976. Cellulose microfibril orientation and cell shaping in developing guard cells of Allium. The role of microtubules and ion accumulation. Planta 132: 71-93.

Parke, M. and I. Adams. 1960. The motile (Crystallolithus hyalinus Gaarder and Markali) and nomotile phases in the life history of Coccolithus pelagicus (Wallich) Schiller. J. Mar. Biol. Assoc. U.K. 39: 263-264.

Pautard, F. G. E. 1970. Calcification in unicellular organisms. Pages 105-201 in H. Schraer, ed. Biological Calcification: Cellular and Molecular Aspects. Appleton-Century-Crofts, New York.

Pearse, A. G. E. 1968. Histochemistry Theoretical and Applied. Vol. 1. Little, Brown, and Company, Boston. 759 pp.

Pickett-Heaps, J. D. 1967. The use of radioautography for investigating wall secretion in plant cells. Protoplasma 64: 49-66.

Pickett-Heaps, J. D. 1968. Further ultrastructural observations on polysaccharide localization in plant cells. J. Cell Sci. 3: 55-64.

Pienaar, R. N. 1969a. The fine structure of Cricosphaera carterae. I. External morphology. J. Cell Sci. 4: 561-567.

Pienaar, R. N. 1969b. The fine structure of Hymenomonas (Cricosphaera) carterae. II. Observations on scale and coccolith production. J. Phycol. 5: 321-331.

Pienaar, R. N. 1971a. Acid phosphatase activity in the cells of the coccolithophorid Hymenomonas. Proc. S. Afr. Electron Microsc. Soc. Pretoria 1971: 8-9

Pienaar, R. N. 1971b. Coccolith production in Hymenomonas carterae. Protoplasma 73: 217-224.

Pienaar, R. N. 1976. The microanatomy of Hymenomonas racuna sp. Nov. (Haptophyceae). Mar. Biol. Assoc. U.K. 56: 1-11.

Preston, R. D. 1974. The physical biology of plant cell walls. Chapman and Hall Ltd., London. 491 pp.

Rayle, D. L. and M. H. Zenk. 1973. Cell extension growth: Some recent advances. Pages 235-246 in T. W. Goodwin and R. M. S. Smellie, eds. Nitrogen Metabolism in Plants. Biochemical Society, London.

Rayns, D. G. 1962. Alternation of generations in a coccolithophorid, Cricosphaera carterae (Braarud and Fagerl.) Braarud. J. Mar. Biol. Ass. U.K. 42: 481-484.

Reeve, J. N. and N. H. Mendelson. 1973. Pronase digestion of amino acid binding components on the surface of Bacillus subtilis cells and minicells. Biochem. Biophys. Res. Comm. 53: 1325-1330.

Reynolds, C. S. 1963. The use of lead citrate at high pH as an electron-opaque stain in electron microscopy. J. Cell Biol. 17: 208-212.

Roberts, K. 1974. Crystalline glycoprotein cell walls of algae: Their structure, composition, and assembly. Phil. Trans. Roy. Soc. London. Series B 268: 129-146.

Roberts, K. and G. J. Hills. 1976. The crystalline glycoprotein cell wall of the green alga Chlorogonium elongatum: A structural analysis. J. Cell Sci. 21: 59-71.

Roberts, K., M. Gurney-Smith, and G. J. Hills. 1972. Structure, composition, and morphogenesis of the cell wall of Chlamydomonas reinhardi. I. Ultrastructure and preliminary chemical analysis. J. Ultrastruct. Res. 40: 599-613.

Roland, J.-C. 1973. The relationship between the plasmalemma and plant cell wall. Int. Rev. Cytol. 36: 45-92.

Roland, J.-C. and P.-É. Pilet. 1974. Implications du plasmalemme et de la paroi dans la croissance des cellules vegetales. Experientia 30: 441-451.

Roland, J.-C., B. Vian, and D. Reis. 1975. Observations with cytochemistry and ultracryotomy on the fine structure of the expanding walls in actively elongating plant cells. J. Cell Sci. 19: 239-259.

Roland, J.-C., B. Vian, and D. Reis. 1977. Further observations on cell wall morphogenesis and polysaccharide arrangement during plant growth. Protoplasma 91: 125-141.

Romanovicz, D. K. and R. M. Brown, Jr. 1976. Biogenesis and structure of Golgi derived cellulosic scales in Pleurochrysis. II. Scale composition and supramolecular structure. Appl. Polym. Symp. 28: 587-610.

Ruel, K., J. Comtat, and F. Barnond. 1977. Ultrastructural and histological localization of xylans in the primary walls of Arunda donax tissues. C.R. Acad. Sci. (Paris) Series D 284: 1421-1424.

Russin, D. J., B. F. Floyd, T. P. Toomey, A. H. Brady, and W. M. Awad. 1974. The proteolytic enzymes of the K-1 strain of Streptomyces grieseus obtained from a commercial preparation (pronase). J. Biol. Chem. 249: 6144-6148.

Schlosser, U. G., H. Sachs, and D. G. Robinson. 1976. Isolation of protoplasts by means of a "species-specific" autolysin in Chlamydomonas. Protoplasma 88: 51-64.

Seed, J. R., J. Byram, and A. A. Gam. 1967. Characterization and localization of acid phosphatase activity of Trypanosoma gambiense. J. Protozool. 14: 117-125.

Segrest, J. P. and R. L. Jackson. 1972. Molecular weight determinations of glycoproteins by polyacrylamide gel electrophoresis in SDS. Methods Enzymol. 28: 54.

Sigma Chemical Company. Sigma Technical Bulletin, Sigma Chemical Company, St. Louis, Mo.

Spurr, A. R. 1969. A low viscosity epoxy resin embedding medium for electron microscopy. J. Ultrastruct. Res. 26: 31-43.

Srivastava, L. M., V. K. Sawhney, and M. Bonettemaker. 1977. Cell growth, wall deposition, and correlated fine structure of colchicine-treated lettuce hypocotyl cells. Can. J. Bot. 55: 902-917.

Stadelmann, E. J. and H. Kinzel. 1972. Vital staining of plant cells. Pages 329-372 in D. M. Prescott, ed. Methods in cell physiology. Vol. 5. Academic Press, New York.

Stosch, H. A. Von. 1967. Haptophyceae. Encycl. Plant Phys. 18: 646-656.

Swift, E. and W. R. Taylor. 1966. The effect of pH on the division rate of the coccolithophorid Cricosphaera elongata. J. Phycol. 2: 121-125.

Talmadge, K. W., K. Keegstra, W. D. Bauer, and P. Albersheim. 1973. The structure of plant cell walls. I. The macromolecular components of the walls of suspension-cultured sycamore cells with a detailed analysis of the pectic polysaccharides. Plant Physiol. 51: 158-173.

Taylor, I. E. P. and D. S. Cameron. 1973. Preparation and quantitative analysis of fungal cell walls: Strategy and tactics. Ann. Rev. Microbiol. 27: 243-257.

Thorne, K. J. I., M. J. Thornley, P. Naisbitt, and A. M. Glauert. 1975. The nature of the attachment of a regularly arranged surface protein to the outer membrane of an Acinetobacter sp. Biochim. Biophys. Acta 389: 97-116.

Trout, J. J. 1977. Morphological, cytochemical, and biochemical effects of Triton WR1339 on rat hepatocytes. Ph.D. Thesis. Iowa State University. 186 pp.

Ulrich, F. 1976. Effects of trypsin on protein synthesis in macrophages. Exp. Cell Res. 101: 267-277.

Van der Valk, P. and J. G. H. Wessels. 1976. Ultrastructure and localization of wall polymers during the regeneration and reversion of protoplasts of Schizophyllum commune. Protoplasma 90: 65-87.

Van Der Woude, W. J., C. A. Lembi, J. Morri, J. I. Kindinger, and L. Ordin. 1974. β-glucan synthesis of plasma membranes and Golgi apparatus from onion stem. Plant Physiol. 54: 333-340.

Venable, J. H. and R. Coggeshall. 1965. A simplified lead citrate stain for use in electron microscopy. J. Cell Biol. 25: 407-408.

Wachstein, M. and E. Meisel. 1957. Histochemistry of hepatic phosphatases at a physiological pH. Am. J. Clin. Path. 27: 13-23.

Waechter, C. J. and W. J. Lennarz. 1976. The role of polyprenol-linked sugars in glycoprotein synthesis. Ann. Rev. Biochem. 45: 95-112.

Washitani, I. and S. Sato. 1976. On the reliability of the lead salt precipitation method of acid phosphatase localization in plant cells. Protoplasma 89: 157-170.

Watabe, N. 1967. Crystallographic analysis of the coccolith of Coccolithus huxleyi. Calc. Tiss. Res. 1: 114-121.

Watabe, N. and K. M. Wilbur. 1966. Effects on growth, calcification, and coccolith form in Coccolithus huxleyi (coccolithinae). Limnol. Oceanogr. 11: 567-575.

Weber, K. and M. Osborn. 1969. The reliability of molecular weight determinations by dodecyl sulfate-polyacrylamide gel electrophoresis. J. Biol. Chem. 244: 4406-4412.

Weiss, R. E., P. L. Blackwelder, and K. M. Wilbur. 1976. Effects of calcium, strontium, and magnesium on the coccolithophorid Cricosphaera (Hymenomonas) carterae. II. Cell division. Mar. Biol. 34: 17-22.

Westafer, J. M. and R. M. Brown, Jr. 1976. Electron microscopy of cotton fibre: New observations on cell wall formation. Cytobios 15: 111-138.

Westbroek, P., E. W. deLong, W. Dam, and L. Bosch. 1973. Soluble intracrystalline polysaccharides from coccoliths of Coccolithus huxleyi (Lohmann) Kampther (1). Calc. Tiss. Res. 12: 227-238.

Whaley, W. G. and H. H. Mollenhauer. 1963. The Golgi apparatus and cell plate formation - a postulate. J. Cell Biol. 17: 216-221.

White, A., P. Handler, and E. L. Smith. 1968. Principles of Biochemistry. Fourth Edition. McGraw-Hill Book Company, New York. 1187 pp.

Wilbur, K. M. and N. Watabe. 1963. Experimental studies on calcification in molluscs and the alga Coccolithus huxleyi. Ann. N.Y. Acad. Sci. 190: 82-112.

Williams, D. C. 1972. Golgi associated calcification in the coccolithophorid phytoflagellate Hymenomonas carterae. Ph.D. Thesis. Iowa State University (Lib. Congr. Card No. Mic. 72-26,951). 159 pp. Univ. Microfilms, Ann Arbor, Michigan.

Williams, D. C. 1974. Studies on protistan mineralization. I. Kinetics of coccolith secretion in Hymenomonas carterae. Calc. Tiss. Res. 16: 227-237.

Williamson, F. A., L. C. Fowke, F. C. Constabel, and O. L. Gamborg. 1976. Labelling of concanavalin A sites on the plasma membranes of soybean protoplasts. Protoplasma 89: 305-316.

Williamson, F. A., L. C. Fowke, G. Weber, F. Constable, and O. Gamborg. 1977. Microfibril deposition on cultured protoplasts of Vicia hajastana. Protoplasma 91: 213-219.

Willison, J. H. M. 1976. Synthesis of cell walls by higher plant protoplasts. Pages 283-297 in J. F. Peberdy, A. H. Rose, H. J. Rogers. E. C. Cocking, eds. Microbiol and Plant Protoplasts. Academic Press, Inc., London.

Willison, J. H. M. and E. C. Cocking. 1975. Microfibril synthesis of the surfaces of isolated tobacco mesophyll protoplasts, a freeze-etch study. Protoplasma 84: 147-159.

Wilson, C. L. 1973. A lysosomal concept for plant pathology. Ann. Rev. Phytopath. 11: 247-272.

Wolter, K. and R. Tawashi. 1977. Calcite growth under controlled diffusion. Experientia 33: 584-586.

ACKNOWLEDGMENTS

I wish to express my appreciation to Dr. D. E. Outka for his guidance and counsel during the course of this work. I would like to thank Drs. M. A. Rougvie and J. M. Viles for the use of their respective laboratory facilities and equipment. In addition I would like to thank the Bessey E M Facility for providing access to the scanning electron microscope. Also I wish to thank the Graduate College for its financial support.

I would particularly like to thank my uncle, Gerald D. Flesch, for his encouraging discussions during our stay in Ames.

I would finally, and by no means least, like to acknowledge the patience and courage which my wife, Joan, has exhibited during this endeavor.